2

SQT

NAS10-7679

DRA

A Reproduced Copy

OF

Part I & 2 part ?

Reproduced for NASA

by the

NASA Scientific and Technical Information Facility

NOTICE

This report was prepared as an account of Government-sponsored work. Neither the United States, nor the National Aeronautics and Space Administration (NASA), nor any person acting on behalf of NASA:

A.) Makes any warranty or representation, expressed or implied, with respect to the accuracy, completeness, or usefulness of the information contained in this report, or that the use of any information, apparatus, method, or process disclosed in this report may not infringe privately-owned rights; or

B.) Assumes any liabilities with respect to the use of, or for damages resulting from the use of, any information apparatus, method or process disclosed in this report.

As used above, "person acting on behalf of NASA" includes any employee or contractor of NASA, or employee of such contractor, to the extent that such employee or contractor of NASA or employee of such contractor prepares, disseminates, or provides access to any information pursuant to his employment or contract with NASA, or his employment with such contractor.

NAS10-7679
SD 72-SH-0001

A STUDY OF SPACE SHUTTLE STRUCTURAL INTEGRITY TEST AND ASSESSMENT

Final Report
Part 1

R.E. Anderson - R.G. Poe
January 1972

Prepared for

NATIONAL AERONAUTICS AND SPACE ADMINISTRATION
JOHN F. KENNEDY SPACE CENTER, FLORIDA

Space Division
North American Rockwell

PREFACE

This report summarizes the results of the tasks conducted in support of NASA Contract NAS10-7679, "Space Shuttle Structural Integrity Test and Assessment." The study was conducted by the Space Division of North American Rockwell Corporation for the John F. Kennedy Space Center of the National Aeronautics and Space Administration. The Kennedy Space Center's Contracting Officer's Representative is Mr. Rocco A. Sannicandro.

The following individuals contributed to this report: F. H. Stuckenberg and W. McMahon of North American Rockwell.

For convenience and economy, the report is divided into two parts. Part I includes the report, the glossary, and bibliography. Part II is made up of three appendixes showing the microphone and accelerometer response curves from the noise tests. Distribution of Part II is limited to those persons requiring that level of detail.

PRECEDING PAGE BLANK NOT FILMED

CONTENTS

Page

APPENDIXES

PRECEDING PAGE BLANK NOT FILMED

ILLUSTRATIONS

TABLES

INTRODUCTION

Ultrasonic nondestructive evaluation (NDE) has been recommended as one of two candidate methods for on-board assessment of advanced space vehicle structures. Acoustic emission NDE is the second method that has been recommended for structural monitoring of structures and assemblies. Both of these nondestructive technologies have been shown in the laboratory to have the capability for flaw detection in larger structures from stationary locations.

Acoustic emission is currently being studied as an on-board structural monitor for S-II cryogenic storage containers under contract to the Marshall Space Flight Center. In addition, some effort is being expended in developing ultrasonic NDE to support S-II Advanced Technology.

Earlier contractual effort with the Kennedy Space Center (NASA Contract NAS10-7250, "Methods of Assessing Structural Integrity for Space Shuttle Vehicles") surveyed the NDE field and recommended, among others, that ultrasonics and acoustic emission be prime candidates for further development. Acoustic emission was recommended as an area monitor to provide data from large surfaces; ultrasonics was selected as the prime method for localized area monitoring. Further development of these methods was recommended for follow-on effort.

In studying the results of the initial program, the NASA/KSC management team, in concert with NR study team personnel, selected the development of on-board ultrasonic structural monitoring technology as the subject of a follow-on contract. For the first time, specific parameters that would ultimately define an on-board monitoring device for basic shuttle structure would be formalized. Specific points to be studied during the follow-on effort would include ultrasonic transducers and couplants, structural flaw analysis, the effect of standing members, surface roughness, material thickness, background noise on ultrasonic propagation, and the postulation of on-board system design parameters.

OBJECTIVE

It is the stated objective of this study to demonstrate and evaluate the ultrasonics technique for assessing the structural integrity of the primary structure of the space shuttle vehicles.

PRECEDING PAGE BLANK NOT FILMED

SUMMARY OF RESULTS

A comparison of shear and surface wave modes of ultrasonic propagation conducted during this study showed that more favorable flaw responses with respect to distance, sensitivity, and resolution were achieved using the Rayleigh or surface wave mode. The frequency ranges selected for ultrasonic testing purposes were 2.25 and 5.0 MHz. Transducer orientation with respect to flaws is critical when using current narrow-beam transducers.

Liquid and bondable couplants were selected. The liquid couplant selected is Cakurd, an NR-developed, viscous water-soluble solution. Lefkoweld 109 was selected as the bondable couplant from the eight adhesives evaluated.

Standing members do represent a restricting factor upon the usefulness of surface wave ultrasonics, the magnitude of the problem being proportional to the number and location of the standing numbers.

Surface roughness below 100, as measured in microinches root mean square (RMS), has no adverse effects upon the propagation of ultrasonic surface waves.

Background noise from ambient levels to 160 decibels has no detrimental effects upon flaw monitoring.

Initial factors of cost, weight, power, and schedule requirements have been postulated for an ultrasonic flaw detection system to be established on-board a Space Shuttle vehicle.

Assessment of the state of the art of several current NDE technologies has been completed. Those technologies assessed are: acoustic emission, ultrasonics, holographic NDE, thermography, fiber optics, and radiography.

CONCLUSION

The tests conducted within the confines of this study and the results from other related NR programs have shown that ultrasonic techniques, using various beam propagation modes and instrumentation, can be utilized as an on-board monitoring system. Although such a system possesses the necessary potential for implementation on board a shuttle vehicle, specific limitations are evident that would restrict its application. These limitations, such as standing members, structure configuration, probable defect location and orientation, present sensor capability, etc., indicate that such a system would be best utilized on only specific critical, highly stressed members rather than large or complex structures. Even in these localized areas, in-depth analysis of many factors would be required prior to system deployment.

Cost, weight, power, and schedule factors relative to three types of postulated systems were developed during this study. This analysis indicated that a ground supported system, wherein only the system sensors and cables were installed on board the vehicle, possessed the highest merit as a structural monitoring system.

Current instrumentation technology has been used as a basis for cost and schedule considerations because it reflects many similar requirements and applications; operational implementation of a nondestructive evaluation system should be part of the vehicle instrumentation system on the basis of cost effectivity.

PRECEDING PAGE BLANK NOT FILMED

STUDY APPROACH AND RESULTS

GENERAL

FIGURE 1 illustrates the study logic and presents the relationship of the specific tasks to be performed. Tasks 1 through 5 serve to develop the data necessary to demonstrate the ultrasonic method for assessing the structural integrity of the primary structure of a space shuttle vehicle. Task 6 is a parallel effort designed to provide NASA/KSC with a current overview of the NDE state of the art with respect to those methods that could be used in performing structural integrity monitoring of a shuttle vehicle. Each operational task will be discussed in detail in ensuing sections of this report and a special section on state-of-the-art assessment will be included.

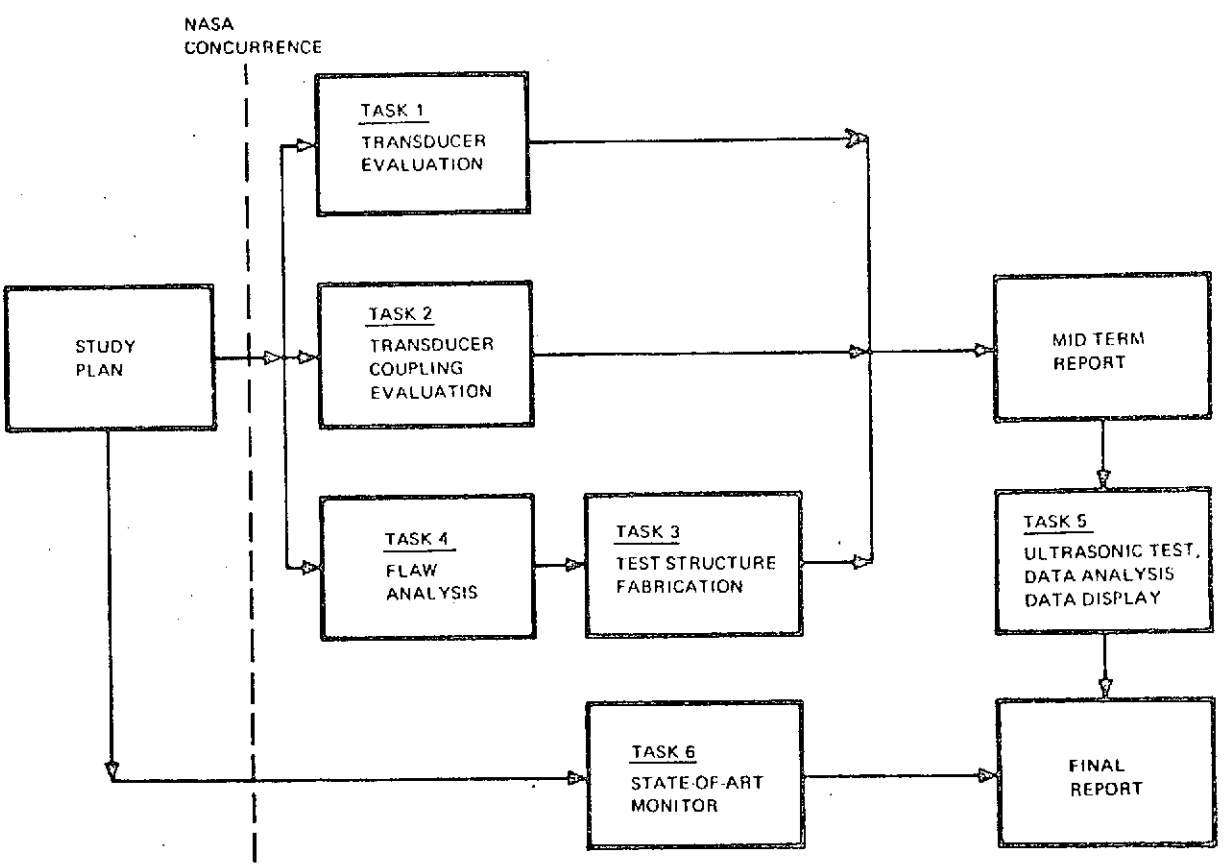

Figure 1. Study Logic Flow Diagram

Nondestructive Testing

Ultrasonic nondestructive testing was performed by NR Space Division's Ultrasonic Technology laboratory. A Sperry Reflectoscope was utilized for transmission and reception of ultrasonic surface waves and, initially, standard laboratory couplants were utilized to transfer the ultrasound into the workpiece. Ultrasonic data was taken in an A trace mode where flaw signals appeared as a function of amplitude variable displacements along a time baseline on an oscilloscope. Data recording was provided by photographing the oscilloscope pattern, utilizing a Hewlitt-Packard Model 196B oscilloscope camera.

Special Specimen Preparation

It became apparent during the course of the study that standard fracture mechanics considerations for shuttle-type structures could not be utilized due to unavailable loading and configuration data. It was decided that special dogbone specimens would be made with predetermined-sized flaws grown into them, based upon calculations for the dogbone configuration. Additional plates of the selected test thicknesses would be fabricated into which would be machined flaws of varying depths in increments of 0.005-inch to 0.010-inch depending upon plate thickness. Correlation would be established between actual flaw response from the dogbone specimens and the response from the artificially produced flaws in the test plate. The particular flaw depth giving the same response as the corresponding dogbone flaw was selected to be machined into the final test specimens for acoustic conditioning during ultrasonic testing.

Fatigue-type flaws were grown into the specially fabricated dogbone specimens utilizing two special laboratory testing devices. The first, a Sonntag Universal Fatigue Bending machine, as shown in FIGURE 2, introduced a cyclic bending moment into the specimen. After a predetermined number of cycles at a prescribed load, cyclic tension was introduced utilizing a Tinius-Olsen Cyclic Tensile Fatigue machine, as shown in FIGURE 3. Final crack growth was achieved and, subsequently, all starter notched were removed by machining.

Environmental Testing

Implementation of Task 5, Ultrasonic Test Data Analysis and Display, required that the effect of high-intensity acoustic noise be introduced as a variable into the test specimens during ultrasonic testing. The required acoustic environment was provided by NR's Dynamics Test engineering group. A Ling Acoustic Reverberant Chamber and its associated electronic control equipment was used to provide the acoustic environments.

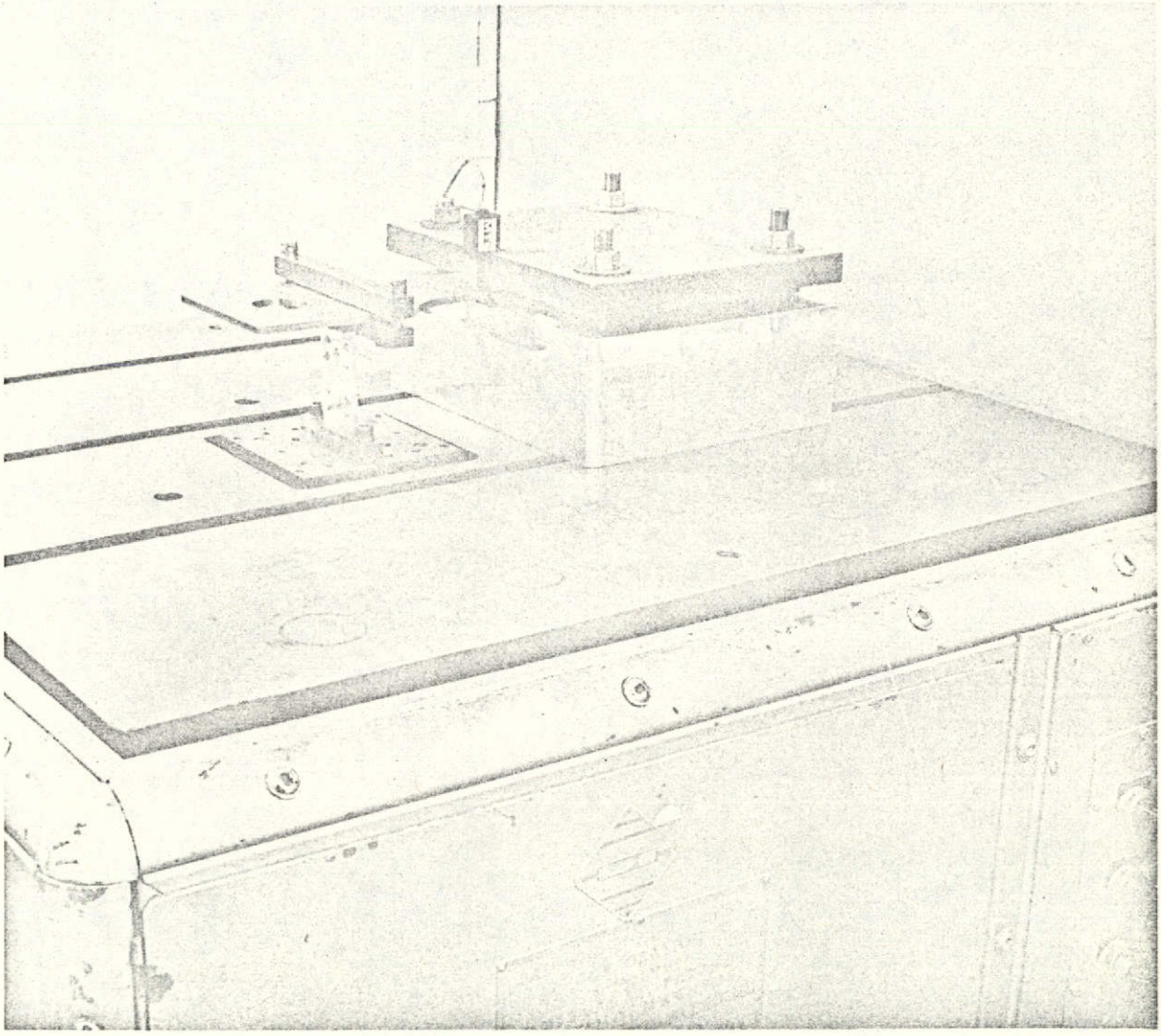

700-81-1418C

Figure 2. Sonntag Universal Fatigue Bending Machine

TRANSDUCER EVALUATION

S-II Technology Data Evaluation

A basic requirement for conducting the follow-on study was to secure applicable data developed during the performance of the MSFC study mentioned previously. All primary information regarding the design of the ultrasonic transducers for the study was to come from the MSFC effort. The S-II Advanced Technology Study No. 4, "On-Board Checkout of the Structural Integrity of Cryogenic Tanks" is being directed towards the development of an on-board acoustic emission and ultrasonic inspection system as applied to cryogenic storage containers. A major task of the ultrasonic development

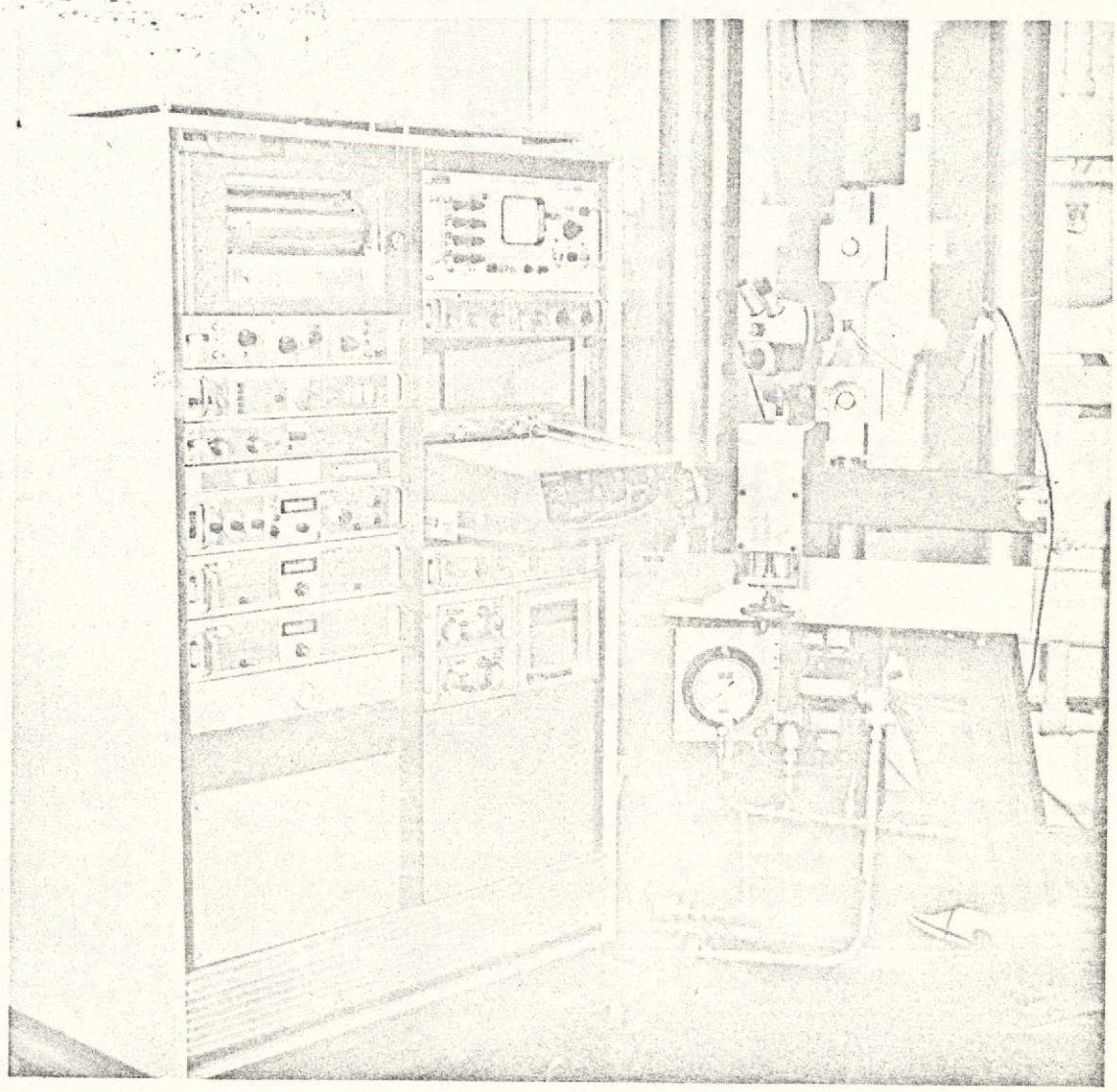

700-81-1415A

Figure 3. Tinius/Olsen Cyclic Tensile Fatigue Machine

program was the definition of specific transducers small enough to be considered for permanent installation within a shuttle structure, yet powerful and responsive enough to provide reliable data about flaw initiation and propagation. A requirement existed at the beginning of the subject study that as much data as possible from the MSFC program with respect to transducer development be utilized. It was felt that the depth of transducer development being conducted for that program would most certainly provide all of the the design data necessary to conduct the initial transducer design and development necessary for the current study.

A review of the transducer data generated during the S-II Advanced Technology, Study No. 4 revealed that a broad range of transducers

(longitudinal, shear, surface, etc.) and the design of the transducer (strip type, point source, multiangle, rotating, etc.) had been investigated.

A trade table containing various attributes of performance of the transducer types and design factors was developed. The ratings established by this matrix revealed that point source shear wave propagation possessed the largest potential for use in the S-II No. 4 study.

Based upon the transducer evaluations conducted in this S-II Study, the utilization of transducers that would produce a shear wave mode of propagation were initially pursued.

Transducer Design Factors

Various 5.0 MHz and 10 MHz standard shear wave transducers, with beam propagation angles of 45, 60, 70, and 80 degrees, were obtained for preliminary testing purposes. These transudcers, as shown in FIGURE 4, contained lead zirconate titanate piezoelectric elements with an effective active element area of 1/4-square inch.

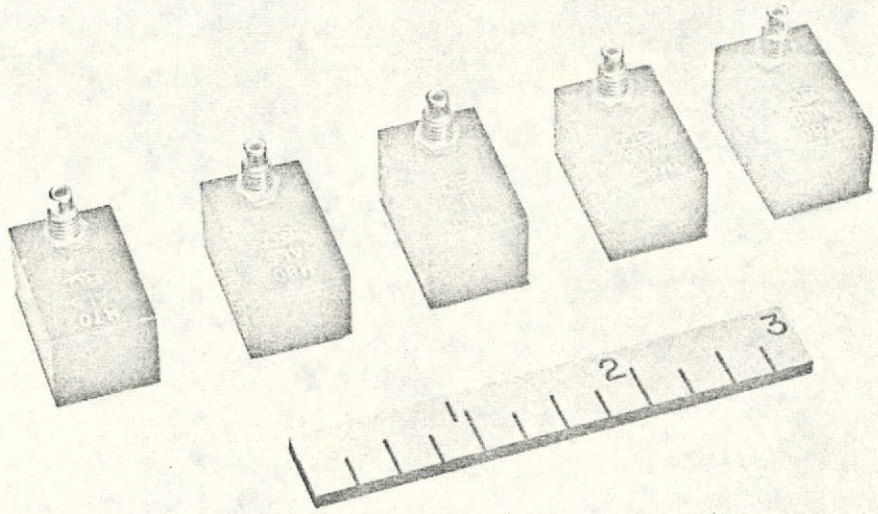

700-81-1622C

Figure 4. Shear Wave Transducers

To facilitate initial testing of the transducers, five test specimens, as shown in FIGURE 5, were fabricated from a 7075 aluminum sheet. These test specimens measured 2 x 36 inches, with individual thickness of 0.032, 0.050, 0.063, 0.090, and 0.125 inch. Simulated defects were introduced into each of the five test specimens to provide a means of monitoring the resolution capability of the ultrasonic beam being propagated by each of the transducers. One of the artificial defects consisted of a 0.047-inch diameter hole located one inch from the end of each specimen. The other defect consisted of a 0.002-inch-wide slot located one inch from the opposite end of each specimen.

To obtain basic data regarding optimum transducer frequency ranges and beam propagation angles, preliminary tests were initiated utilizing the aforementioned transducers and test specimens in conjunction with a Sperry Reflectoscope, Model 700. The results of these tests revealed that although defect detection was possible with all four beam propagation angles, the maximum transducer-to-defect distance at which detection was possible varied. It was shown from the tests utilizing the 60-, 70-, and 80-degree transducers that, as the beam propagation angle of the transducer increased, the transducer-to-flaw distance at which response was obtained also increased. It was concluded from these tests that the desired ultrasonic response was the result of a Rayleigh or surface wave rather than a shear wave. The transducers with the 45-degree propagation angle, which produces primarily all shear waves into the test structure, provided minimal distance capability.

As the beam propagation angle increased, a larger percentage of the ultrasonic energy introduced into the specimens was in the form of surface waves and increased distance coverage was achieved. These tests also revealed that the 10-MHz frequency range was generally more effective in the thinner specimens, 0.032-, and 0.050-inch, while the 5.0 MHz range was superior in the 0.063-, 0.090-, and 0.125-inch specimens. The maximum distance of detection as a function of beam propagation angles is illustrated in TABLE 1. Typical ultrasonic responses obtained during these tests, as displayed on the CRT presentation, are shown in FIGURE 6.

Based upon the data obtained from these initial shear-wave transducer tests, four 90-degree surface wave transducers, with frequency ranges of 2.25, 5.0, 10.0, and 15.0 MHz, were procured from Automation Industries, Inc. These four surface wave transducers are shown in FIGURE 7.

Utilizing the 90-degree surface wave transducers, supplemental tests were conducted on the artifically flawed test specimens to establish distance capability of these units. The results of these tests using the 2.25 and 5.0 MHz transducers are also shown in TABLE 1. No photographs of the CRT presentations during these tests were taken.

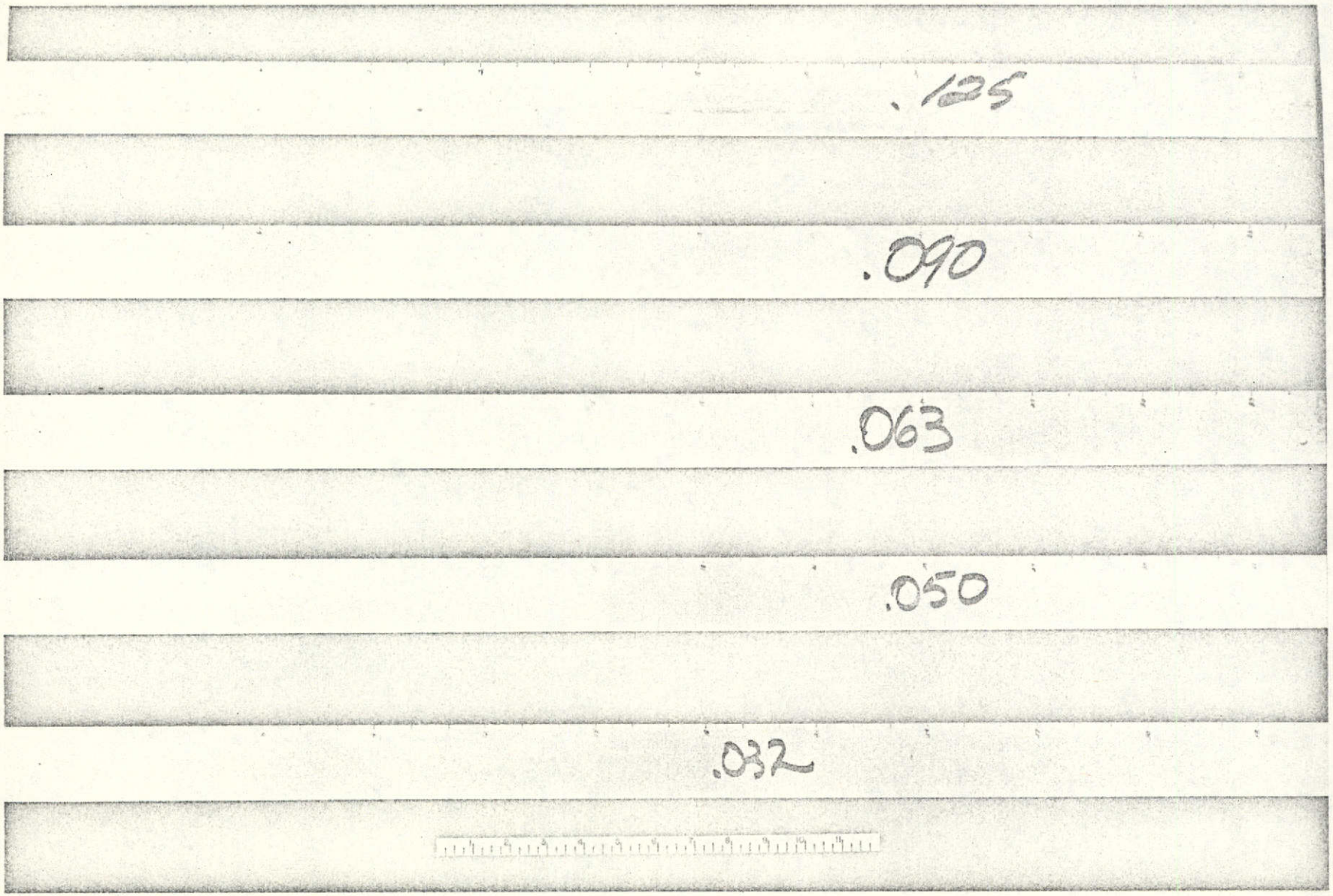

Figure 5. Resolution Capability Test Specimens

5.0 MHz, 45° TRANSDUCER

SPECIMEN THICKNESS

.032"

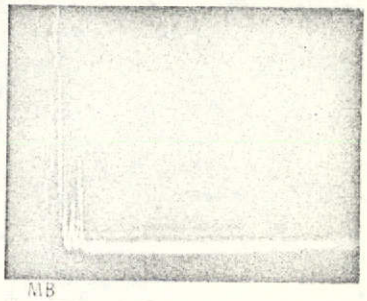

.050"

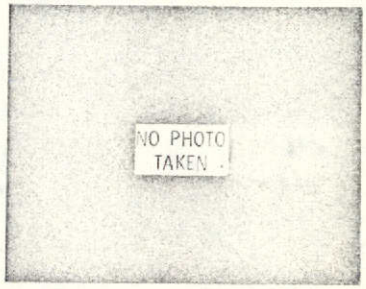

.063"

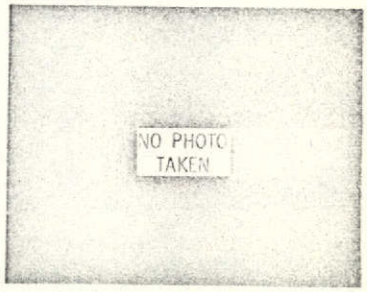

.090"

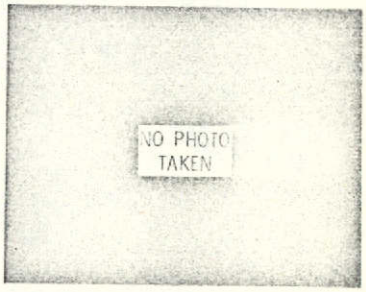

.125"

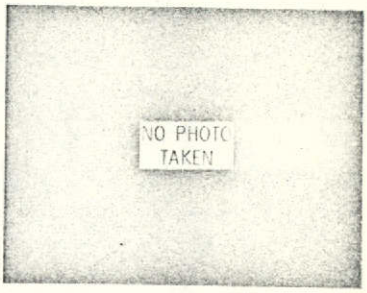

MB - MAIN BANG
H - HOLE
E - SPECIMEN EDGE

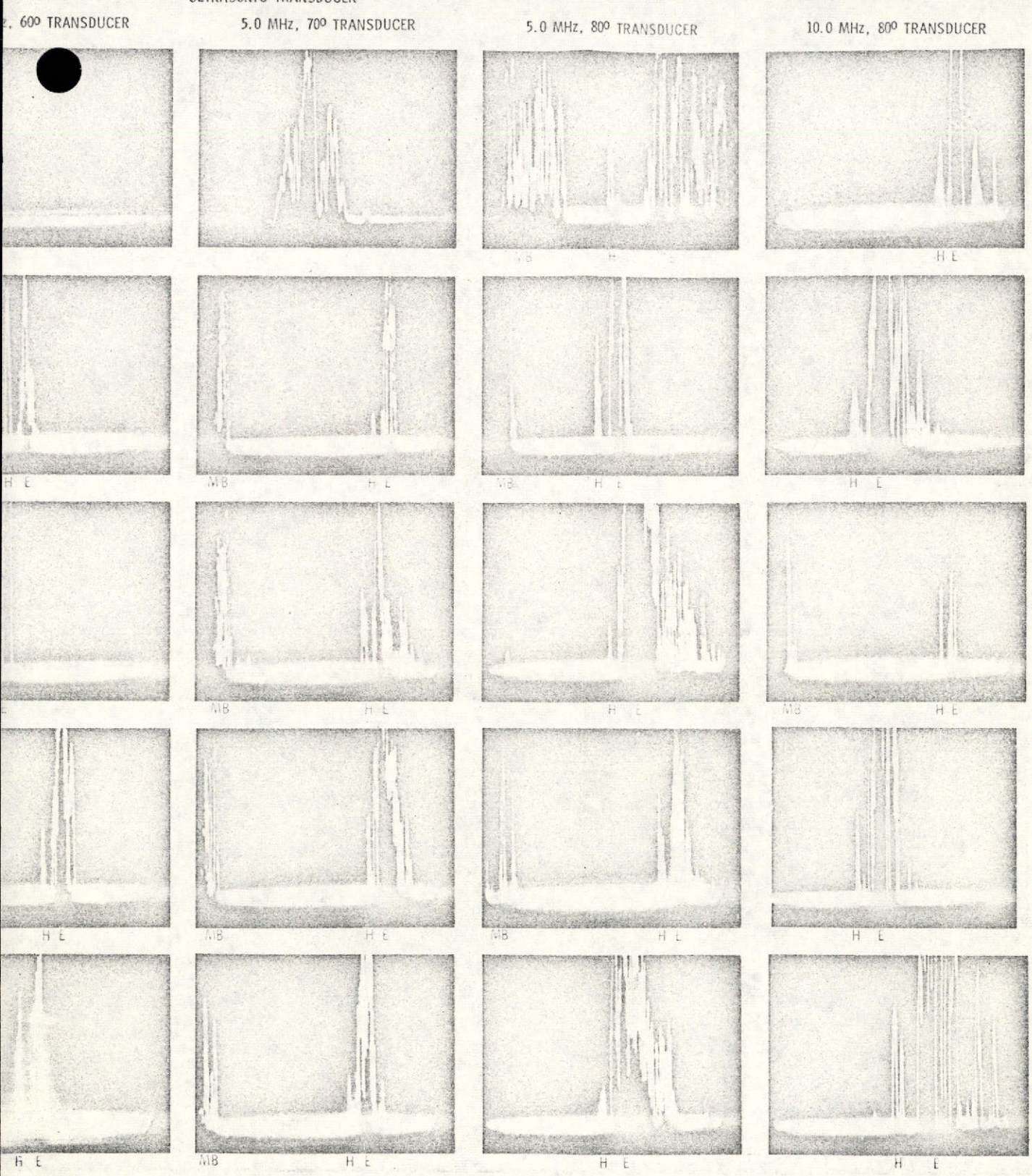

Figure 6. Typical Ultrasonic Responses From 0.047-Inch-Diameter Artificial Defect

Table 1. Detection Distance Versus Beam Propagation Angle

SPECIMEN THICKNESS (IN.)	DETECTION DISTANCE (INCHES) ULTRASONIC TRANSDUCER - PROPAGATION ANGLE					
	5 MHz 45 deg	5 MHz 60 deg	5 MHz 70 deg	5 MHz 80 deg	10 MHz 80 deg	2.25 MHz 5 MHz 90 deg
0.032	No response	No response	No response	2.75	15.5	36*
0.050	No response	4	9	6	15	36*
0.063	1	6	9.5	21	15	36*
0.090	No response	6	9.5	34	21	36*
0.125	1	5	9	21	15	36*

*Maximum specimen length

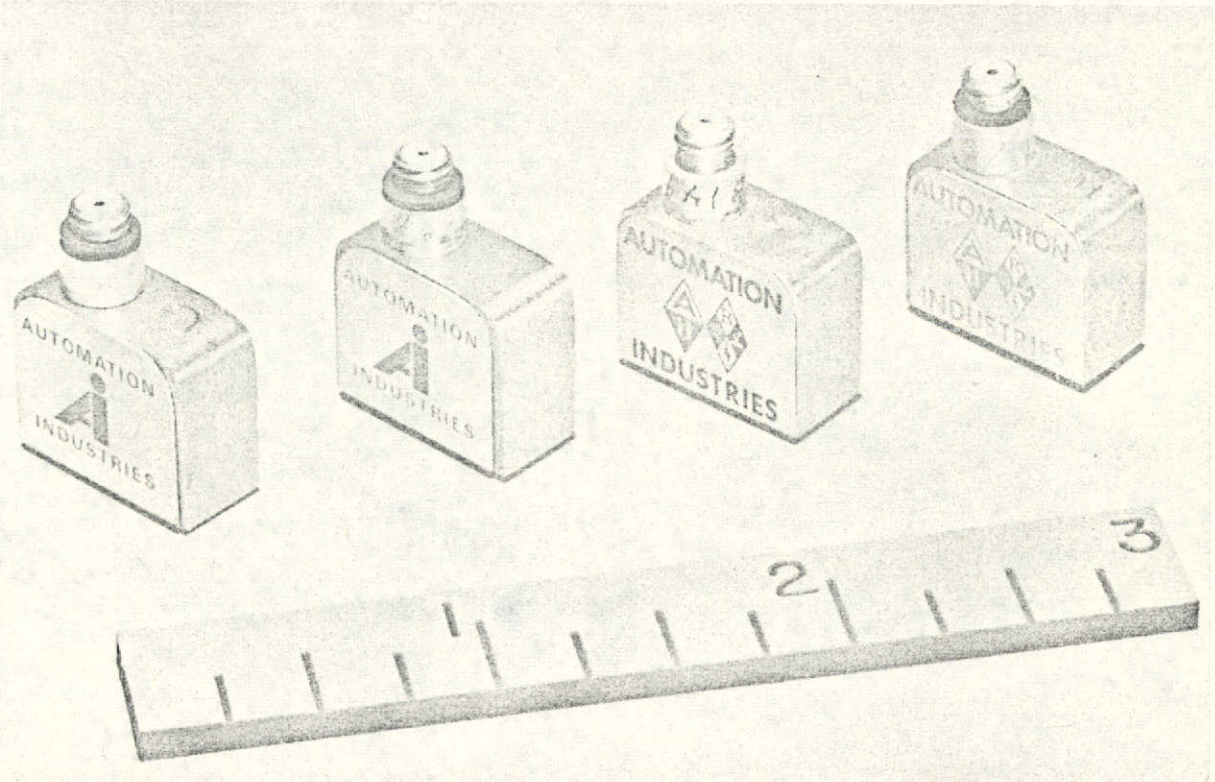

Figure 7. Surface Wave Transducers

Frequency Optimization

A new series of transducer evaluation tests utilizing the 0.002-inch slot was initiated to establish the optimum frequency range of the surface wave transducers with respect to the material thicknesses being investigated. The need to optimize beam angle was not required since all the surface wave transducers utilize a 90-degree beam propagation angle.

The results of these tests indicated that ultrasonic frequencies of 2.25 and 5.0 MHz provided excellent power, sensitivity, and resolution to detect flaws in the 2-inch by 36-inch aluminum test panels. The 10.0 and 15.0 MHz transducers suffered a large loss in all these parameters but still were able to detect the simulated flaws when placed in relatively close proximity. This loss of power in the 10.0 and 15.0 MHz surface wave transducers compared to the original shear wave units used in the initial tests was attributed to the reduced active element area of piezoelectric elements.

These tests demonstrated the ability to transmit an ultrasonic surface wave in simple structures. To establish extended distance capability, the transducers were used to monitor the edge of an aluminum strip from the opposite end. The sheet edge was clearly detectable at 10 feet (maximum sheet size) with less than 50 percent gain.

Utilizing the five aluminum specimens, tests were conducted with the transducers placed at 22 inches from the slot type flaws to obtain comparative data on the gain required at each frequency to achieve a 50-percent scope amplitude response from the flaws. The overall power requirements for each individual test were obtained by dividing the gain value by the percent of reject or dampening used. The results of these tests are listed in TABLE 2.

Table 2. Surface Wave Transducer Flaw Detection Capabilities (Gain)—Frequency Versus Material Thickness

Material Thickness (in.)	1.0 MHz, 90 deg	2.25 MHz, 90 deg	5.0 MHz, 90 deg	10.0 MHz, 90 deg	15.0 MHz, 90 deg
	Gain ÷ % Reject = Total Gain	Gain ÷ % Reject = Total Gain	Gain ÷ % Reject = Total Gain	Gain ÷ % Reject = Total Gain	Gain ÷ % Reject = Total Gain
0.032	No response	(1.0X1.4) ÷ 0.8 = 1.8	(1.0X1.2) ÷ 1.0 = 1.2	(10.0X8.0) ÷ 0.1 = 800	No response
0.050	No response	(.1X.8) ÷ 0.25 = 0.32	(.1X8.4) ÷ 0.25 = 3.3	(10.0X10.0) ÷ 0.1 = 1000	No response
0.063	No response	(.1X10.0) ÷ 1.0 = 1.0	(1.0X7.0) ÷ 1.0 = 7.0	No response	No response
0.090	No response	(.1X8.0) ÷ 0.5 = 1.6	(.1X10.0) ÷ 0.25 = 4.0	No response	No response
0.125	No response	(.1X10.0) ÷ 0.8 = 1.2	(1.0X5.0) ÷ 0.8 = 6.2	No response	No response

These tests verified the excellent power, sensitivity, and resolution capabilities of the 2.25 and 5.0 MHz transducers. As can be seen from the test results, the 2.25 MHz transducer has generally better power and distance capability. It should be noted, however, that the scope presentation is much cleaner when using the 5.0 MHz transducer, especially in the thinner specimen thickness (0.032- and 0.050-inch).

TRANSDUCER COUPLING EVALUATION

During the transducer coupling evaluation task, two separate groups of materials were evaluated: liquid couplants and semipermanent or bondable couplants. The primary consideration was the ability of the couplant materials to provide optimum signal coupling between the transducer and the test specimens. Results obtained from this task have indicated the liquid couplant that will be used for the laboratory tests and the bondable couplant that will be used for the tests to be conducted during the background noise evaluation.

Liquid Couplants

Prior to initiating the ultrasonic evaluation of the liquid couplants, a selection of various greases and viscous water-soluble solutions was obtained for evaluation. The initial selection of candidate liquid materials included Cakurd (an NR-developed viscous water-soluble solution), Krytox-240 grease, Kel-F-Oil, Halocarbon-1425-E Oil, tap water, and a dry lube film. To determine the ultrasonic coupling characteristics of these materials, a test was conducted using a 2.25-MHz, 90-degree surface wave transducer and an 0.125-inch thick aluminum plate. The transducer was placed at a standard position of 12 inches from the specimen edge, and tests were conducted with each couplant to determine its ultrasonic coupling ability by establishing the gain required to achieve an edge response equal to a set amplitude level on the CRT presentation. The ultrasonic responses obtained with the various couplants were basically similar with only slight variations in signal stability. These variations were attributed to couplant migration from the transducer to specimen interface. Tests also were conducted using no couplant; these resulted in good signal response, provided proper transducer-to-defect orientation and adequate hold-down pressure was achieved. A summary of the gain values required for each couplant material during these tests is shown in TABLE 3.

Since the results of these tests showed only minimal differences in the couplants tested, no additional materials were evaluated. It was surmised that if any reasonable degree of transducer-to-specimen coupling is achieved, an adequate surface wave can be generated. A general requirement was established during this evaluation that no couplant can be tolerated in the frontal area of the transducer, due to resultant damping of the surface wave propagated by the transducer.

Table 3. Ultrasonic Gain Values for Selected Liquid Couplants

Couplant	Scope Gain Settings	Edge Distance
Cakurd	1.0 x 1.0 = 1.0	12.0 in.
Krytox 240 Grease	0.1 x 6.0 = 0.6	12.0 in.
Kel-F No. 10	1.0 x 1.0 = 1.0	12.0 in.
Halocarbon 1425 E	0.1 x 9.0 = 0.9	12.0 in.
Water	1.0 x 3.8 = 3.8	12.0 in.
No couplant	0.1 x 2.9 = 0.29	12.0 in.

The liquid couplant material selected at the conclusion of these tests was the Cakurd viscous water-soluble solution. This decision was based on the fact that consistently good results have been obtained in the past at the Space Division with this material. In addition, the viscosity of the solution can be varied to meet the necessary test requirements, and post-test cleaning is simplified since the material is water-soluble.

Bonding Couplants

Since the limited number of available transducers could not be permanently attached to test specimens for this evaluation, candidate adhesive bondlines were fabricated on test plates to specific requirements. These requirements included stability, low temperature curing, low bondline thickness (approximately 0.003 to 0.005 inch), final bond line homogeneity, and a straight frontal edge of the bondline to allow liquid coupling between the transducer and adhesive. Based upon these basic adhesive requirements, a series of bondable materials was selected. The resultant list of materials for testing included epoxy polyamide, Epon 954, Lefkoweld 211, Lefkoweld 109, Stabond U-135, AG filled epoxy type 1, Class A, and AG filled epoxy type 2, Class A. A set of bondlines using these adhesives was prepared on aluminum plates for use as ultrasonic test specimens.

Pertinent data regarding adhesive curing characteristics are detailed in TABLE 4.

Table 4. Adhesive Curing Requirements

Couplant	Remarks
Epoxy Polyamide	Epon 828 and Versamid 115. 50% to 50% by weight, deairate in vacuum bell jar, 24-hour room temperate cure.
Epon 954	27 parts by weight of component A to 100 parts by weight of component B. Catalyze component A with component B, 24-hour room temperature cure.
Lefkoweld 109	Modified epoxy system, low temperature properties (-200 F to 250 F). 100 parts by weight of base component to 74 parts by weight of catalyst, 24-hour room temperature cure.
Lefkoweld 211	Modified epoxy system, elevated temperature properties (RT to 300 F). 3 component system. 100 parts base 0.77 parts LO-2 } by weight 9.9 parts LO-1 24-hour room temperature cure.
Stabond U-135	100 parts by weight of base to 12.5 parts by weight of catalyst. 12-hour room temperature cure followed by 4 hours at 160 F.
AG Epoxy, Class A, Type 1	Strain gage adhesive, MITHRA No. 200 (silver). Equal parts by weight of component A to component B. Spec requires cure for 16 hours at 175 F. Test sample-room temperature cure only.
AG Epoxy, Class A, Type 2	Epibond 8246 100 parts by weight of component A to 10 parts of component B. 5-day room temperature cure.

Prior to actual ultrasonic coupling tests, the thickness of the bondlines was measured, using a sheet metal micrometer. The thickness of each adhesive sample is shown in TABLE 5. As can be seen in the table, the Lefkoweld 211 and AG filled epoxy, Type 2 Class A samples were much thicker than considered desirable.

Table 5. Adhesive Thickness

Adhesive	Overall Thickness (in.)	Plate Thickness (in.)	Adhesive Thickness (in.)
Lefkoweld 211	0.155	0.131	0.024
Stabond U-135	0.136	0.127	0.004
Lefkoweld 109	0.138	0.127	0.011
Epon 954	0.138	0.127	0.011
Epoxy Polyamide No. 1	0.134	0.130	0.004
Epoxy Polyamide No. 2	0.136	0.130	0.006
AG Filled Epoxy Class A, Type 1	0.140	0.130	0.010
AG Filled Epoxy Class A, Type 2	0.171	0.131	0.040

Following the appropriate curing of the adhesive samples, a series of ultrasonic tests was conducted utilizing a 2.25-MHz transducer to determine the coupling characteristics of each adhesive. These tests were conducted by coupling between the transducer and the adhesive with the Cakurd liquid couplant selected earlier. Gain settings required to obtain a predetermined level of amplitude response from the plate edge were used as a measure of the signal coupling characteristics of each adhesive. The gain settings obtained during these tests are shown in TABLE 6. Based upon these test results, and the adhesive data obtained from the S-II technology study, the Lefkoweld 109 adhesive was selected as the optimum material to be used as the couplant during the acoustic tests that will be conducted during the remaining phase of this program. This material provided optimum bonding and signal coupling parameters.

TEST STRUCTURE FABRICATION

A machined waffle aluminum panel with intersecting ribs on four-inch centers was selected as the basic ultrasonic test structure (FIGURE 8). From this basic configuration, three specimen types were evolved.

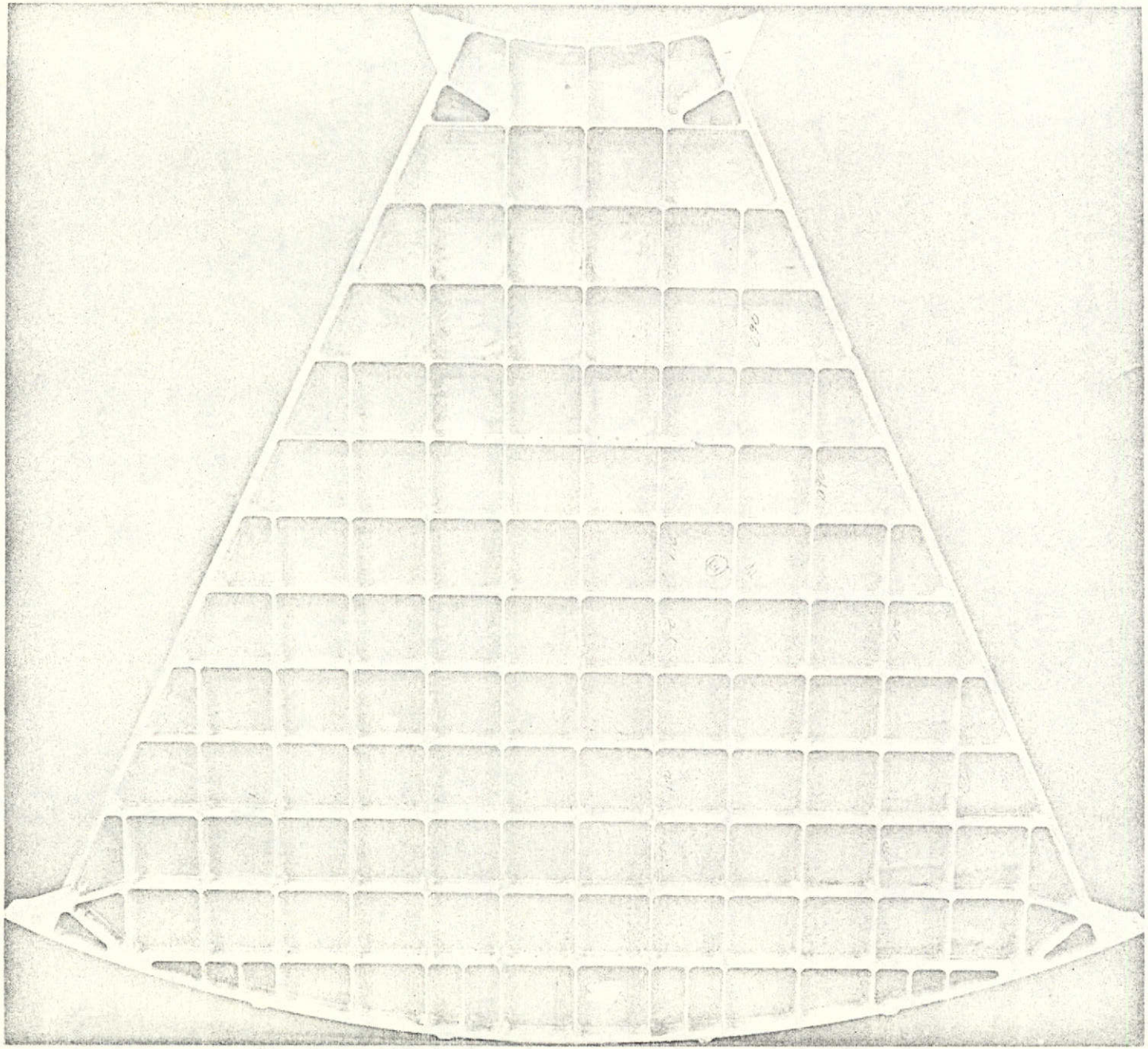

Figure 8. Basic Ultrasonic Test Structure

Table 6. Ultrasonic Gain Values for Selected Bondable Couplants

Adhesive	Scope Gain Settings	Edge Distance
Lefkoweld 211	0.1 x 3.6 = 0.36	8.75 in.
Stabond U-135	0.1 x 6.5 = 0.65	8.75 in.
Lefkoweld 109	0.1 x 1.1 = 0.11	8.75 in.
Epon 954	0.1 x 1.8 = 0.18	8.75 in.
Epoxy Polyamide	0.1 x 1.6 = 0.16	8.75 in.
Epoxy Polyamide	0.1 x 4.2 = 0.42	8.75 in.
AG-Epoxy Class A, Type 2	10.0 x 1.0 = 10.0	8.75 in.
AG-Epoxy Class A, Type 1	0.1 x 2.5 = 0.25	

Series A

FIGURE 9 depicts a series of five individual test specimens which comprise this set of test structures. Each specimen has a constant thickness base upon which are five integral, equally spaced, standing members four inches apart. Base plate thickness for the specimens was machined to be 0.030, 0.045, 0.060, 0.090, and 0.120 inches, respectively. These specimens were used to support the ultrasonic test program conducted during Task No. 5.

Specimen B

FIGURE 10 illustrates the test specimen that originally was to be used to determine the effect of surface roughness on Rayleigh or surface wave detection of flaws. Initial tests with this specimen revealed that the standing members had an adverse effect upon the ultrasonic response and negated the use of this specimen for the roughness tests. This panel was then reconfigured into five individual test specimens, measuring 22 inches in length with base plate thickness of 0.030, 0.045, 0.065, 0.090, and 0.125 inch, respectively. Three of the five original standing members were removed so that only two standing members 8 inches apart remained. These specimens, shown in FIGURE 11, were then utilized to establish the effect of standing members upon the propagation of Rayleigh or surface waves.

Roughness Specimen

Since the original specimen to be used for these tests was unsatisfactory, and was reconfigured for use in the standing member tests, an additional surface roughness test specimen, as shown in FIGURE 12, was

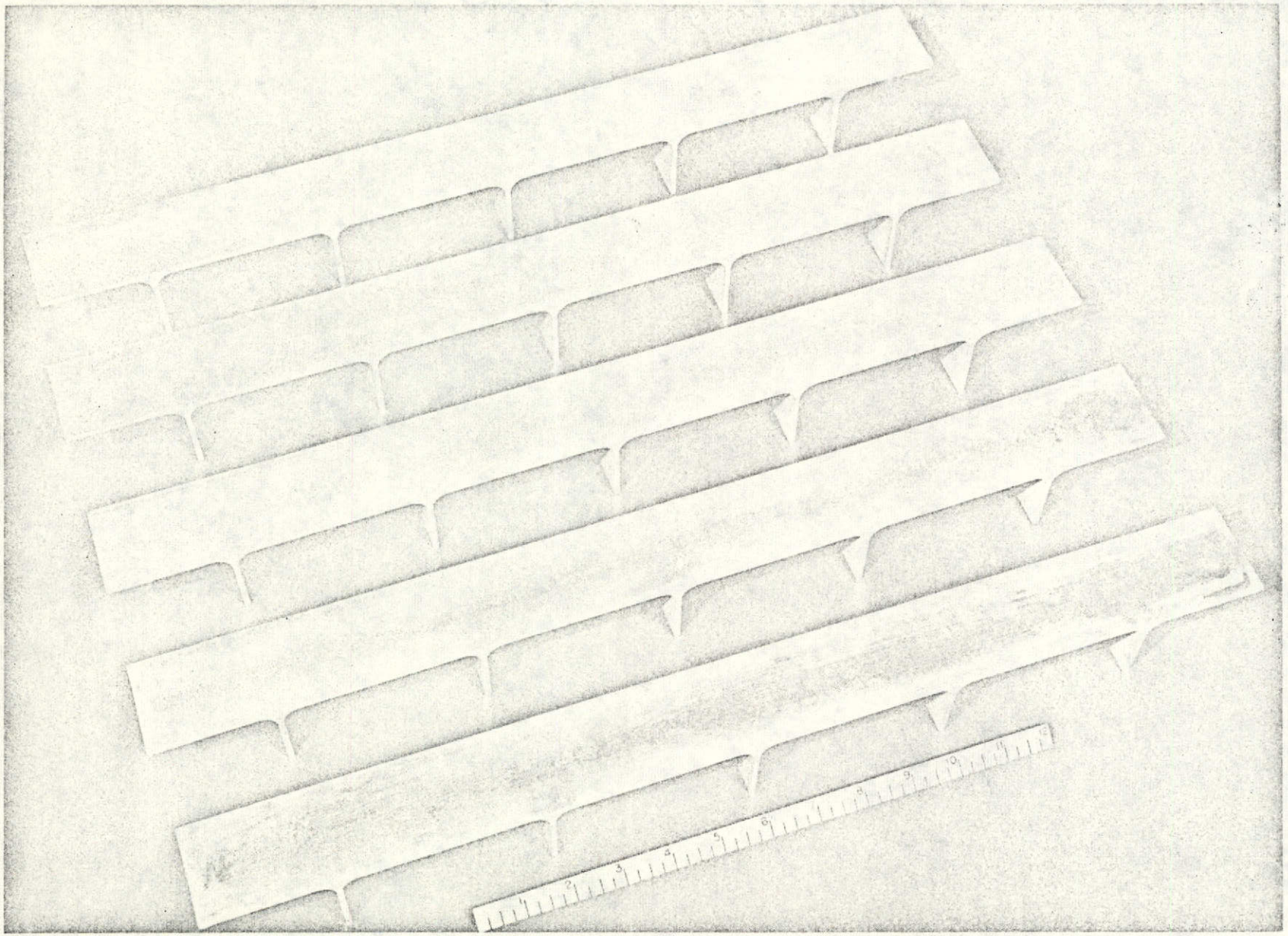

Figure 9. Flaw Detection Test Specimens

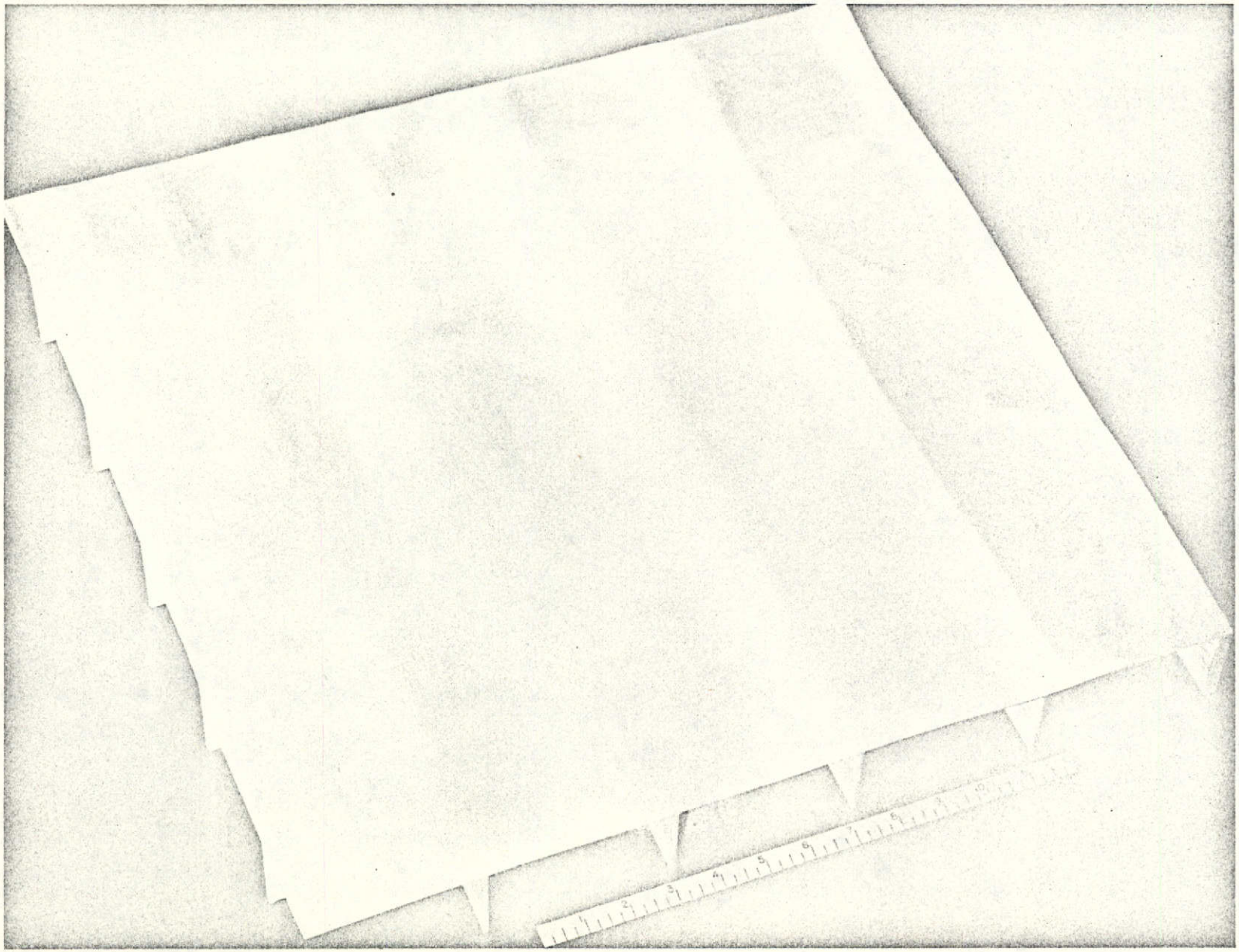

Figure 10. Surface Roughness Test Specimen (Initial Configuration)

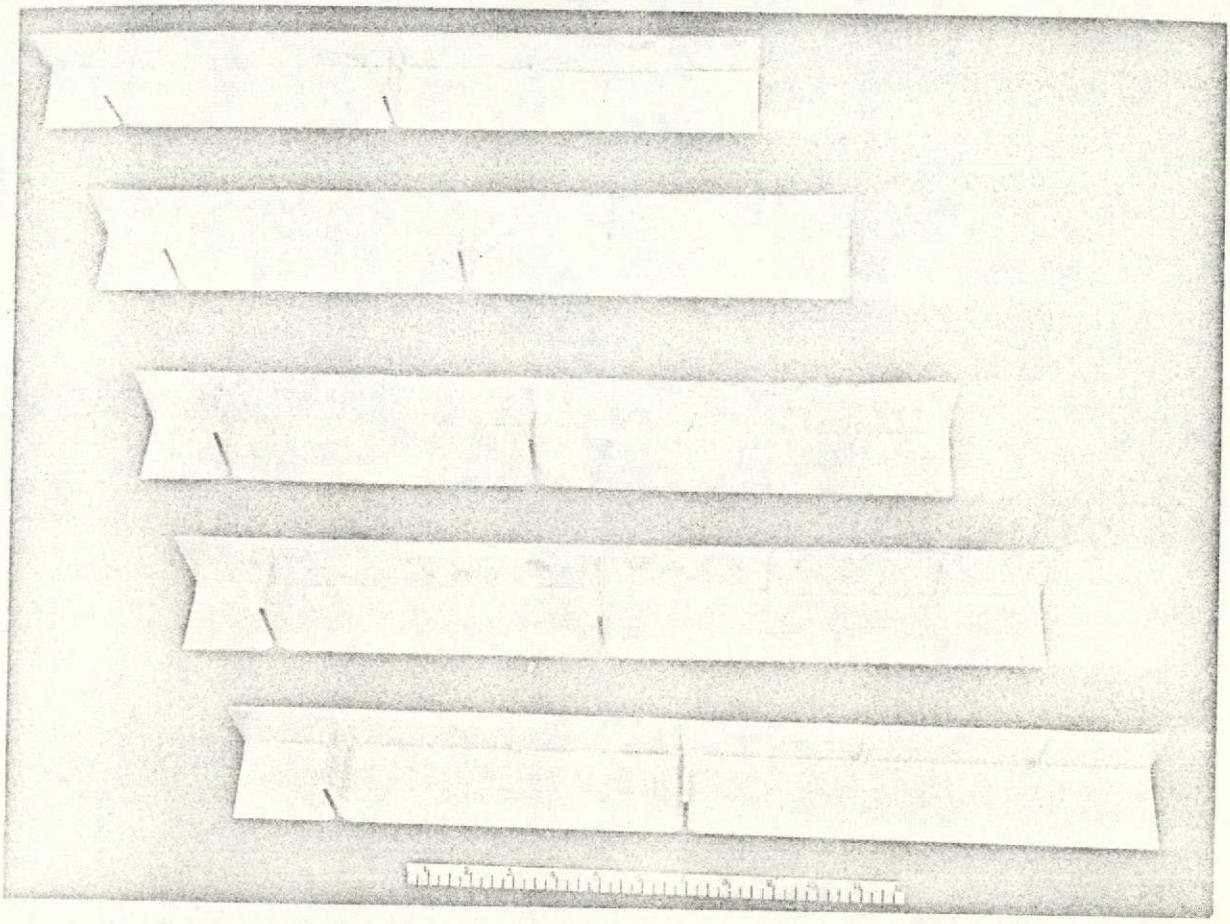

700-86-1056

Figure 11. Initial Standing Member Test Specimens (Two-Ribbed)

fabricated from an aluminum plate. The surface of this specimen, which measured 24 x 24 inches with a constant thickness of 0.135 inch, was machined to various finishes in five strips across the plate. The five finishes, shown in TABLE 7, are measured in microinches (RMS).

No flaws were introduced into this specimen. The specimen edge was utilized as the ultrasonic response point to determine the effect of surface roughness.

Specimen C

FIGURE 13 illustrates the first specimen type used to obtain data indicating the effect of high acoustic noise levels on the transmitted ultrasonic signal. No specific flaws were introduced and ultrasonic response was monitored from a standing member echo.

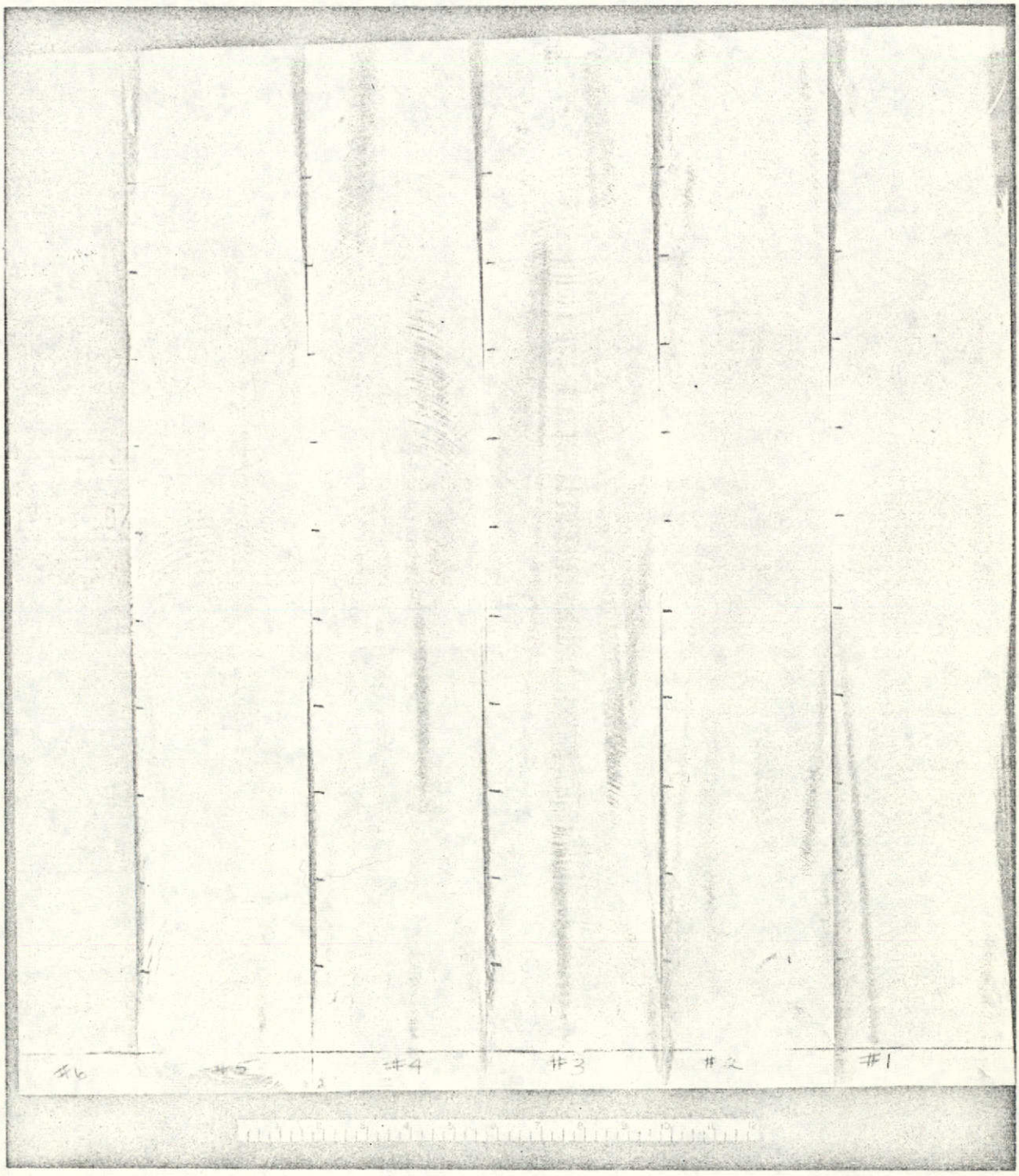

700-81-1657B

Figure 12. Surface Roughness Test Specimen (Final Configuration)

Table 7. Surface Finish Values

Finish Number	Roughness Value Microinches - RMS
1	60(-)
2	60(+)
3	75(+)
4	85(+)
5	100
6	5 (as received)

Fatigue Crack Specimens

As part of the flaw analysis task of the study, three fatigue crack specimens were fabricated using present fracture mechanics data to determine the flaw dimensions.

These specimens, as shown in FIGURE 14, were fabricated utilizing the following procedure:

1. Machine three specimens to final configuration from 2219 aluminum alloy 0.250-inch thick.

2. Introduce appropriate starter notches with a fly cutter.

3. Grow fatigue cracks to a predetermined size by the application of tensile loads.

4. Machine the specimens to remove the starter notches with the final thickness of each specimen to be 0.030, 0.065, and 0.125 inch.

Concurrently, three aluminum plate specimens of 0.030, 0.065, and 0.125 inch were prepared with a series of varying depth simulated slot defects. These test specimens are shown in FIGURE 15.

Flaw Introduction

Optimum flaw introduction methods include, primarily, those techniques that create "natural" cracks within the test areas of assemblies. Specific operations that must be performed in order to create natural cracks include cyclic bending and tension conditioning. These processes are time-consuming and extremely expensive when only a relatively few cracks are to be created. During the course of this study, for example, three natural cracks were initiated and grown, which required an average expenditure of 20 man-hours per crack.

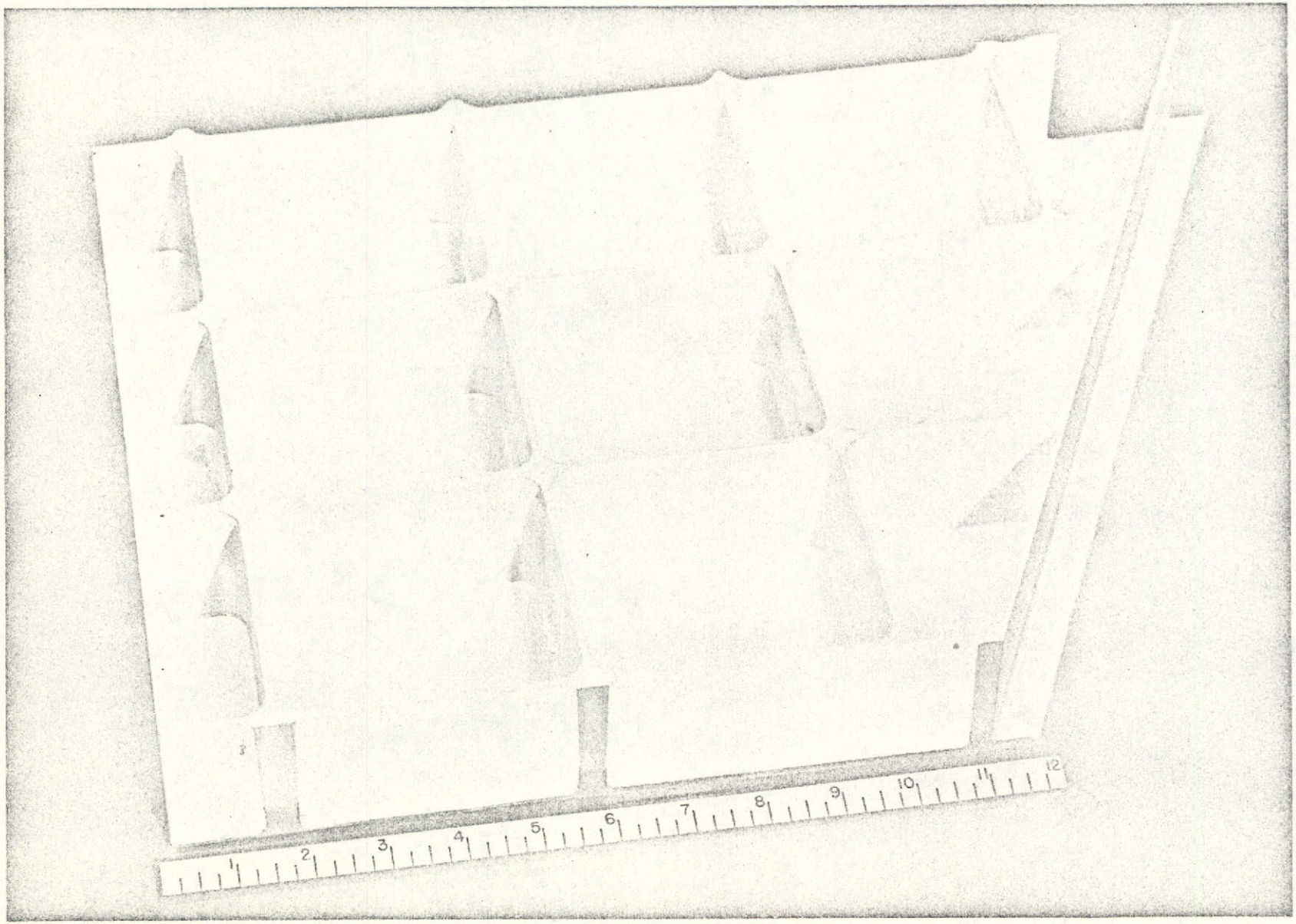

Figure 13. Acoustic Noise Test Specimen

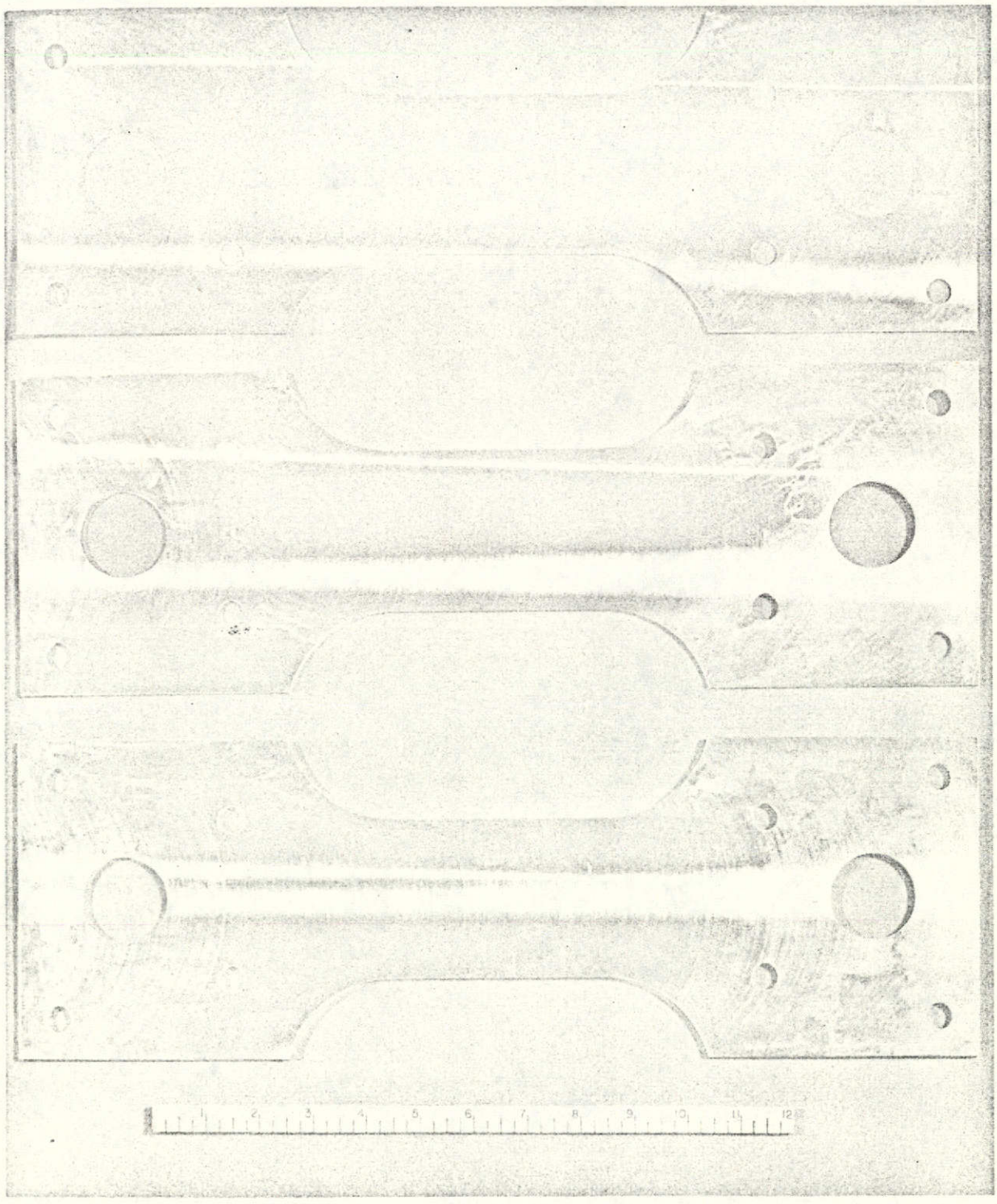

700-86-1048

Figure 14. Fatigue Crack Test Specimens

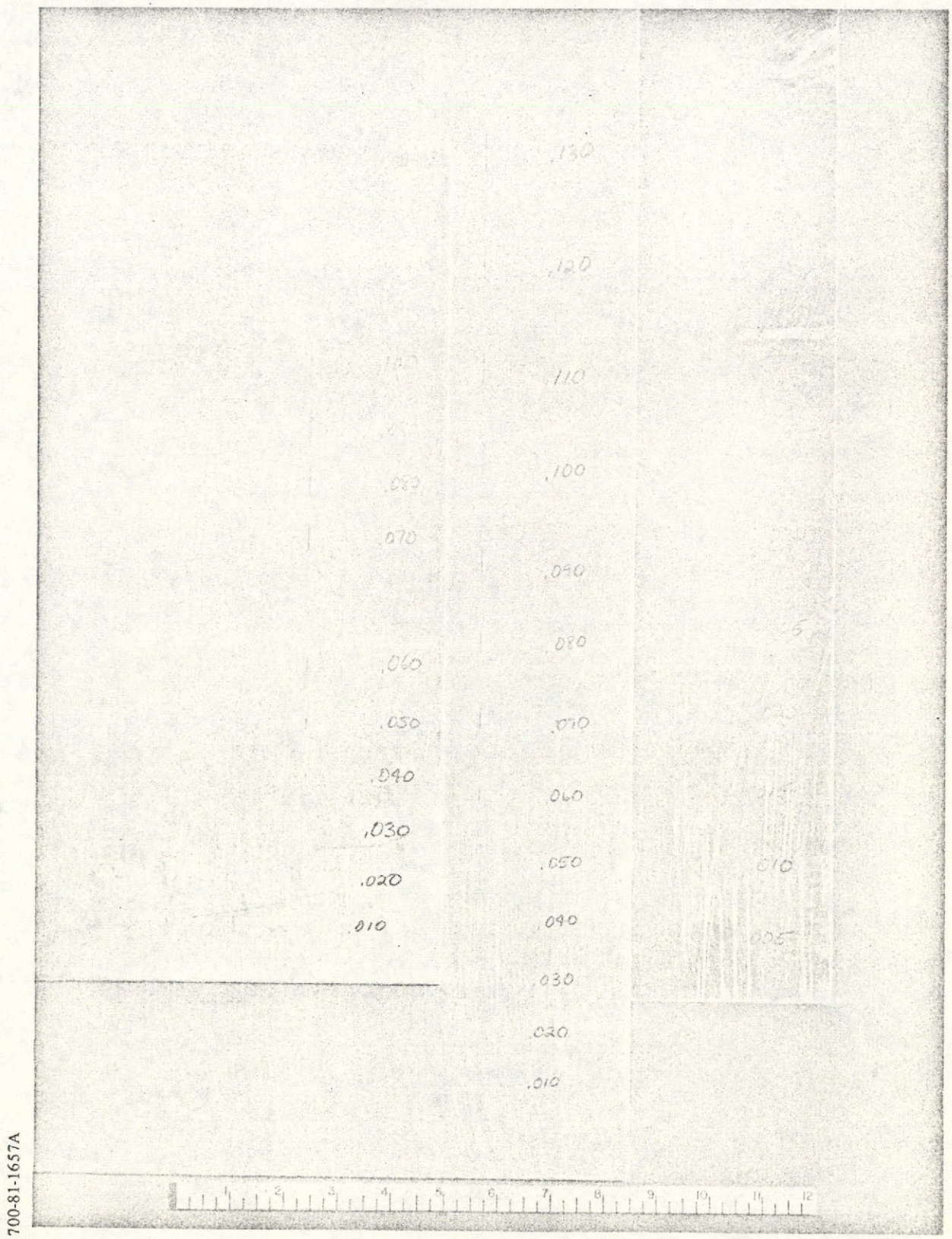

Figure 15. Aluminum Plate Test Specimens--Incremental Artificial Flaw Depths

Consideration was given to utilizing the electrical discharge machining method (ELOX) for producing artificial defects in the test pieces. This method has been used for many years to introduce artificial cracks in ultrasonic test standards for shear and surface wave inspection of tubing. Cracks produced by this method range in width from 0.010 to 0.015 inches. It was felt that for the purposes of this study, ELOX-produced cracks would be too wide. In service, shuttle structures would be subject to fatigue-type cracks that are inherently extremely tight, with both sides of the crack area in intimate contact with each other.

No other method for artifically producing cracks in aluminum was readily available or apparent. A small effort was undertaken within the scope of the study to produce an artificial crack from 0.001 to 0.003 inches in width using a mechanical approach. As a result of this effort, a cutter was developed that was able to continually produce cracks up to 0.0025 inches in width. The cutter was made from a 0.010-inch-thick, 1.25-inch-diameter cobalt steel disc. This disc was mounted on a preground magnetic chuck and reduced to a thickness of 0.002 inches using a special lathe. After thickness reduction; 78 teeth per inch were ground into the circumference of the disc with special machining techniques. A flute depth of 0.150 inches was attained. A low-velocity manual-feed technique was employed to produce the artificial cracks. The cutting compound used was a specially prepared combination of sperm oil and beeswax. FIGURE 16 shows a typical disc used as the cutter wheel.

FLAW ANALYSIS

Effort scheduled during this task was to establish specific locations of crack-like flaws and their dimensions for introduction into the test specimens. These criteria were to be primarily based upon current fracture mechanics data available for the Space Shuttle vehicle. Upon completion of this task, the flaws were to be introduced into the test specimens using the low velocity machining method described in the previous section.

The initial plan to establish flaw sizes from fracture mechanics analysis data proved impractical due to the lack of information as to the specific load factors applicable to the test structure. A decision was made to establish standard flaw sizes and configurations in laboratory-fabricated, fatigue-type specimens to correlate actual fatigue-crack response to artificial-crack response in the primary test specimens. In fact, ultrasonic calibration standards were fabricated to properly compare the basically unknown response from the artificial defects.

The first task in the revised approach involved the preparation of three actual fatigue-crack specimens using present fracture mechanics data to determine the flaw dimensions.

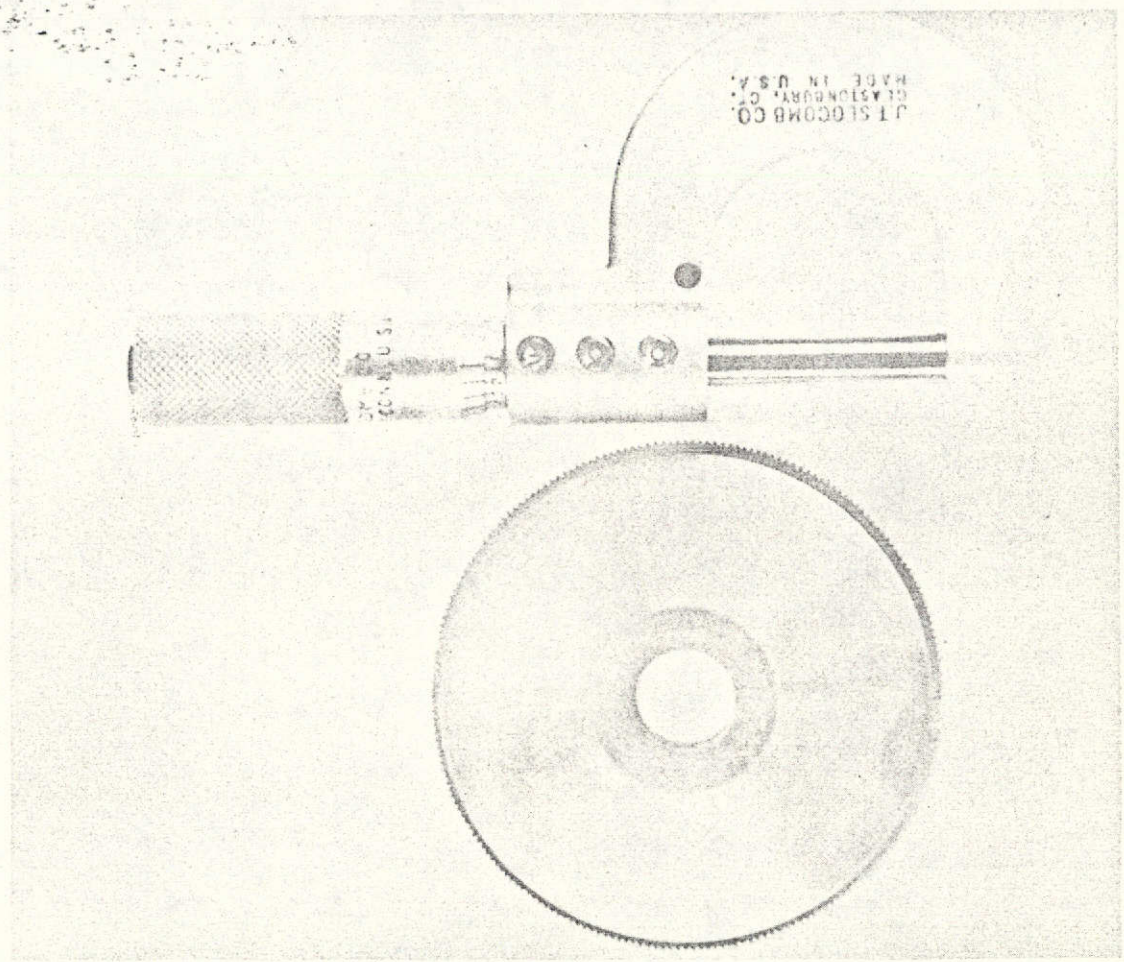

Figure 16. Artificial Flaw Cutter Wheel

Three, 0.249-inch-thick 2219 aluminum specimens were prepared for crack propagation by machining starter notches 0.040 inch deep and 0.600 inch wide (cutter radius = 1.14 inches). Cracks were initiated in the specimens through bending fatigue, followed by tension fatigue to a normalized crack size of 0.091 inch.

Upon completion of the crack growth phase, the three specimens were machined to the desired thicknesses of 0.125, 0.065, and 0.030 inch respectively. These fatigue crack specimens are shown in FIGURE 14.

Preliminary tests were conducted using these specimens to determine the response of surface waves to the fatigue cracks. The results of these tests confirmed the detectability of the natural fatigue cracks by ultrasonic surface waves. This ultrasonic response is shown in FIGURE 17, photos of the reflectoscope presentation obtained during these tests.

Concurrently, three aluminum specimens containing varying depth artificial flaws were prepared. These specimens, with thicknesses of 0.130, 0.097 and 0.033 inch, are shown in FIGURE 15.

0.030-INCH SPECIMEN

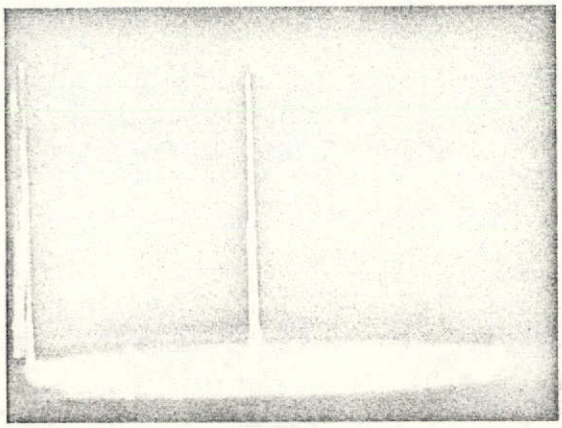

MB CK

0.065-INCH SPECIMEN

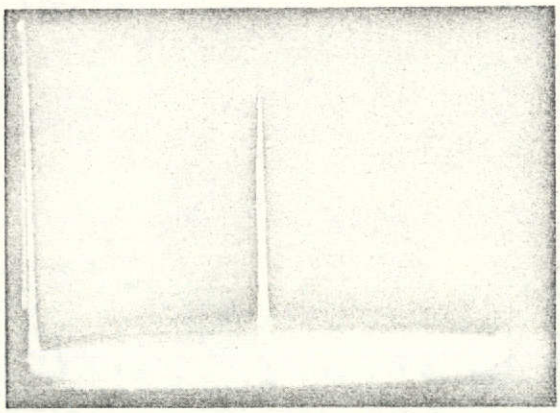

MB CK

0.125-INCH SPECIMEN

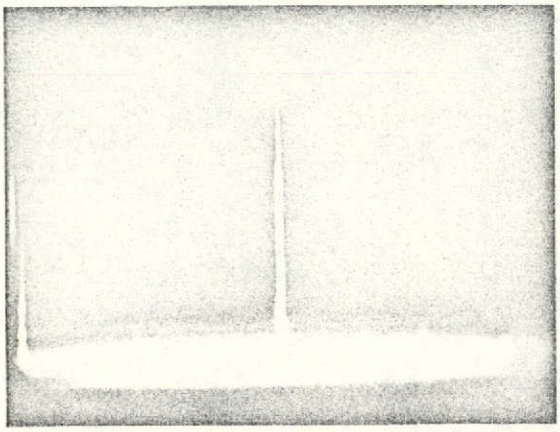

MB CK

LEGEND

MB: MAIN BANG
CK: CRACK

Figure 17. Ultrasonic Response From Fatigue Cracks

Upon completion of the fabrication of the various test specimens, ultrasonic tests were initiated to correlate the response of the natural fatigue cracks with those of the artificial flaws. These tests were conducted by determining the gain required to obtain a predetermined level of scope amplitude with the transducer placed at a constant 6-inch distance from the flaws. Several series of tests were conducted on each specimen to achieve consistent readings, since transducer orientation and coupling caused variances in response with respect to the gain values. The results of these tests are summarized in TABLES 8, 9, and 10.

Table 8. Low-Range Thickness Specimens

0.030-Inch Specimen and 0.030-Inch Dogbone				
	Scope Gain Settings			
Flaw Depth	Test 1	Test 2	Test 3	
Frequency	2.25	2.25	5.0	Average Values
0.035	3.8	2.2	0.10	2.0
0.030	3.0	2.6	0.10	1.9
0.025	3.8	1.1	0.10	2.0
0.020	3.4	1.9	0.10	1.8
0.015	5.8	1.7	0.16	2.6
0.010	8.5	3.5	0.25	4.1
0.005	4.0	16.0	0.89	7.0
Fatigue crack (F/C)	5.1	—	0.07	2.6

The results of the individual test series were then averaged to eliminate, to some degree, the variances. The average values were then plotted to determine the artificial flaw size which equaled the natural fatigue crack with respect to ultrasonic response. These graphs are shown in FIGURES 18, 19, and 20.

The artificial flaw sizes for each specimen thickness were then used to generate a curve that would serve as a means of determining appropriate artificial flaw depth for any specimen with a thickness between 0.010 and 0.130 inch. This final graph is shown in FIGURE 21.

Table 9. Mid-Range Thickness Specimens

0.098-Inch Plate and 0.065-Inch Dogbone				
Flaw Depth	Scope Gain Settings			Average Values
	Test 1	Test 2	Test 3	
Frequency	5.0	5.0	5.0	
0.100	0.10	0.10	0.10	0.10
0.090	0.10	0.10	0.10	0.10
0.080	0.13	0.10	0.10	0.11
0.070	0.11	0.10	0.10	0.10
0.060	0.15	0.10	0.10	0.11
0.050	0.17	0.10	0.10	0.12
0.040	0.17	0.10	0.10	0.12
0.030	0.36	0.11	0.10	0.18
0.020	0.18	0.18	0.26	0.21
0.010	0.38	0.30	0.26	0.31
F/C	0.16	0.15	0.20	0.17

Table 10. High-Range Thickness Specimens

0.130-Inch Plate and 0.116-Inch Dogbone				
Flaw Depth	Scope Gain Settings			Average Values
	Test 1	Test 2	Test 3	
Frequency	2.25	2.25	5.0	
0.130	0.20	0.16	0.10	0.18
0.120	0.22	0.18	0.10	0.17
0.110	0.34	0.21	0.10	0.21
0.100	0.22	0.15	0.10	0.19
0.090	0.36	0.16	0.10	0.21
0.080	0.40	0.24	0.10	0.25
0.070	0.38	0.26	0.10	0.25
0.060	0.38	0.36	0.10	0.28
0.050	0.40	0.52	0.10	0.34
0.040	0.42	0.56	0.10	0.36
0.030	0.45	0.74	0.10	0.43
0.020	0.43	0.93	0.13	0.49
0.010	0.92	1.23	0.14	0.86
F/C	0.56	0.75	0.08	0.29

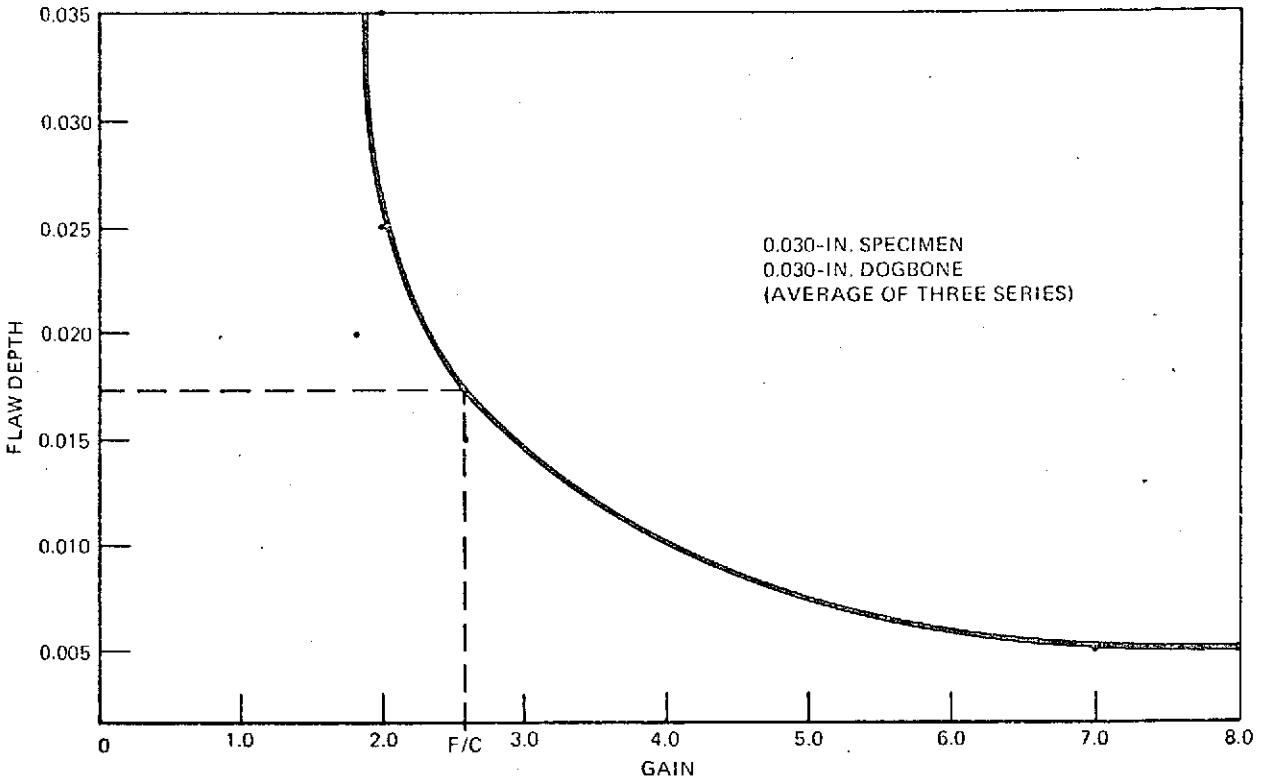

Figure 18. Ultrasonic Response Vs. Flaw Depth for Low-Range Thickness Specimens

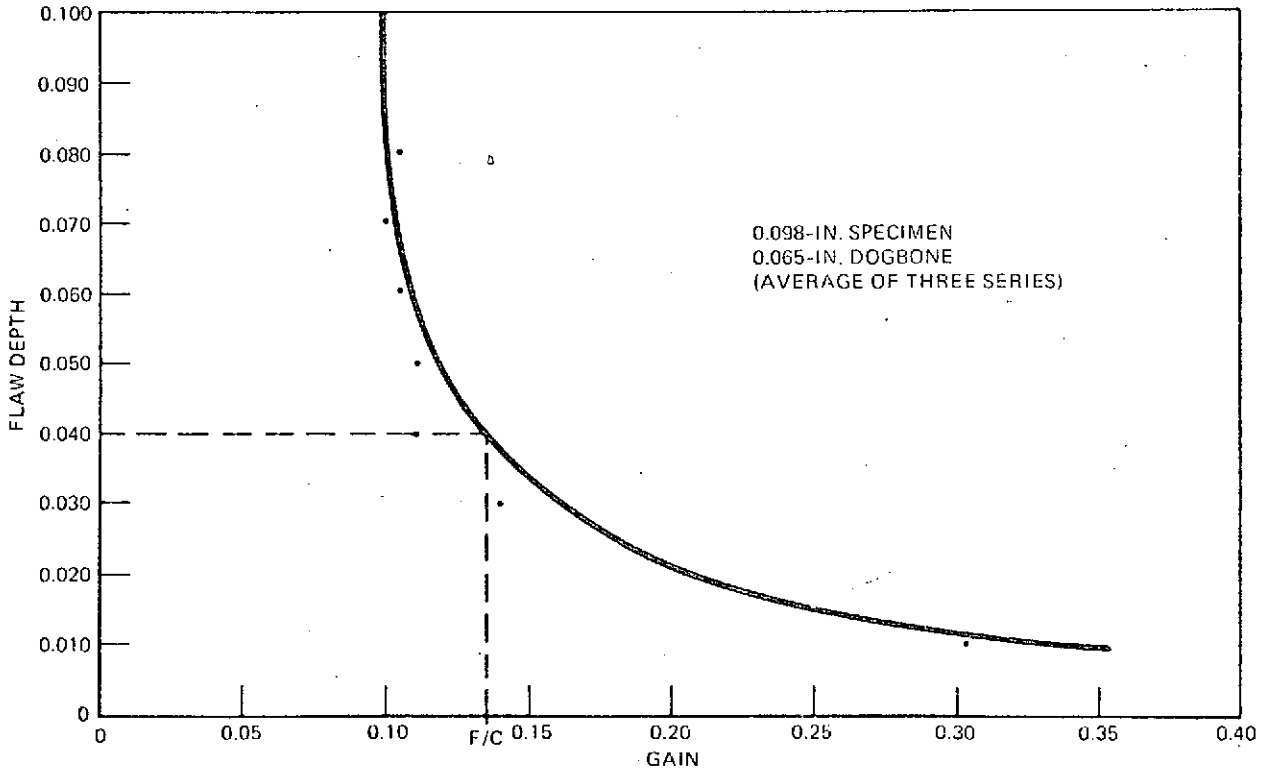

Figure 19. Ultrasonic Response Vs. Flaw Depth for Mid-Range Thickness Specimens

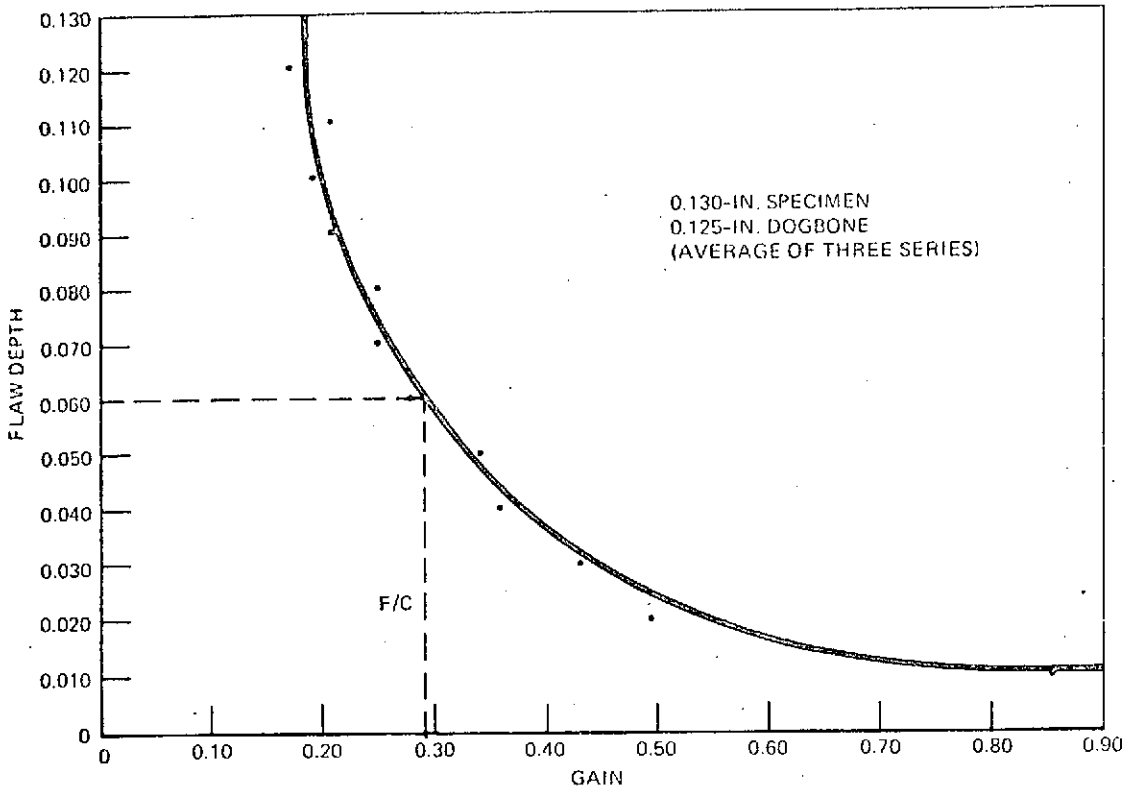

Figure 20. Ultrasonic Response Vs. Flaw Depth for High-Range Thickness Specimens

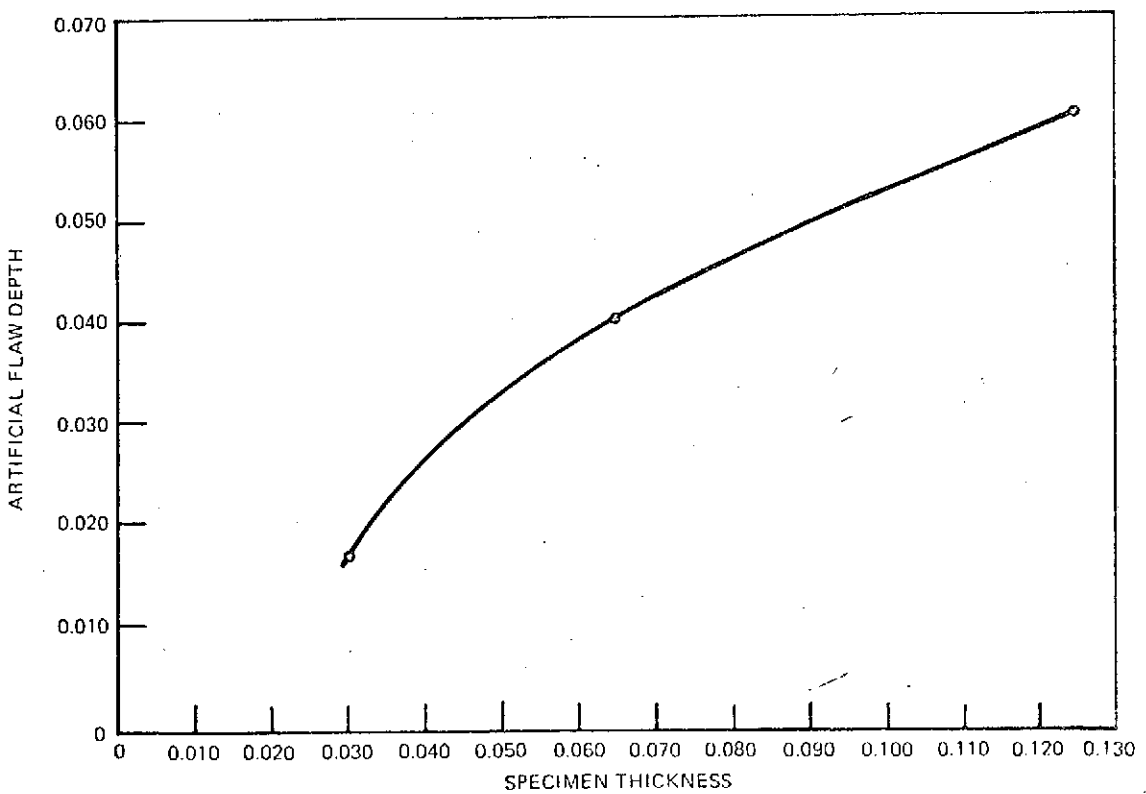

Figure 21. Artificial Flaw Depth Vs. Specimen Thickness

Upon completion of the ultrasonic testing of the specimens utilized during this task, destructive analysis was performed to verify the actual size of the fatigue cracks. The dimensions of the cracks in the three specimens are shown in TABLE 11. The shape and dimensions of the fatigue cracks after fracture of the specimen are shown in FIGURES 22, 23 and 24.

Table 11. Actual Fatigue Crack Size

Specimen (In.)	Crack Width (Front) (In.)	Crack Width (Back) (In.)	Crack Depth (In.)
0.116	0.515	—	0.071
0.065	0.405	0.106	0.065
0.030	0.363	0.262	0.030

ULTRASONIC TESTING

Initial Noise Test

Although shown in the study schedule as part of the Task 5 ultrasonic testing, a series of initial noise tests were conducted as a supplement to the Task 1 transducer evaluation on four surface wave transducers. The objective of these tests was to determine if the background noise environment had an adverse effect upon the ultrasonic response at any of the specific frequencies at which the subject transducers operated.

These tests were conducted by attaching the appropriate ultrasonic transducers to the test specimen, as shown in FIGURE 13, by the use of F88 CCP dental adhesive. The test specimen was subsequently suspended in the reverberation chamber of the LTV acoustic system. A pink noise environment was then introduced into the chamber at levels of 140 db, 145 db, 150 db, 155 db, and 160 db. The spectrum input, as shown in Appendix A, at each of these levels was monitored by a microphone mounted within the chamber. The ultrasonic response obtained from the first standing member in the path of ultrasonic beam was recorded directly from the reflectoscope CRT presentation through the use of a 35-mm Mitchell camera with a time lapse attachment and counter. The responses of the ultrasonic wave front, as recorded from the CRT presentations, are shown in FIGURE 25. Monitoring of the first standing member with the 10.0 and 15.0 MHz transducers could not be achieved due to the inherent low transmittive power of these units. However, the initial pulse of these transducers was monitored. No record of the 15.0 MHz transducer is available due to film processing difficulties; however, visual observation of the results during testing were similar to those of the 10.0 MHz transducer.

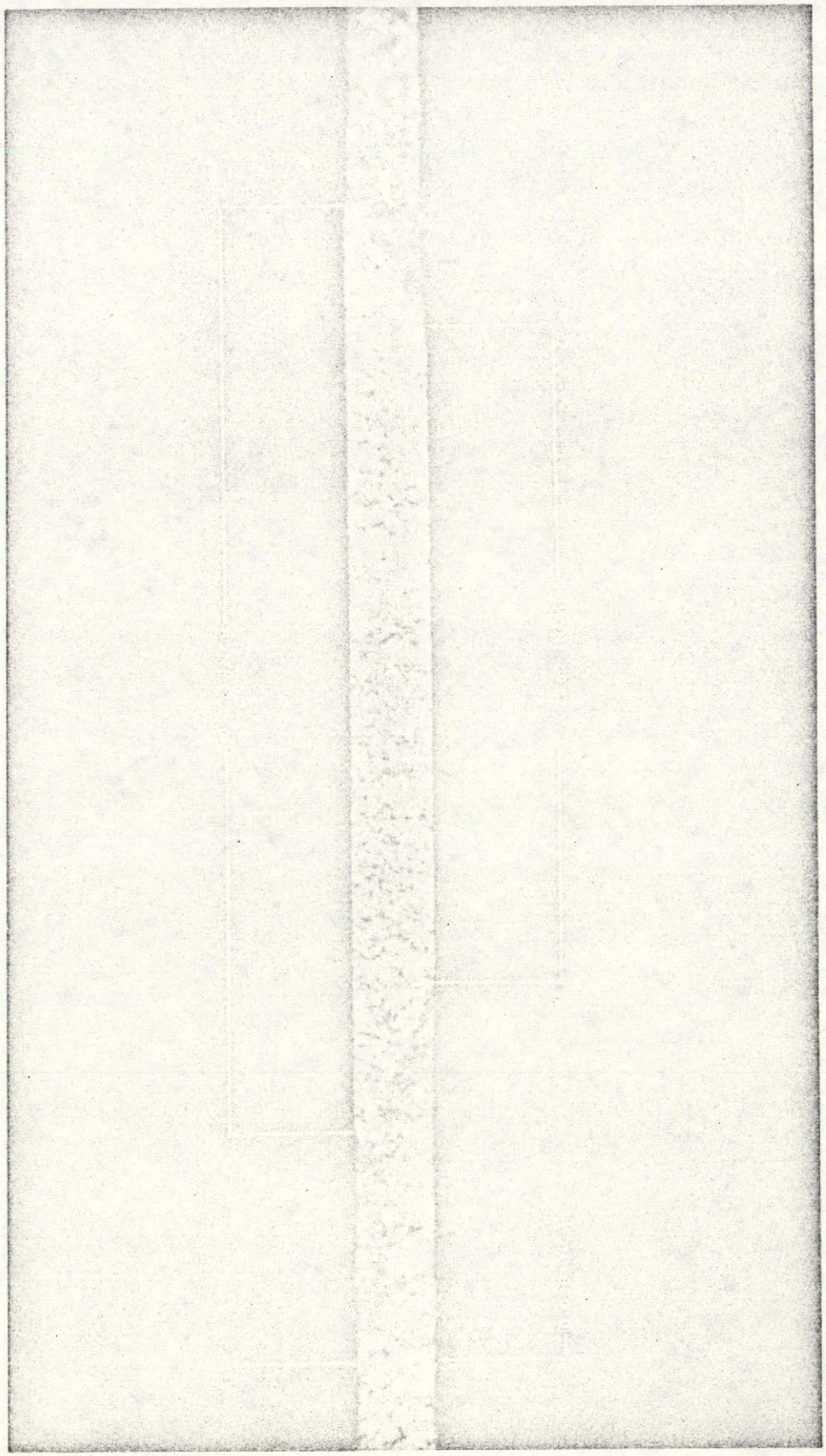

Figure 22. Fatigue Crack Cross Section—0.030-Inch Specimen

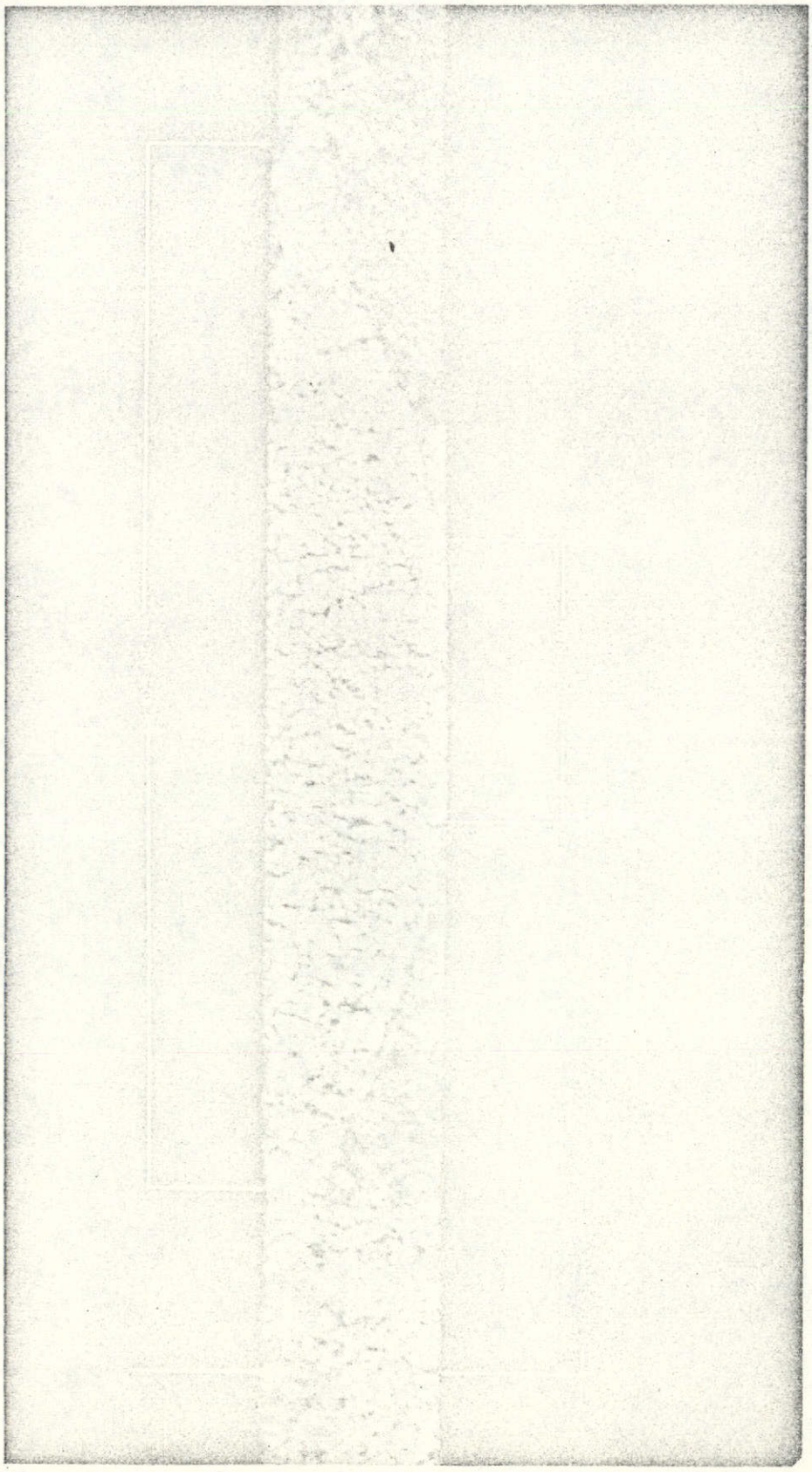

Figure 23. Fatigue Crack Cross Section—0.065-Inch Specimen

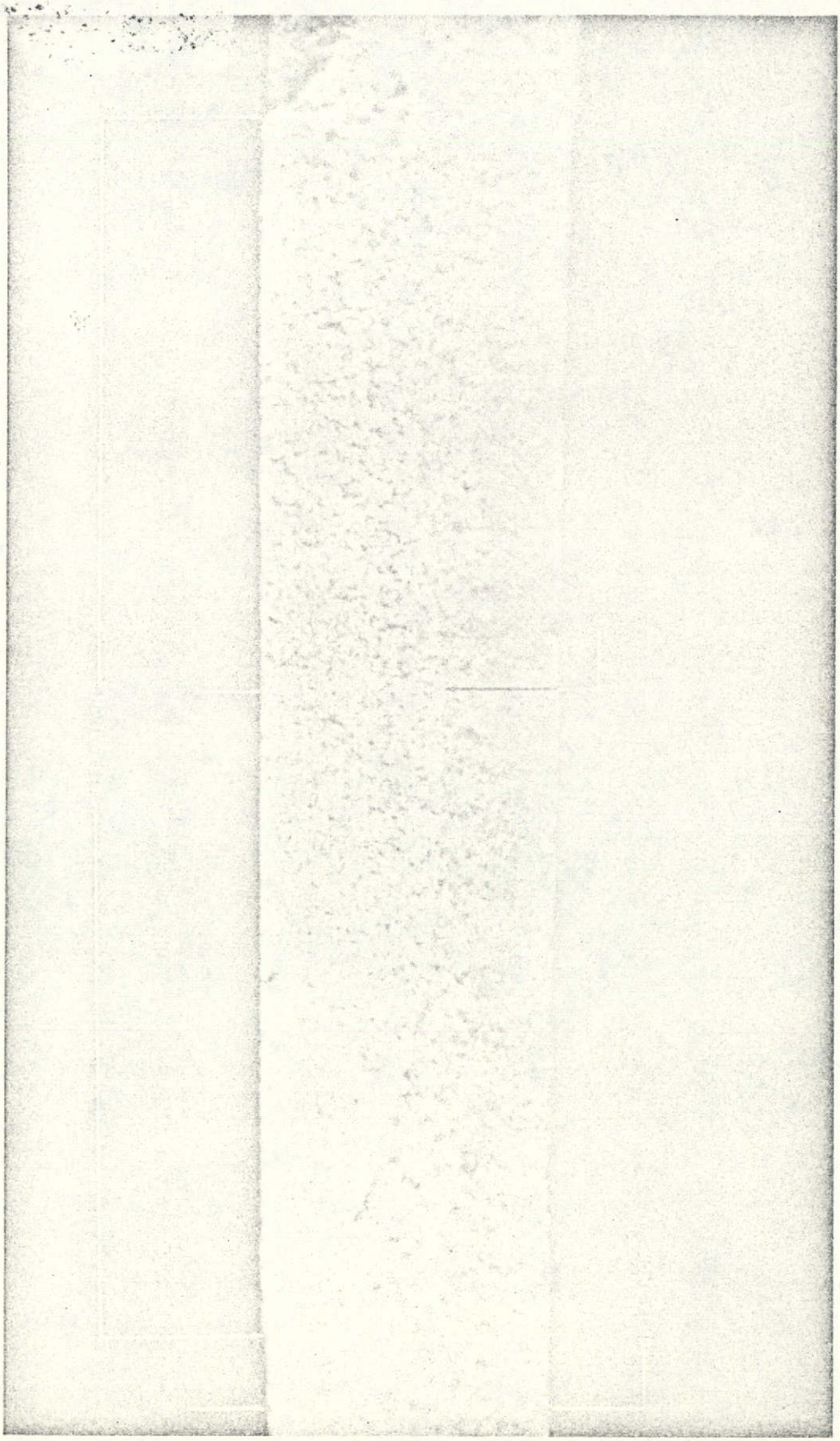

Figure 24. Fatigue Crack Cross Section—0.116-Inch Specimen

Roughness Test

A series of tests were conducted on the specimen shown in FIGURE 12 to determine the effect of various surface finishes upon the propagation of ultrasonic surface waves. During these tests, the 2.25 and 5.0 MHz transducers were maintained at a constant 20-inch distance from the specimen edge, which was used as the monitoring echo. The objective of the tests was to establish the gain requirements necessary at each degree of finish to achieve a predetermined amplitude response from the edge of the specimen.

The gain values obtained at both the 2.25 and 5.0 MHz frequencies are shown in TABLE 12. The values obtained were averaged to allow graphic presentation of the results, which are shown in FIGURE 26. As can be seen from the graph, a direct relatioship between roughness and gain requirements could not be achieved. This was postulated to be the result of varying coupling of the transducer to specimen surface. A more stable and consistently repeatable signal could be obtained on the roughened finishes as compared to the as-rolled and finer ones. The conclusions drawn from these tests is that a surface finish of 100 microinches RMS or less has only minimal effects upon surface wave propagation.

Thickness Test

The effort conducted in support of this task was to establish the transducer type and frequency range appropriate for the various material thicknesses being evaluated during this study. As shown during the early testing phases, the transducer types to be used on all the various thicknesses were of the type that yielded a surface wave mode of ultrasonic propagation. During the frequency optimization and flaw analysis tasks, data regarding the appropriate frequencies for use on the various individual material thicknesses was generated.

Table 12. Roughness Test Data-Surface Finish Versus Gain

Surface Finish Value	Scope Gain Settings						Average Gain Value
	2.25 MHz			5.0 MHz			
	Test 1	Test 2	Test 3	Test 4	Test 5	Test 6	
6	0.36	0.32	0.13	0.88	0.43	0.08	0.37
1	0.54	0.45	0.20	0.99	0.58	0.53	0.55
2	0.54	0.36	0.18	0.60	0.53	0.42	0.44
3	0.30	0.20	0.10	0.65	0.44	0.27	0.33
4	0.40	0.29	0.25	0.48	0.84	0.27	0.42
5	0.38	0.25	0.13	1.20	1.40	1.00	0.73

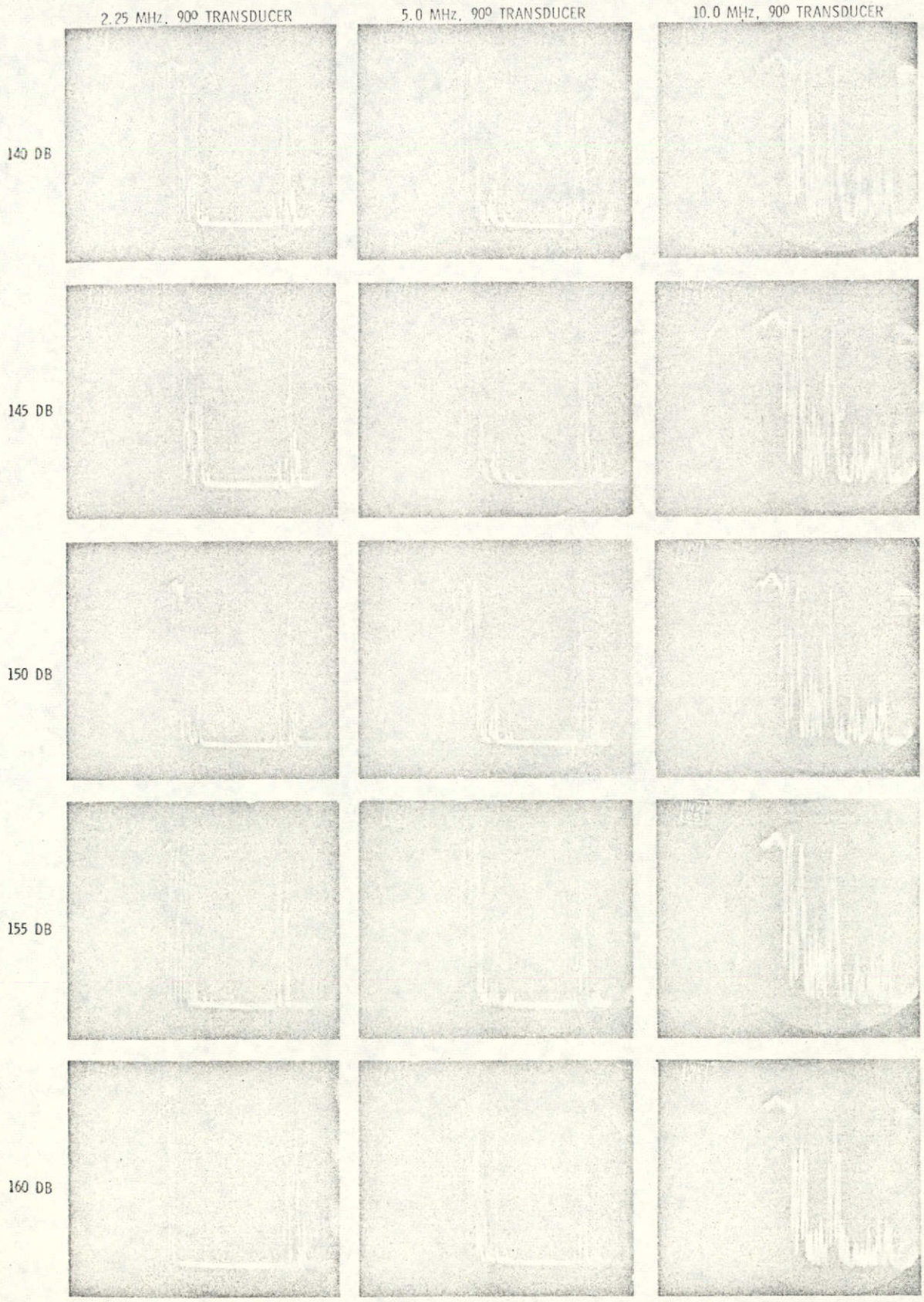

Figure 25. Ultrasonic Signals During A High Acoustic Noise Environment

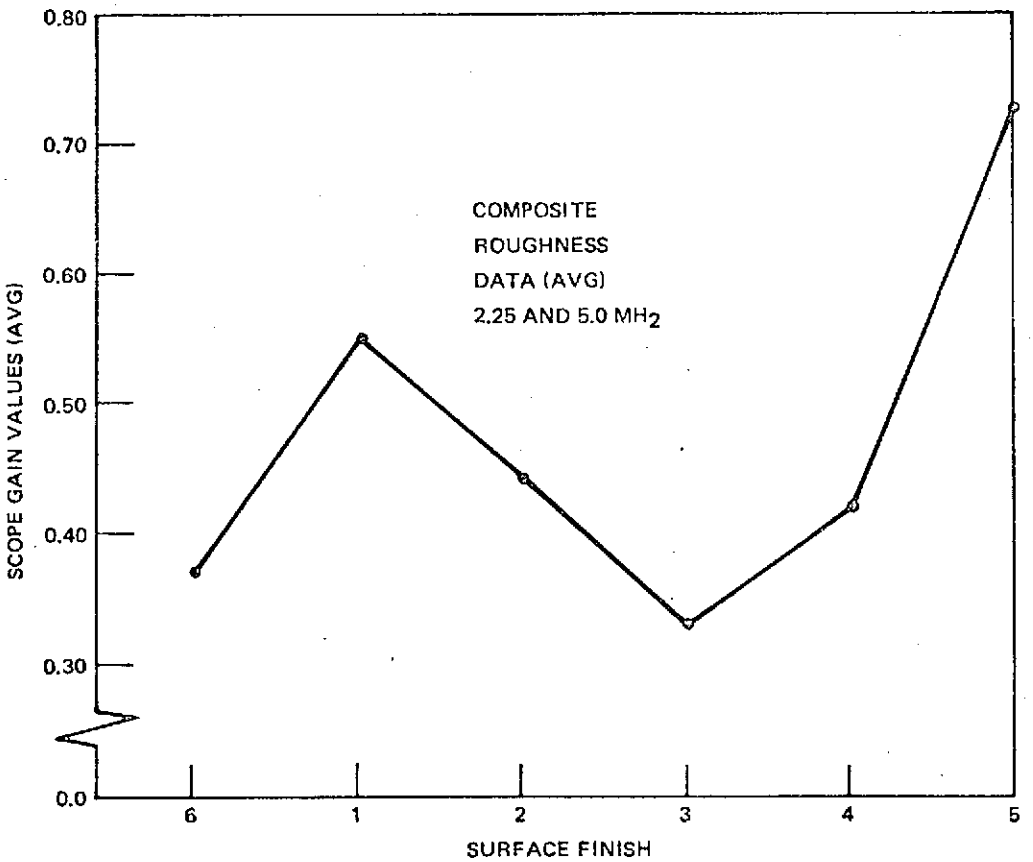

Figure 26. Gain Vs. Surface Finish—Average Values

The frequency optimization tests conducted in support of Task 1, the results of which are shown in the matrix in TABLE 2, established the 2.25 and 5.0 MHz frequencies as the ranges that provided the best results among those tested. Although both frequencies exhibited ample power and resolution capability for the material thicknesses being evaluated, the 5.0-MHz transducer yielded a cleaner scope presentation and slightly better resolution in the 0.032- and 0.050-inch specimens. This fact was postulated as being a result of the wavelength of the sound beam being propagated into the specimens. It should be noted that either frequency range would have provided the desired results; however, the 5.0-MHz range was selected for use with specimens less than 0.050-inch thick. It was felt this improved scope presentation would be advantageous on the thinner specimens during the standing member and final acoustic tests.

Standing Member Test

In order to determine the effect of standing members upon the ultrasonic surface waves, tests were conducted on two similarly configured test specimens, one set with two vertical ribs and the other with five vertical ribs. These test specimens are shown in FIGURES 11 and 9. The objective

was to determine the effect the ribs would have with respect to monitoring the opposite edge of the test specimen using 2.25 and 5.0 MHz surface wave transducers. The transducers were placed at two locations on each specimen, on one end of the panel so the ribs stood in the path of beam propagation and the other with the transducer positioned on the smooth surface opposite where the ribs intersected the base material.

These tests revealed that regardless of whether or not the ribs were in the path of the propagated sound beam, the edge of the specimen could be located. Photos taken of the scope presentation of the echos obtained during these tests are shown in FIGURES 27 and 28. As can be seen in the figures, multiples resulting from the standing members would prove to be a major obstacle to the detection of flaws in the specimens containing five ribs. The specimens with two ribs did not represent as severe a problem since flaws could be located. FIGURE 29 illustrates the major paths of ultrasonic propagation that are hypothesized to exist in the two-ribbed specimen. Rib radii, rib tops, and the specimen edge all provide permanent responses. The photographs below the specimen drawing show the actual responses from the rib and edge reflectors on a 0.09-inch-thick test specimen used in this study. The photos were taken prior to flaw introduction in the specimen. It could be concluded that standing members do represent a restricting factor upon the usefulness of surface wave ultrasonics, the magnitude of the problem being proportional to the number and location of the standing members.

Weld Specimen Tests

During the course of this study, an interest was shown as to the effect of weldments upon ultrasonic surface waves. A test specimen of 2219 aluminum of 0.250-inch thickness with a weld located at the centerline of the panel was obtained for test purposes. Four artificial flaws of 0.030-inch depth were introduced into the specimen at various locations to provide different flaw orientation with respect to the weld. This test specimen and the flaw locations are shown in FIGURE 30. A series of tests were conducted using a 2.25 MHz transducer to evalute the propagation and detection capabilities of surface waves on this weld specimen. In the first test, the transducer was placed at an 8-inch distance from the parent metal flaw so that the weld was in the path of ultrasonic propagation from the transducer to the flaw. In the second test the transducer was placed at a 5-inch distance from the weld and the longitudinal flaw in the weld was monitored. During the third test, the transducer was positioned on the weldment itself, which had been machined to remove the majority of the weld reinforcement, and the transverse flaw in the weld was monitored at a 7-inch distance. In the final test, the flaw in the weld heat-effected zone was monitored by placing the transducer parallel to the weld at a distance of 5 inches from the flaw. During all these tests, the artificial flaws were easily detected using surface waves and the presence of the weld proved to have no adverse effects upon either the prop-

SPECIMEN THICKNESS TRANSDUCER FREQUENCY	FRONT SURFACE (RIBS IN SOUND PATH)	BACK SURFACE (RIBS NOT IN SOUND PATH)
0.030 INCH 5.0 MHz	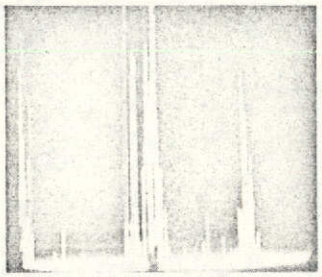 MB E	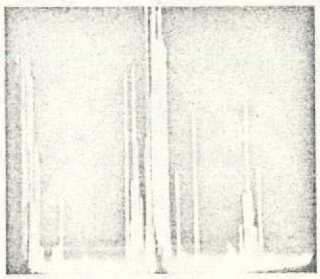 MB E
0.045 INCH 5.0 MHz	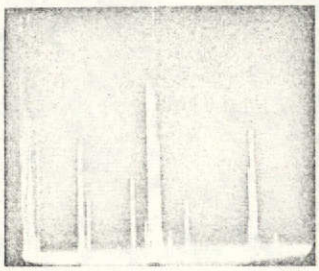 MB E	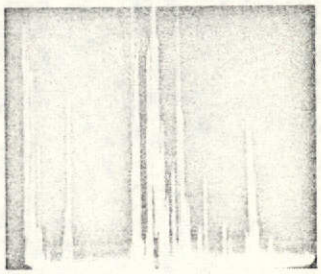 MB E
0.065 INCH 2.25 MHz	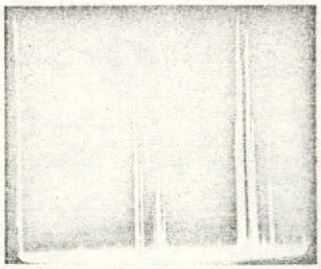 MB E	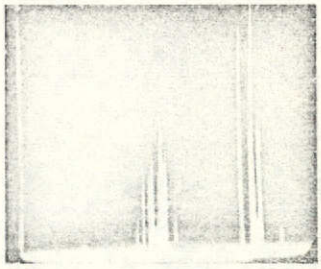 MB E
0.090 INCH 2.25 MHz	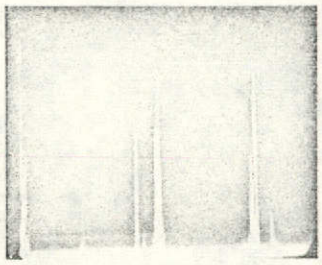 MB E	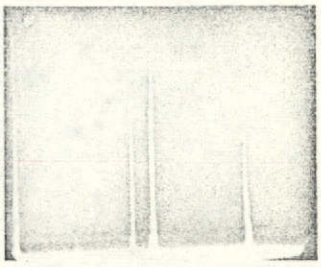 MB
0.125 INCH 2.25 MHz	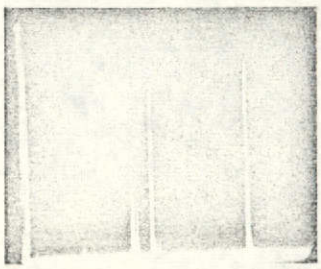 MB	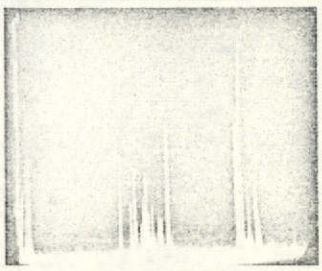 MB E

LEGEND

MB: MAIN BANG
E: EDGE

Figure 27. Standing Member Tests (Two-Rib Specimens)

SPECIMEN THICKNESS TRANSDUCER FREQUENCY	FRONT SURFACE (RIBS IN SOUND PATH)	BACK SURFACE (RIBS NOT IN SOUND PATH)
0.045 INCH 2.25 MHz	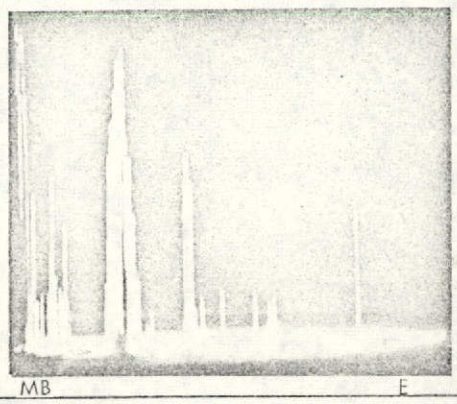 MB E	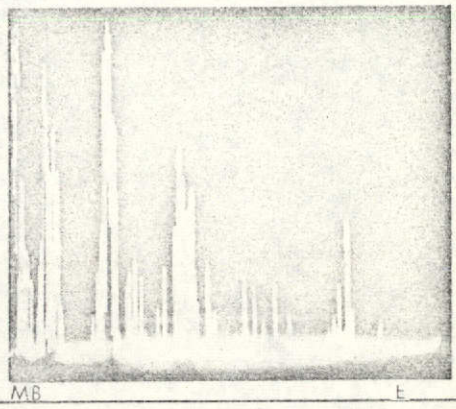 MB E
0.045 INCH 5.0 MHz	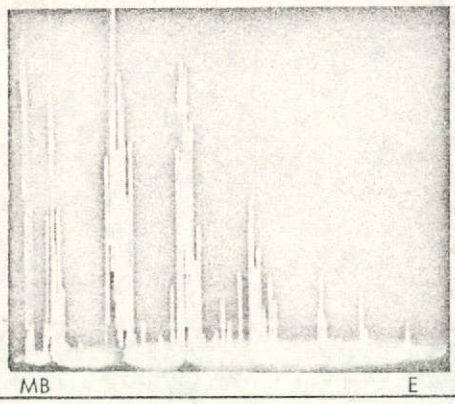 MB E	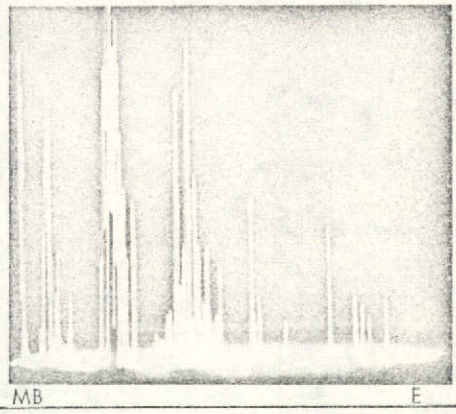 MB E
0.065 INCH 2.25 MHz	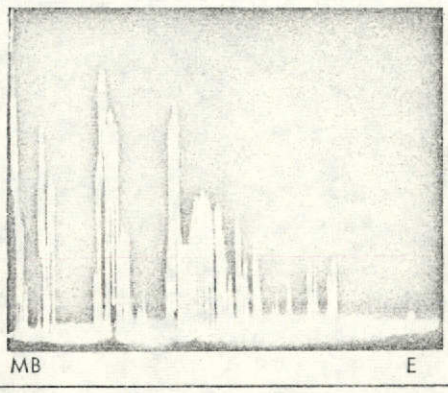 MB E	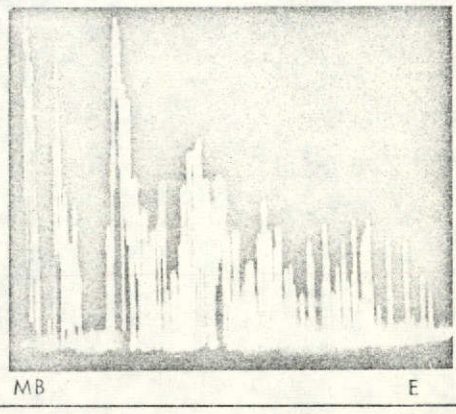 MB E
0.065 INCH 5.0 MHz	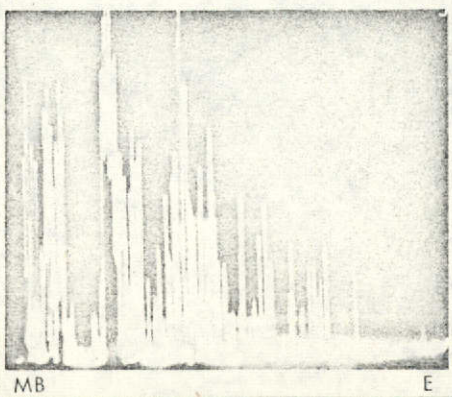 MB E	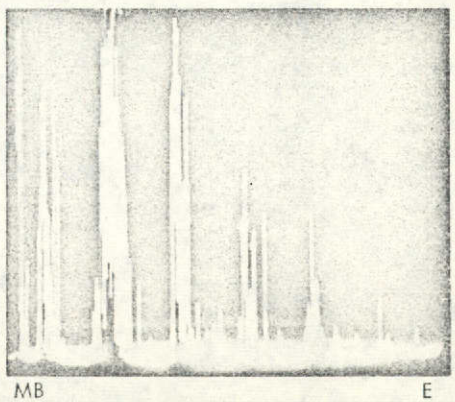 MB E
LEGEND MB: MAIN BANG E: EDGE		

Figure 28. Standing Member Tests (Five-Rib Specimens)

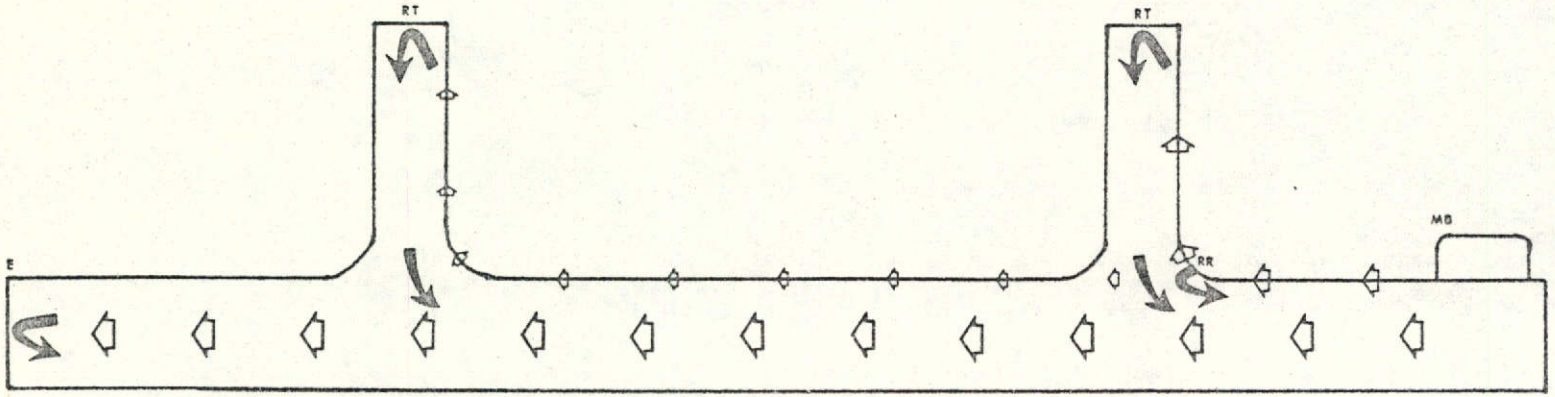

HIGH GAIN

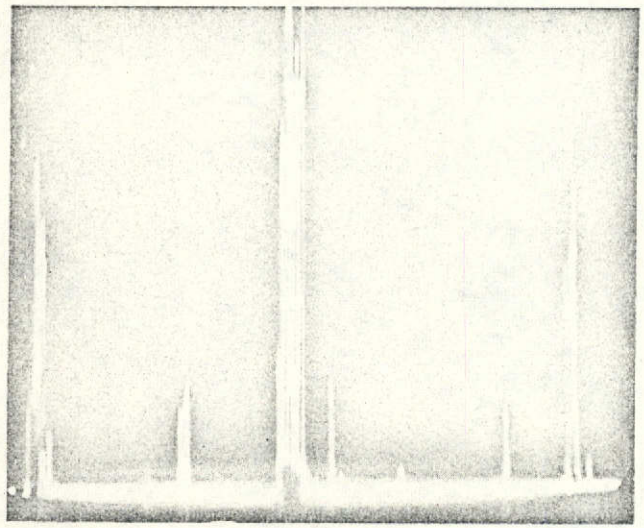

LEGEND

MB - MAIN BANG
RR - RIB RADIUS
RT - RIB TOP
E - EDGE

LOW GAIN

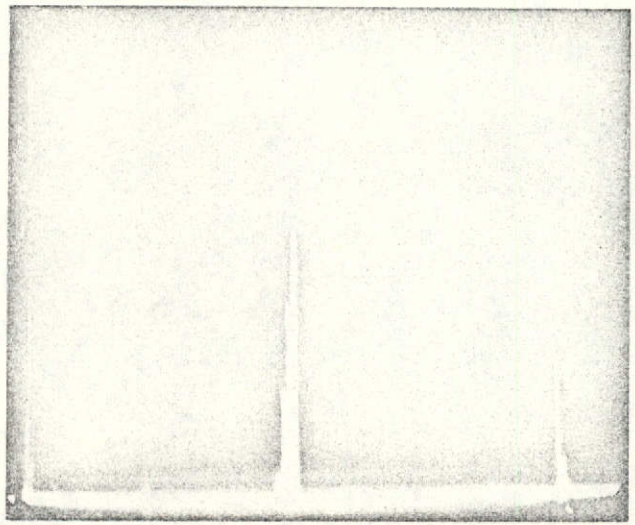

Figure 29. Hypothesized Ultrasonic Propagation Paths in Two-Ribbed Test Specimen

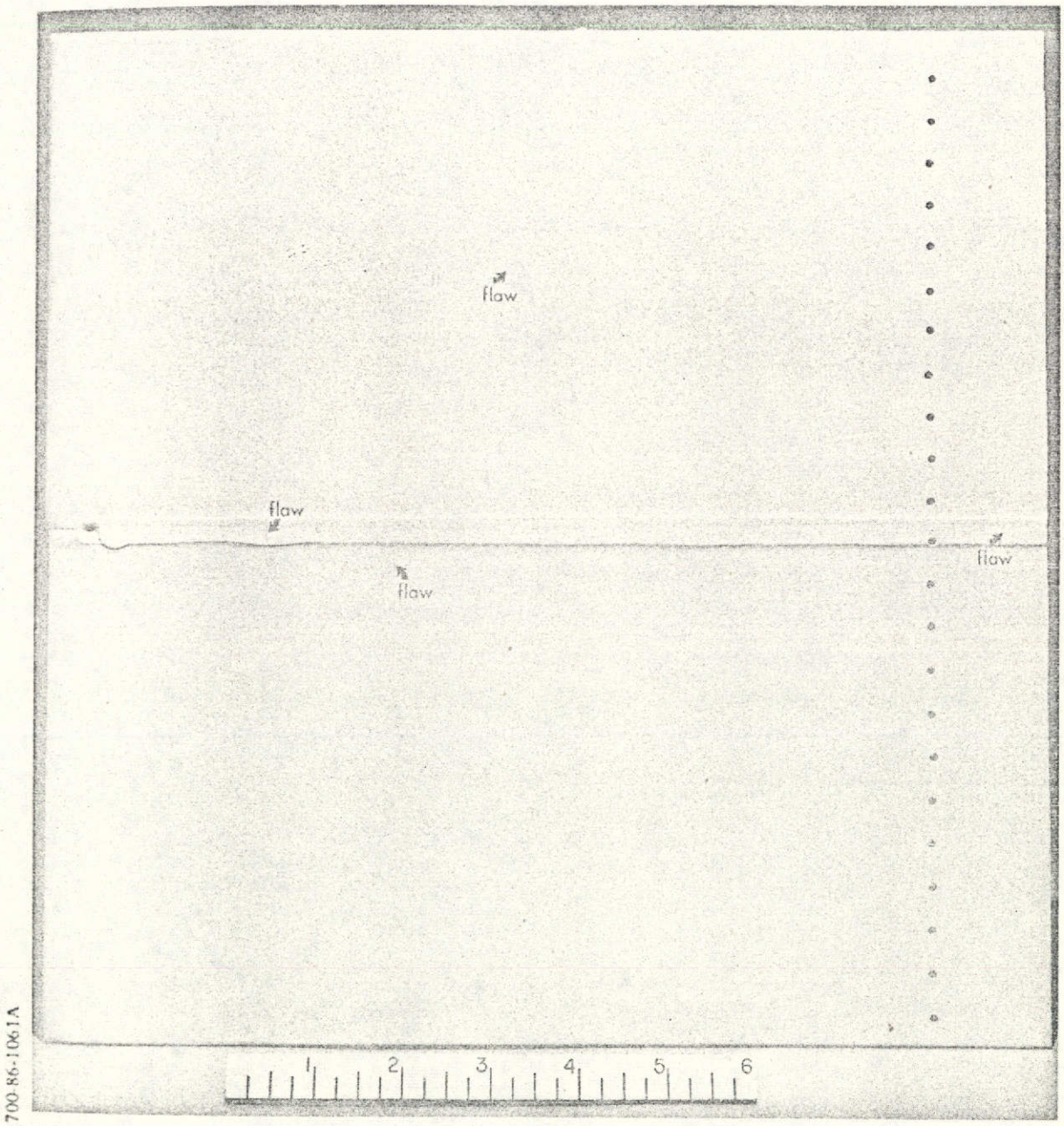

Figure 30. Weld Test Specimen

agation or the detection capabilities of the ultrasonic technique. The ultrasonic responses obtained from each of the flaws during these tests are illustrated in FIGURE 31.

Acoustic Chamber Tests

Acoustic environmental testing was conducted in the same manner as outlined in a previous section of this report. Three test specimens were utilized to determine the effect of extreme acoustic noise on ultrasonic flaw detection. Base plate thicknesses were 0.045, 0.065, and 0.090 inch respectively and each test specimen contained two standing members spaced 8 inches from each other. Flaws were machined into eact test specimen at the location shown in FIGURE 32 to the following depths:

0.045 specimen - 0.030 inch
0.065 specimen - 0.040 inch
0.090 specimen - 0.049 inch

Transducers were then bonded to the test specimens utilizing Lefkoweld 109 adhesive, as illustrated in FIGURE 33. Upon completion of adhesive curing, the ultrasonic responses from the artificial flaws were documented prior to acoustic testing. These ultrasonic responses are shown in FIGURE 34.

To facilitate the acoustic testing, each specimen was individually suspended in the test chamber as shown in FIGURE 35. A test run for each transducer was conducted with two-minute holds at each selected decibel level. An accelerometer was bonded to each test specimen and Appendix B shows the reaction of the test specimens to the acoustic environment. A specially constructed microphone was suspended in the chamber to monitor the noise being applied to the test specimens. The noise levels generated as detected by the microphone are shown in Appendix C.

No effect of severe acoustic environments was noted upon the ability of surface wave ultrasonic flaw detection techniques to detect or monitor crack-like flaws in the test structure. The only noticeable effect on the signal at all was a slight vibratory motion in the amplitude mode. FIGURES 36, 37, and 38 show individual scope patterns for each of the six runs made indicating flaw location from ambient noise conditions to levels of 160 db. It should be noted that the markings below the CRT baseline in FIGURES 36, 37, and 38 were used only as an aid during the tests to locate the flaw signals.

FIGURE 39 shows the test instrumentation used during the noise testing.

PARENT METAL FLAW

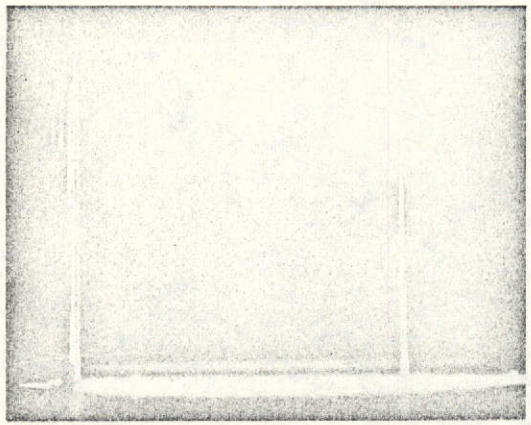

WELD HEAT ZONE FLAW

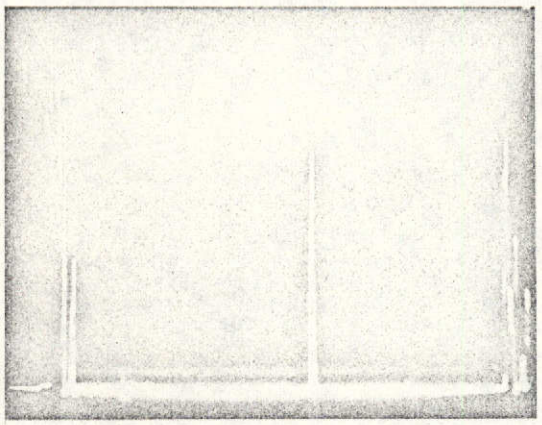

TRANSVERSE WELD FLAW

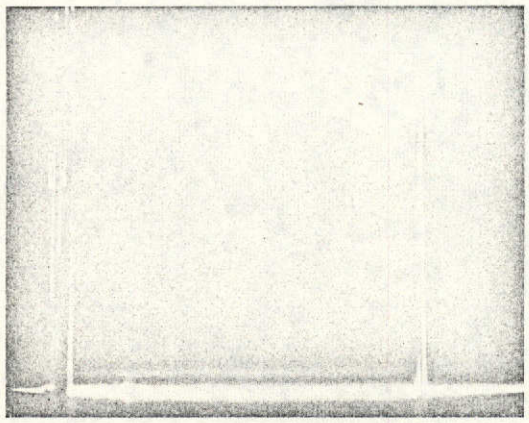

LONGITUDINAL WELD FLAW

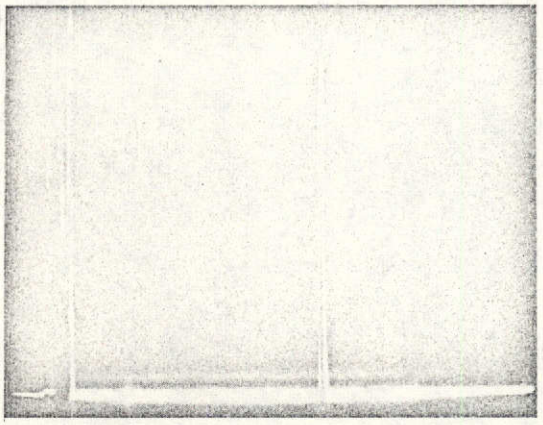

LEGEND

MB: MAIN BANG
F: FLAW
E: EDGE

Figure 31. Ultrasonic Responses From Weld Specimen Flaws

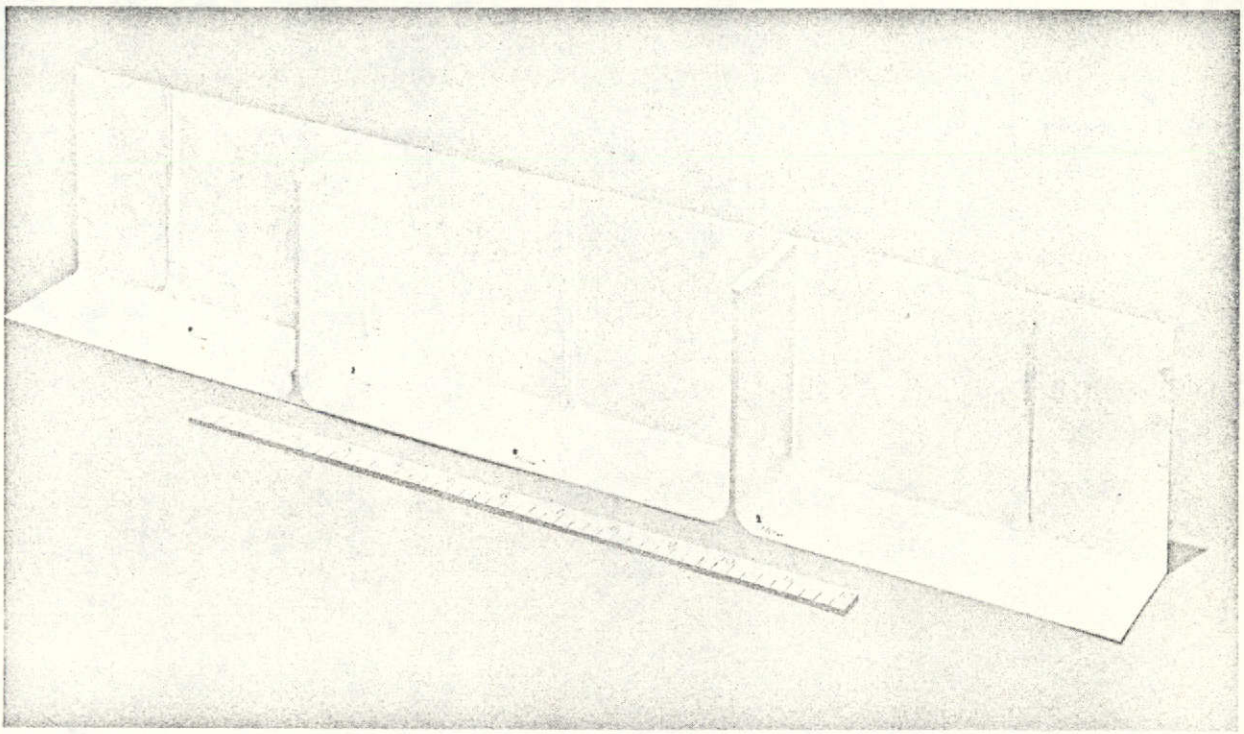

700-86-1061B

Figure 32. Acoustic Chamber Test Specimen With Flaws

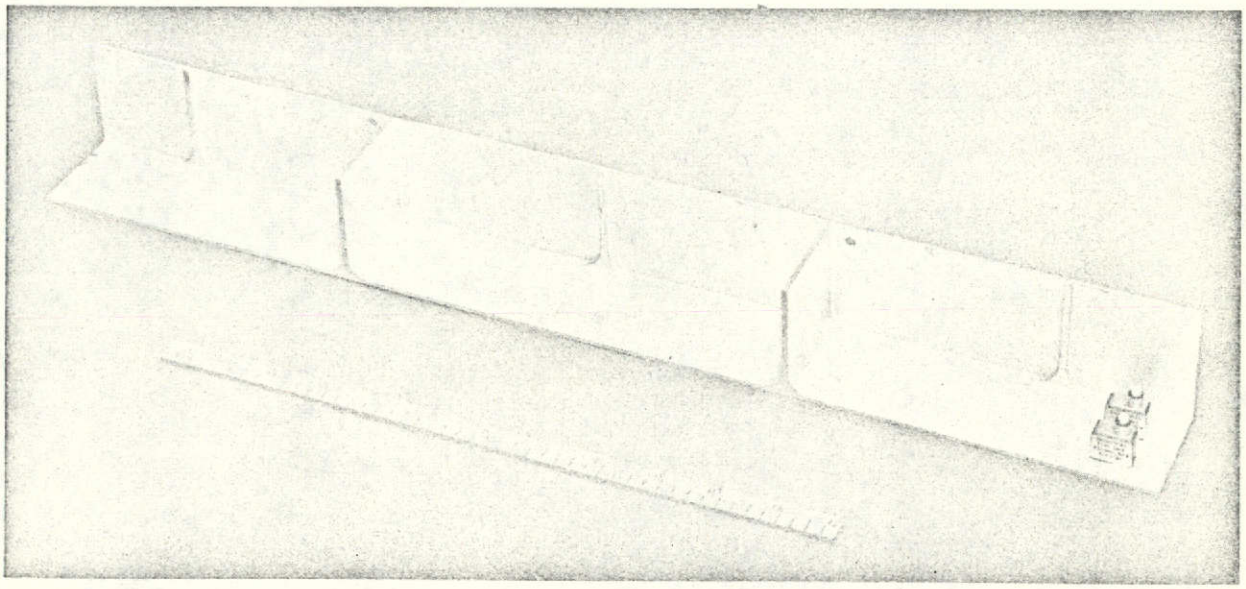

700-81-1683

Figure 33. Acoustic Chamber Test Specimen With Transducers Bonded

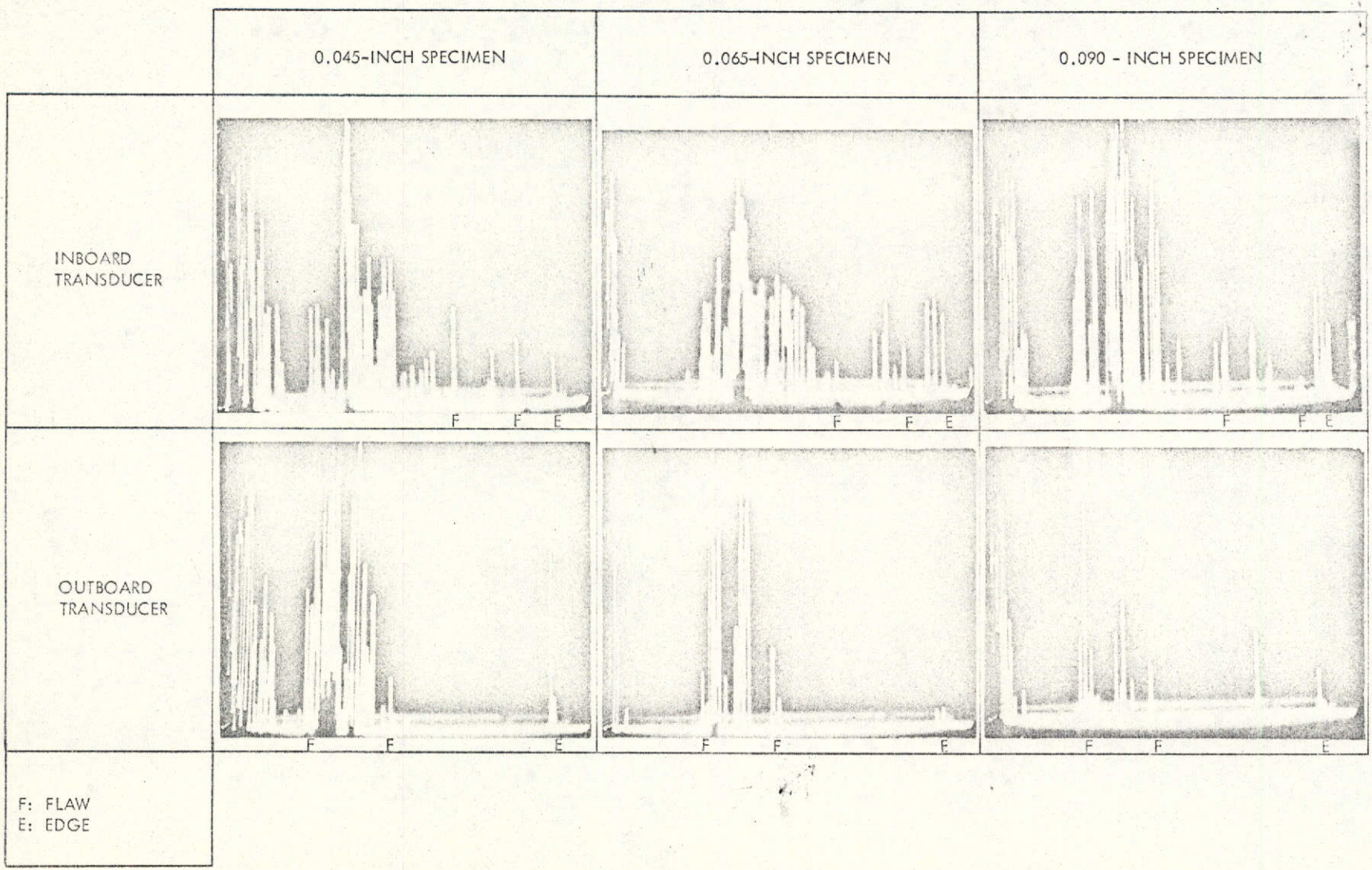

Figure 34. Ultrasonic Responses From Artificial Flaws in Final Acoustic Test Specimens

700-81-1684A

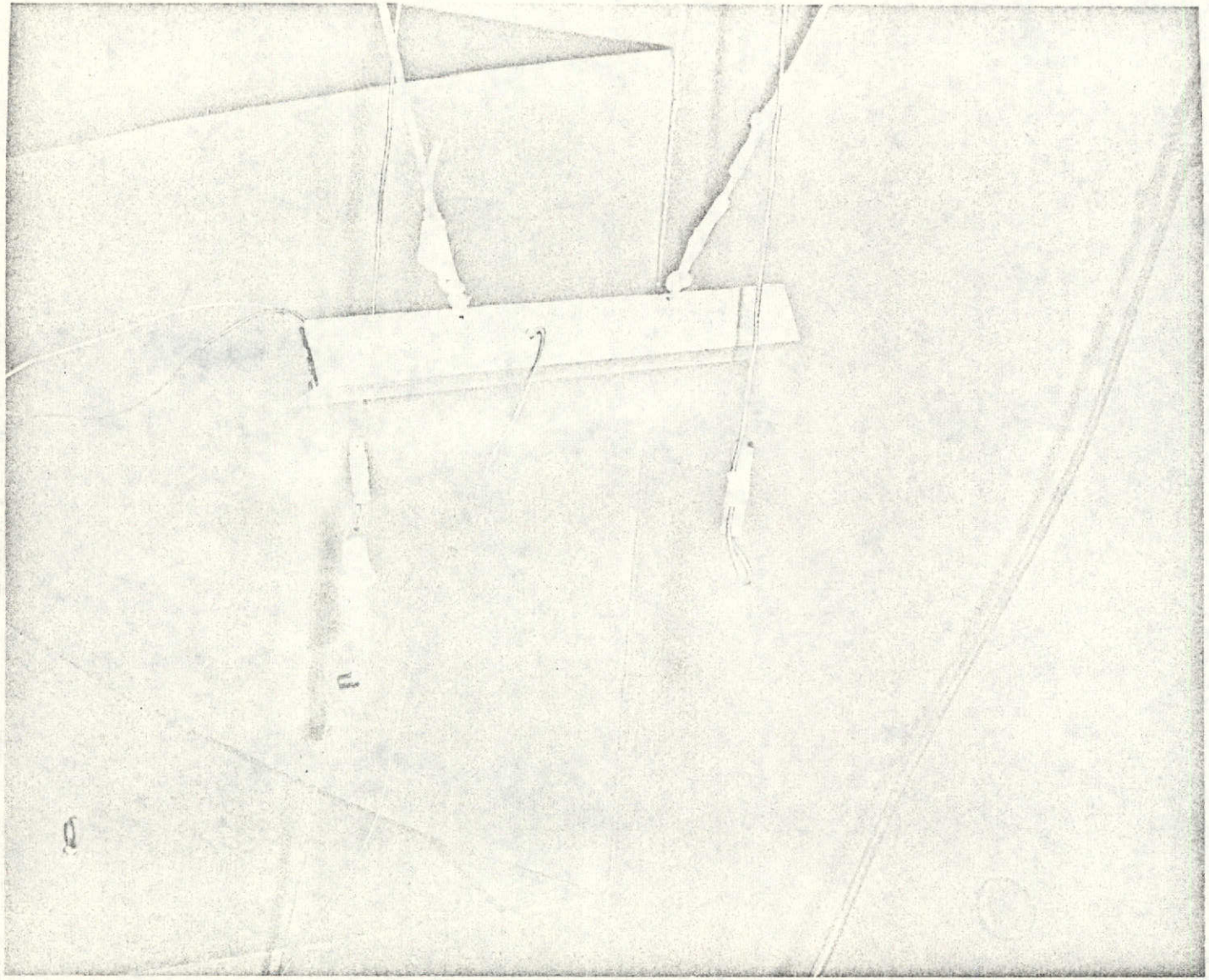

Figure 35. Test Specimen Placement in Acoustic Chamber

DECIBEL LEVEL	INBOARD TRANSDUCER	OUTBOARD TRANSDUCER
LEGEND: ARROW DENOTES FLAW ECHO PRIOR TO ACOUSTIC ENVIRONMENT	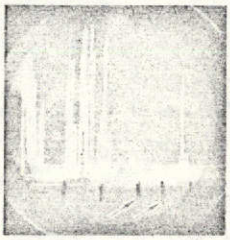	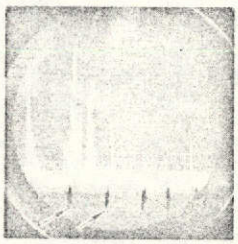
140 db	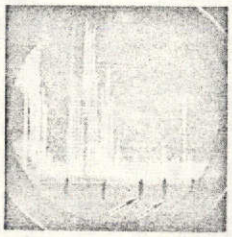	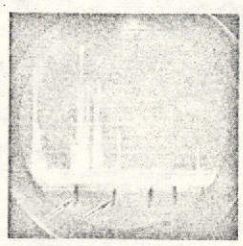
145 db	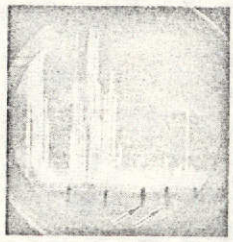	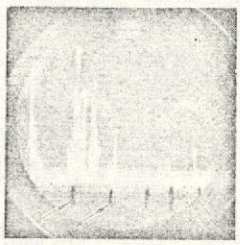
150 db	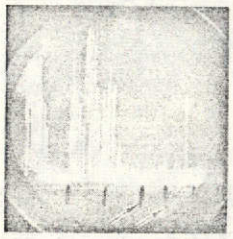	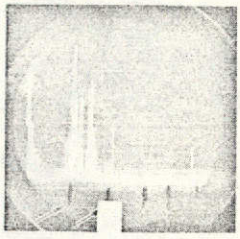
155 db	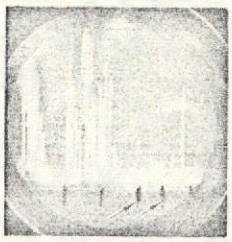	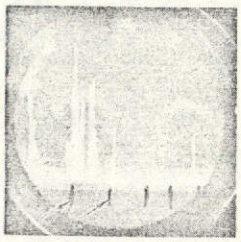
160 db	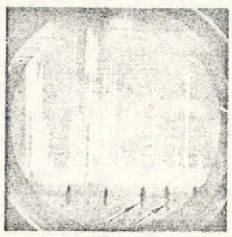	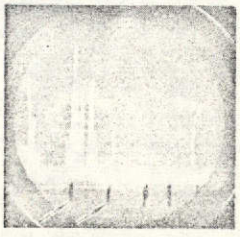

Figure 36. Ultrasonic Responses During Acoustic Tests of 0.045-Inch Ribbed Specimen (5.0 MHz)

DECIBEL LEVEL	INBOARD TRANSDUCER	OUTBOARD TRANSDUCER
LEGEND: ARROW DENOTES FLAW ECHO PRIOR TO ACOUSTIC ENVIRONMENT	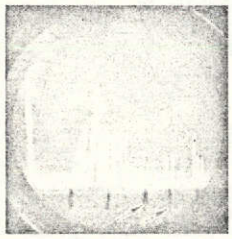	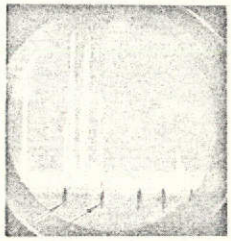
140 db		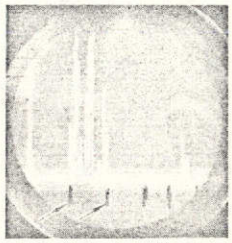
145 db	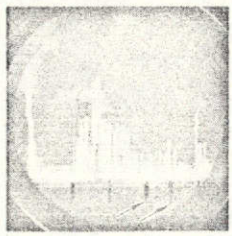	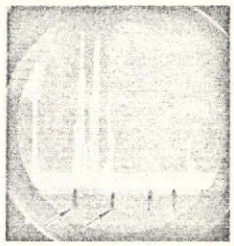
150 db	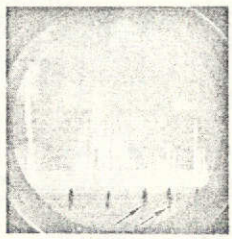	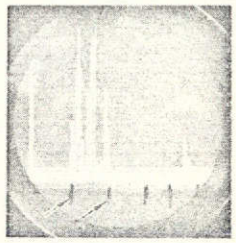
155 db	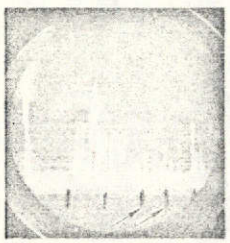	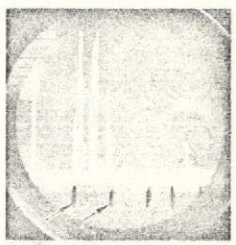
160 db	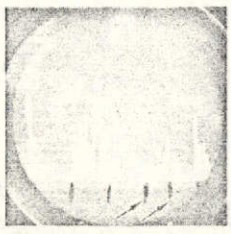	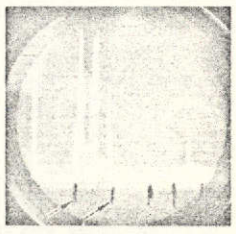

Figure 37. Ultrasonic Responses During Acoustic Tests of 0.065-Inch Ribbed Specimen (2.25 MHz)

DECIBEL LEVEL	INBOARD TRANSDUCER	OUTBOARD TRANSDUCER
LEGEND: ARROW DENOTES FLAW ECHO PRIOR TO ACOUSTIC ENVIRONMENT	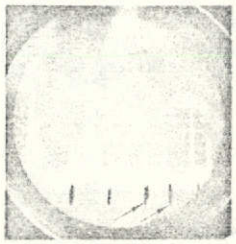	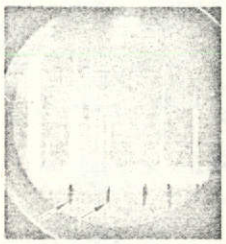
140 db	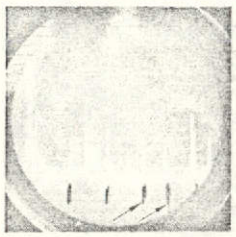	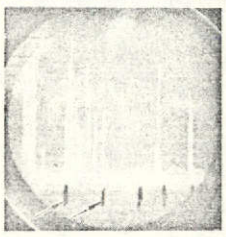
145 db	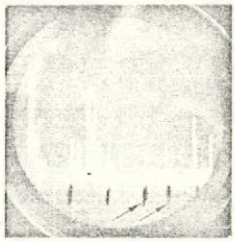	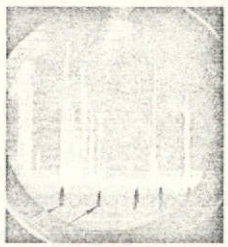
150 db	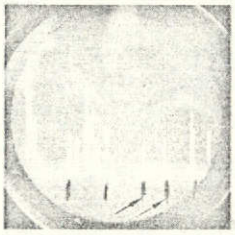	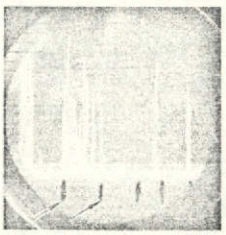
155 db	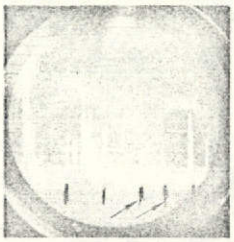	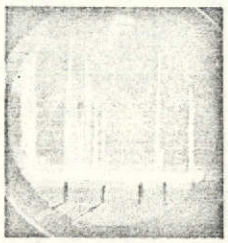
160 db	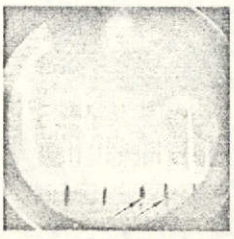	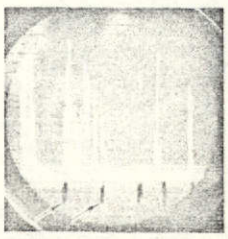

Figure 38. Ultrasonic Responses During Acoustic Tests of 0.090-Inch Ribbed Specimen (2.25 MHz)

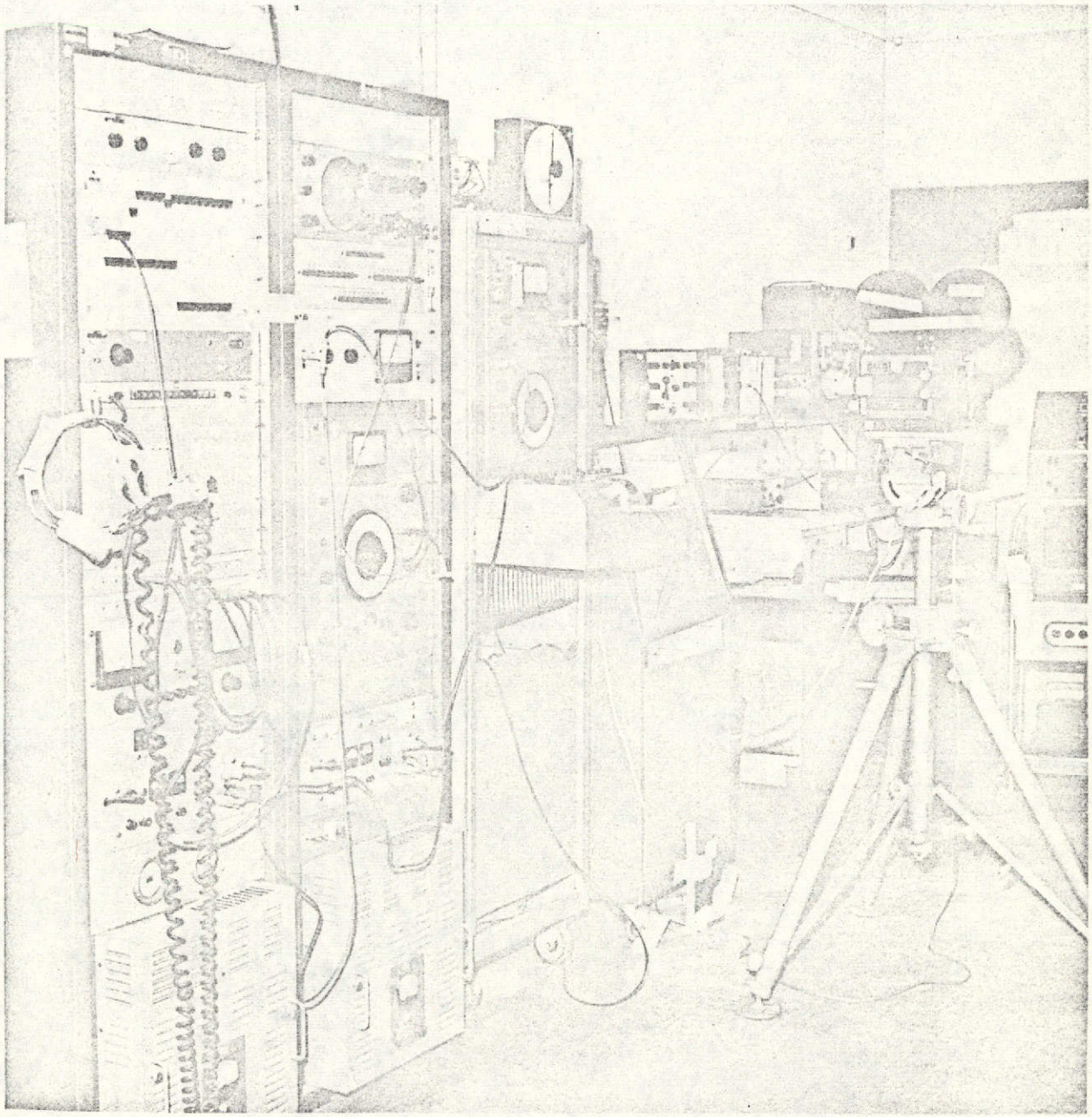

700-81-1684B

Figure 39. Acoustic Noise Test Instrumentation

OPERATIONAL ASSESSMENT

Current space shuttle vehicle design baseline requirements are for 100 mission flights. The requirement for refurbishment, maintenance, and system verification within a two-week span is the basis of the requirements for special ground support and on-board checkout equipment. Among the available methods to accomplish this task are those of nondestructive evaluation. Some of these techniques have been utilized previously on aircraft, spacecraft, and launch vehicles. Presently recognized means of assessing the integrity of structures and assemblies nondestructively include such techniques as penetrants, radiography, C-scan ultrasonics, visual inspection, and eddy currents.

This study identified three general categories of on-board ultrasonic systems: (1) complete system, (2) limited system, and (3) ground supported system.

On-board ultrasonic checkout system is a proposed subsystem that could be part of the overall space shuttle maintenance concept. The space shuttle maintenance plan has been developed to establish, as applicable, requirements and prospective implementation approaches for the conduct of the design, development, and operations of the space shuttle program. The following section is a summary of those aspects of this plan, as detailed in NR SD report SD 71-106, which are pertinent to implementation of an on-board ultrasonic checkout system. This Phase B shuttle effort was conducted for the Manned Spacecraft Center.

The maintenance concept establishes a framework for development of space shuttle maintenance capabilities. As it is refined, the concept influences equipment design, defines the objectives of maintenance and support planning actions, and provides a baseline for the acquisition of maintenance resources.

Three levels of maintenance are defined. Level I maintenance activities will be accomplished to process a postmission vehicle through safing, unloading, and purging functions to the hangar maintenance area. Level II, the secondary maintenance cycle, will be performed to repair a line-replaceable unit (LRU) that has been replaced during turnaround maintenance. Level III maintenance will be provided for extensive rework, repair, and refurbishment of equipment requiring specialized skills, equipment, and facilities not available at the operating site.

The on-board ultrasonic checkout system could be part of the Level I maintenance function. Nondestructive evaluation of critical structural members could be accomplished in support of Level I activities associated with body structures and can be used to conduct flaw isolation operations associated with structural components. For example, if a crack is discovered by an on-board ultrasonic checkout, procedural steps such as penetrant, ultrasonics, X-ray, etc., might be accomplished in progressive steps to assure flaw detection.

SYSTEM DESCRIPTIONS

In order to evaluate on-board ultrasonics, a detailed design of a postulated system should be available. Three general categories of on-board ultrasonic systems are readily identified. A complete system would monitor the majority of the shuttle structures. A limited system would monitor selected critical structures. Both of these systems are envisioned as being self-contained on board the shuttle vehicle. A ground-supported system would monitor selected critical structure with the aid of ground support equipment.

A common component of each of these systems would be the transducers and coax cable. The weight of each individual transducer is expected to be near 8 grams: the weight of the miniature coax cable is 4.5 grams per foot.

Complete System

A complete system would monitor the majority of the structural members. In order to minimize high-voltage switching problems, it is desirable to use individual pulser modules for each transducer channel. A multiplexer would be used to switch to a single channel receiver. Assuming a structural checkout once every half hour, one ultrasonic receiver and processor would be necessary for approximately every 1800 receiver channels. The data display could be either a real-time cockpit display or be stored on the flight record for subsequent analysis. The block diagram shown in FIGURE 40 represents a complete system with complete data display and recording. Basic power consumption would be about 500 watts with an additional 1/4-watt per transducer channel. The 500 watts represent the estimated sum of the total components. Allocations for the components are 260 watts for the pulser receiver, 20 watts for the multiplexer, and 250 watts for the computer. The weight of the basic unit is expected to be near 25 pounds with an increase of 1/4-pound per transducer channel. Each application of a transducer would have to be evaluated individually and configured.

Limited System

A limited system would monitor selected critical structures. The functional electronic processing would be similar to that for a complete system except for having fewer channels. In either case, a multitude of display techniques are possible. FIGURE 41 shows a block diagram for a limited system with historical data management only. The basic power and weight consumption figures developed for the complete system would also apply to a limited system. A limited system has specific weight advantages over a complete system. However, the development risk is about the same as that for a complete system.

Ground-Supported System

The ground-supported system would have only the transducers and associated wiring on-board the shuttle vehicle. The ultrasonic transducers would be bonded in place with associated wiring leading to external connectors. The checkout system would then be interrogated by using associated ground support equipment. No on-board power consumption would be involved, and the weight of the system would be the lowest of the three system concepts. The major disadvantages of the ground-supported system are the labor requirements and time required to interrogate the system during vehicle turnaround. FIGURE 42 shows a block diagram for a ground-supported system. Development cost would be minimal since only standard nondestructive instrumentation would be used. It then appears that the ground-supported on-board system has definite weight and cost savings advantages relative to the other two systems.

System Comparison

A qualitative analysis was performed on the three individual system approaches and is presented in TABLE 13. The evaluation was made by first identifying the primary attributes of the various approaches. A numerical grade between 1 and 10 was assigned to the various attributes, with the high rating reflecting the most desirable condition, for each approach based on the consensus of Space Division personnel who are involved in the analysis. Weights were assigned to each attribute to reflect the relative importance. The rating of each approach is then calculated by summing the attribute rating times the weighting factor, over all attributes.

OPERATIONAL LIMITATIONS

An on-board ultrasonic checkout system would be best utilized to monitor critical, highly stressed structural members. The monitoring of tank welds in high pressure vessels and highly stressed stringers appears

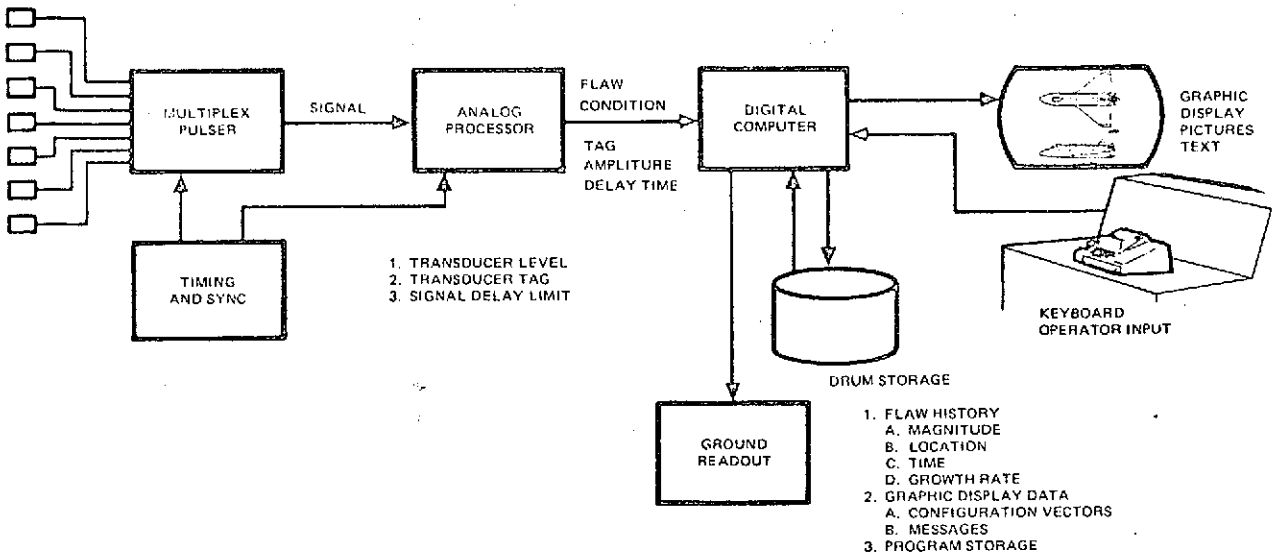

Figure 40. Complete On-Board System Block Diagram

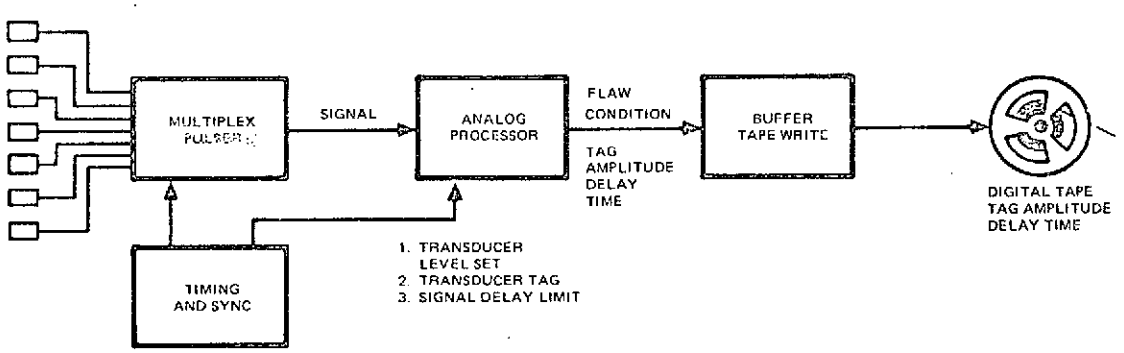

Figure 41. Limited On-Board System Block Diagram

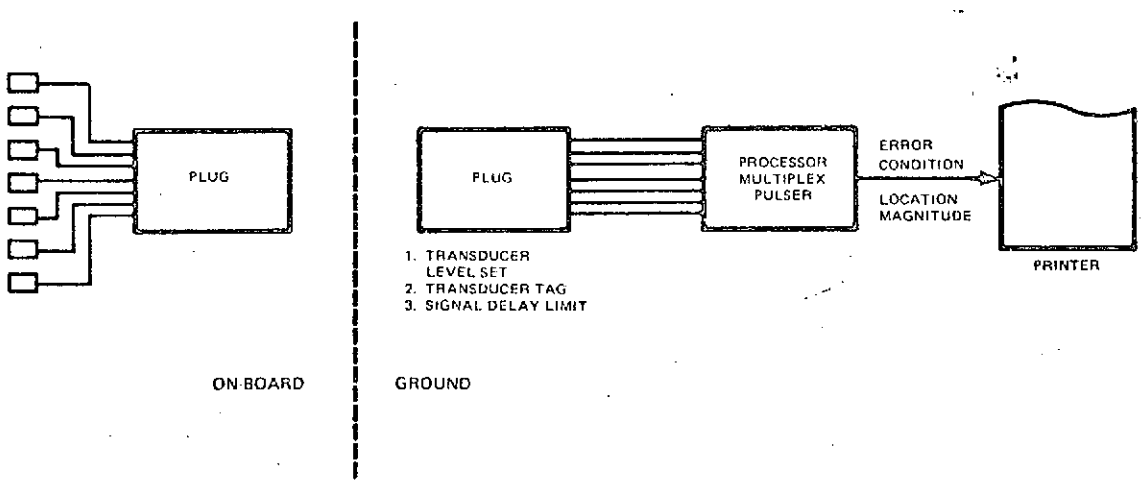

Figure 42. Ground-Supported System Block Diagram

Table 13. Matrix Evaluation of On-Board Concepts

On-Board Ultrasonic Concept	Relative Merit of Ultrasonic Feasibility Factors*							Relative Merit Rating
	Number of Transducers	Amount of Electronic Equipment	Power Requirement	Weight	NDT System Reliability	Cost	System Reliability	
Complete system	2	1	2	2	8	1	8	30
Limited system	8	5	6	6	3	7	2	63
GSE-supported system	6	7	10	8	5	9	4	85
Relative Weight	1	1	2	2	1	3	1	

*High rating reflects most desirable condition

most appropriate. Structurally, members with more then two ribs with a spacing of less than 5 inches apart could not be monitored effectively. It is not possible to monitor the area just adjacent to the reflected pulse from the rib member. Hence, the near-side base of a rib could be monitored while the far-side base could not be monitored. Holes, bolts, and other structural members obstruct the line of sight. The majority of these limitations can be overcome by using additional transducers, which points out the major limitation of on-board ultrasonic monitoring: excessively large numbers of transducers are necessary to completely monitor a complex structure.

Many factors influence the feasibility of installing an ultrasonic system on board the orbiter. Present analysis indicates that it would be impractical to monitor every structural member of the orbiter. This can be seen from the analysis of a typical single structure. Consider the engine support pedestal floor shown as a detailed drawing in FIGURE 43, as obtained from blueprint No. VC70-3084, Aft Fuselage Structural Arrangement. As can be seen from this figure, there are 19 longitudinal ribs protruding from both the top and bottom surface. Axially, there are eight principal ribs or partial ribs. Allowing for propagation over five ribs only and not trying to gate rib spaces less than 6 inches apart, this structure would require approximately 100 transducers to completely monitor the load-bearing ribs. Even so, the corner of the joined ribs would have dead space left unmonitored. This analysis then suggests that one should be selective as to the areas monitored. These areas would have to be subjected to careful analysis and probably prototype configuring of the structure.

The tests conducted within the confines of this study and the results obtained from other NR programs have shown that ultrasonic techniques, using various beam propagation modes and instrumentation, can be utilized as an on-board structural monitoring system. Although present state-of-the-art technology would allow installation of such a system, certain operational limitations would necessitate consideration. Some of these more evident limitations are discussed in the following paragraphs.

A major potential limitation can be the configuration of the structure to be monitored by the ultrasonic system. Specific physical characteristics of the structure, such as standing members, holes or cutouts, rivets, attached members, etc., in the path of the ultrasonic beam can initiate detrimental echos or complete beam reflection which can obliterate and/or negate defect detection. The degree of this effect for each of these independent physical characteristics depends upon the ultrasonic system's capability and will vary with the location of the area being monitored and the type of beam propagation mode utilized. An example would be the presence of standing members located on the assembly. If transducer placement with

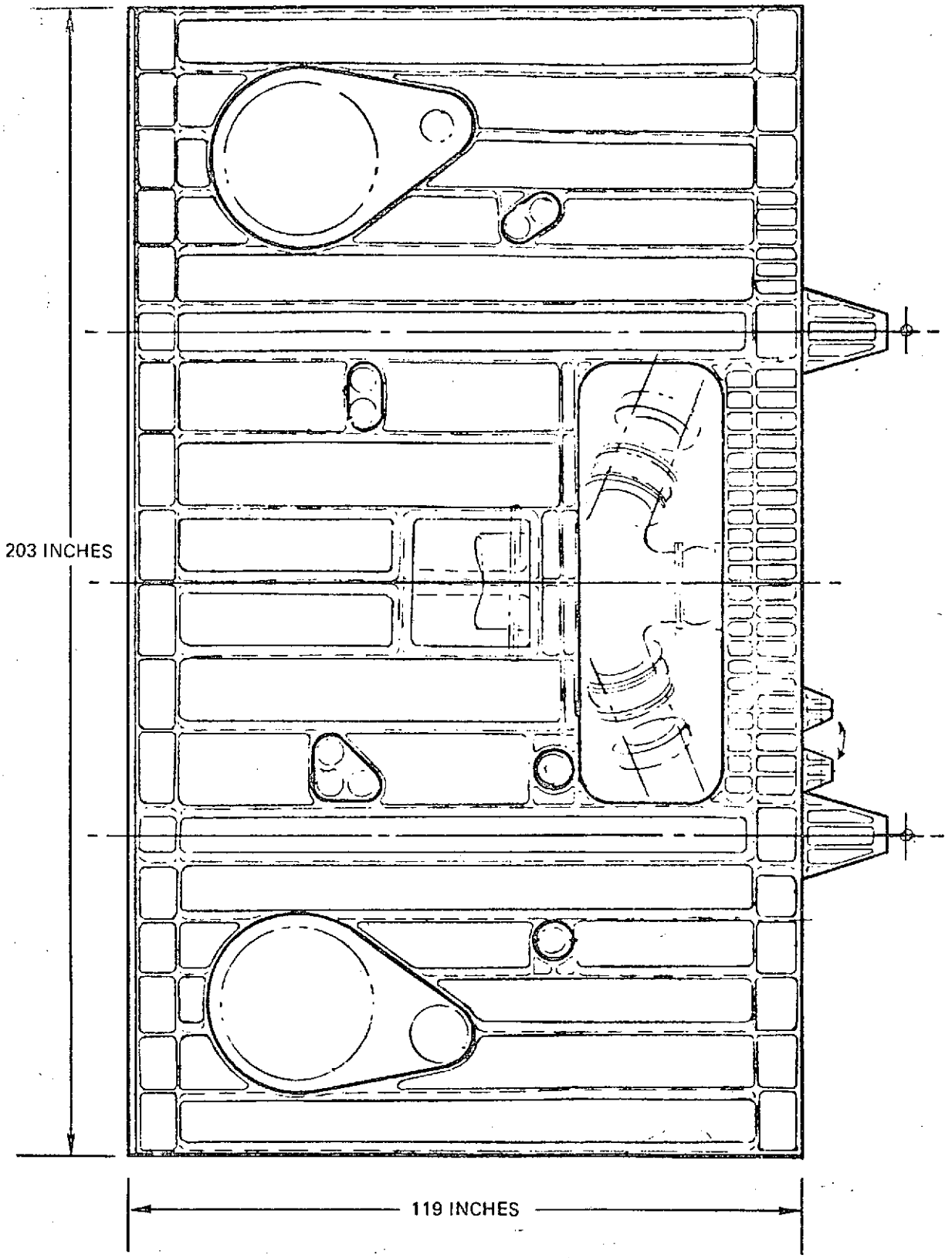

Figure 43. Aft Fuselage Structural Arrangement
(Selected Portion)

respect to the critical area to be monitored can be achieved so that the standing members are not in the beam propagation path, the fact that the standing members are present has no effect. If, however, it is necessary to place the transducer at a location where the standing members are in the path of the propagated ultrasonic beam, the degree of the effect will vary. If the material is sufficiently thick to allow proper shear wave propagation, the standing members will not be restrictive since the sound travels within the material by reflecting from the top and bottom base surfaces and can be passed by the ribs with no resultant effect by proper transducer to rib distance and sound propagation angles within the material. If the structure is so thin that surface waves are required, then the ribs can represent a restrictive factor depending upon the location and number of the standing members as discussed earlier in this report.

Another limiting factor is the present narrow beam transducers and the importance of critical defect to transducer orientation. The use of bonded-in-place, narrow beam transducers allows only small area coverage since the beam spread is approximately 3 percent. This means that if large area coverage is required, multiple sensors will be necessary. This contributes to system weight and cost. This can be diminished somewhat by using strip or mosaic transducers, which, although not necessarily reducing transducer weight, will reduce the number of separate channels and instrumentation since one mosaic transducer will cover the same area that required three to four standard sensors. A related issue is that of transducer to defect orientation since on-board systems are based upon the operational mode of pulse-echo ultrasonics. Pulse-echo ultrasonics operate on the principle of each sensor propagating the sound into the structure and also receiving the resultant defect echos. The defect orientation becomes critical when the long axis of each crack-like flaw varies from a perpendicular plane with respect to the propagated sound. This will result in either the sound passing by the defect and not initiating any reflection or the reflection angle may be such that the echo path will not lead back to the sensor. The degree of effect upon on-board system consideration of these factors are dependent on various issues. Analysis of structural loading data prior to sensor placement can provide data regarding the type of defect and its probable location and orientation within the areas deemed critical. This type of analysis would allow placement of system sensors so that the highest degree of detection sensitivity with fixed transducers could be achieved. The application of multiple rotating sensors which sweep an area could provide a potential means of improvement in the area of narrow beam transducers and defect orientation. The use of this type of sensor requires analysis of the sensor itself, drive mechanisms, and couplants.

It can be seen from the considerations shown above that the use of on-board monitoring will require an in-depth analysis of many factors prior

to its implementation on a shuttle vehicle. The feasibility of using such a system has been demonstrated for limited cases; however, many different factors must be evaluated prior to its implementation. These include areas such as:

(a) Structure to be monitored

(b) Specific critical areas within the structure

(c) Probable defects, critical size, and orientation

(d) System envolvement, i.e., in-flight, turnaround, etc.

(e) Sensor selection

(f) Sensor placement

(g) Instrumentation

(h) Data management

(i) Operational parameters

An analysis and evaluation of these factors are beyond the scope of this study; however, such issues must be considered during the development and implementation of an on-board monitoring system.

DATA MANAGEMENT

Although the data displayed in the tests described in this report were oscilloscope "A" traces, this data can be gated and displayed digitally or as a GO/NO-GO panel light. For a large number of transducer channels, it is possible for one GO/NO-GO panel light to monitor many channels. This monitoring system may be compared with other display methods. Since the pulser-receiver would be multiplexed over many transducer channels, a panel light could just follow this sequencing. This would require an additional digital display indicating which channel was being monitored. In either case, the information status is updated only as the transducer channel multiplexer information is processed by the pulser-receiver. However, with multiple channel monitoring, the status of all channels is readily observable at any one time. In this sense, it is a monitoring real-time system. The other system is best referred to as a sequencing real-time system. These two alternatives represent the most logical ways to integrate the on-board ultrasonic system into a panel display.

Three other alternatives exist for processing the data: (1) the data could be stored on flight record tapes and be analyzed after the flight; (2) the data could be telemetered, to earth for monitoring by an earth-located monitoring station; (3) a limited on-board system could be deployed. In this case, ultrasonic transducers would be bonded in-place with associated wiring leading to external ports. The checkout system would then be interrogated after landing by using associated ground support equipment. The ground support equipment would include the pulser-receiver, gates, multiplexer, and an interpretation-computer.

COST OF AN ON-BOARD ULTRASONIC SYSTEM

In order to estimate the cost of an on-board ultrasonic system, a detailed design of the system should be available. The principle cost parameter will be the number of transducers for a given type of system. The principal cost can be divided into three categories: material costs, installation costs, and operational costs.

The basic material costs would involve the pulser receiver, multiplex units, and computer interpreter for about $20,000 for ten channels with an increase of about $50 per channel. The transducers would cost about $200 each.

It is estimated that the installation costs would be about two man-hours per channel. The operational costs are highly dependent on the type of system employed. A real-time system would not involve any major operational cost while a limited or ground-supported system would cost about five man-minutes for each channel each time the channel is interrogated. Of course, support operations beyond these basic costs would be necessary to support implementation.

Total cost estimating for a system may be approached from many different ways. The previous section developed basic cost data based on foreseeable costing. The general approach to space shuttle costing is based on historical data of analogous functions. The data contained in "Program Cost and Schedule Estimates Plan for Phase C/D," SD 71-107, which is part of the Phase B shuttle effort completed for the Manned Spacecraft Center, provides a basis for such data. Working from the data contained in this report, the following estimates of total implementation costs for an on-board ultrasonic checkout system have been generated.

Cost estimates for the space shuttle are made in three categories. The design, development, testing, and engineering costs (DDT&E) are a nonrecurring cost based on past experiences in similar functional areas (i.e., primary body structures, nose TPS, thrusters, etc.). The second

category is that of production costs, which are a recurring cost. The breakdown here is similarly made by functional elements as related to weight estimates. The last category is that of operations costs, also a recurring cost. The operations cost is derived as a detailed manpower estimate based on historical data. Since no historical data exists for an on-board ultrasonic system, an estimate was made, based on as closely related functions as possible. Consideration would suggest that the "instrumentations" function would serve as the best model; the cost estimates for the orbiter and booster are shown below:

	DDT&E	Production	Operations	TOTAL
Orbiter Avionics Instrumentation (millions of dollars)	$37.2	$4.5	$2.1	$43.9

Probably the best estimate we have on any cost figure is that for production costs with respect to an on-board ultrasonic system. These costs may be estimated to lie between $25,000 and $200,000 with the most probable cost estimated to be $50,000, based on approximately 100 sensors. This then may be extrapolated to program costs based on typical instrumentation costs:

	DDT&E	Production	Operations	TOTAL
On-Board Ultrasonic Instrumentation (thousands of dollars)	$413.0	$50.0	$23.4	$486.4

SCHEDULE FOR IMPLEMENTATION OF ON-BOARD ULTRASONIC SYSTEM

The schedule for implementation and operation of the ultrasonic NDE system must follow a logical development order and must be compatible with the overall shuttle schedule. A logical development plan is outlined in FIGURE 44. The major milestones for shuttle would pace the on-board ultrasonic checkout system development. By combining these data, a schedule for on-board ultrasonic implementation was developed as illustrated in TABLE 14.

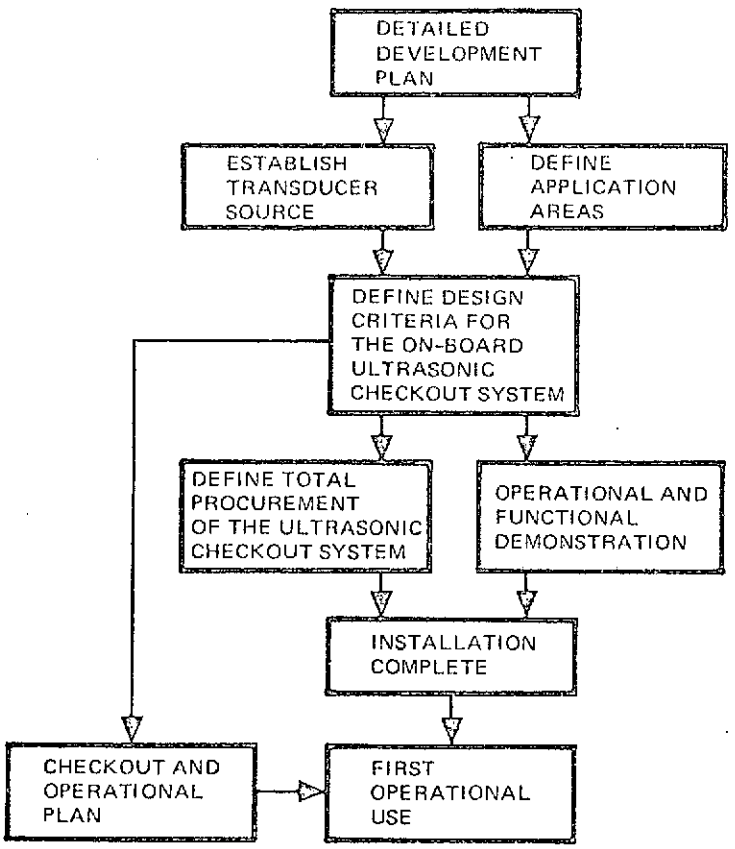

Figure 44. Development Plan Logic

Table 14. Schedule for Implementation of On-Board Ultrasonic Checkout System

Activity	Months After Phase C/D Go-Ahead
Detailed development plan	3
Establish transducer source	6
Define design criteria for the on-board ultrasonic system	8
Define the total procurement of the ultrasonic checkout system	20
Operational and functional demonstration	26
Installation complete	45
Checkout and operational plan	47
First operational use	52

STATE-OF-THE-ART/APPLICABLE NDE METHODS

As a related effort in conjunction with the prime program being conducted in support of this contract, it was required that the current state of the art of a series of nondestructive evaluation methods be monitored. Specifically, acoustic emission and the resonant vibration methods were to be followed. In-house programs being conducted at NR studying these techniques are typical of how the state of the art is being advanced in these methods. In addition, ultrasonics (acoustic spectroscopy), holographic NDE, thermography, fiber optics, and radiography are discussed. These methods were mentioned in the Phase II report of NASA Contract NAS10-7250, "Methods of Assessing Structural Integrity for Space Shuttle Vehicles" as being applicable in the near and intermediate term for shuttle use.

ACOUSTIC EMISSION

Noises from some materials subjected to various modes of deformation have been heard casually for a long time. During the past 20 years, this phenomenon has aroused much interest on the part of numerous investigators who reported their perception of noises (acoustic emissions) emanating from deforming specimens of rock salt and from the single crystals of several metals.

Investigators immediately recognized the practical significance of a diagnostic method that could detect the inception of internal damage and monitor progressive events as they occur. The low-energy signals from internal events are not easily detectable by other means; in most cases, no other expedient exists. The capability to interpret messages from the internal disturbances—however minute—can provide a means of assessing damage done or of predicting incipient failure.

During the recent past, acoustic emission technology was investigated for potential monitoring capabilities in such areas as:

1. Degradation by corrosion and stress corrosion

2. Pressure vessel structural monitoring during proof.

3. Feasibility of on-board monitoring of structural integrity

4. In-process welding control

It has been theorized and widely recognized that two types of acoustic emission exist. The first is the high-frequency, low-amplitude, low-energy emission generated during the deformation of materials. Continuous emissions begin at the onset of plastic deformation and reach a peak rate in the specimen's plastic region. Continuous emissions are associated with microscopic and submicroscopic events such as slips, twinnings, granular reorientations, dislocations, and pile-ups. The second is the large-amplitude burst-type of emission created by fracturing and realignments at the leading edges of flaws. Burst types of emission are associated with macroscopic failures and are estimated to have energy levels 10^{10} to 10^{14} times larger than those of continuous emissions.

If a structure containing a flaw is subjected to any stress (fatigue, dynamic, static), the material in the vicinity of the flaw can undergo plastic deformation because of localized high stresses even though the remainder of the structure is well within the elastic design limit.

Dunegan, Harris, and Tatro state that the degree of damage or criticality can be assessed from acoustic emission data by correlation with previously established fracture toughness data in the following manner:

1. Acoustic emission as a function of the stress intensity factor for the specific materials is determined. The results of several tests with flaws of different sizes would generate an N-K plot The thickness of material to be used in the final structure would be most important; the value of the critical stress intensity factor, K_C, could also be determined in these tests by taking the specimens all the way to failure.

2. The structure is acoustically monitored during initial loading to obtain the value of the emission counts, N_t, corresponding to a given load, F_t.

3. The value of the stress intensity factor, K_t, corresponding to the given load, F_t, is obtained from the typical N-K curve by using the value of N_t determined in step 2.

Fracture load can then be determined from the relationship

$$\frac{F_t}{K_t} = \frac{F_C}{K_C} \text{ (fracture load)}$$

This relationship results from the linear dependence of the stress intensity factor on the applied load.

Thus, quantitative information on the initiation of crack growth and the extent of crack extension can be calculated. In this manner, the current structural integrity or remaining lifetime can be assessed.

Corrosion and Stress Corrosion

Tests on stressed specimens in a corrosive environment revealed the feasibility of detecting stress corrosion cracking with an acoustic emission system. Significant increase in acoustic stress waves presaged impending rapid degradation. Therefore, an acoustic emission system appears feasible for monitoring surface and structure degradation caused by corrosion.

Feasibility of On-Board Systems

Theory and mathematical calculations for an on-board acoustic emission monitoring system have been compiled. These calculations and the preliminary testing indicate a strong potential for employing the method to ensure structural integrity and to assess remaining service life.

Pressure-Vessel Monitoring

The development achieved to monitor the structure of pressure vessels consisted of sensor development and frequency analysis of flaw signals and extraneous noise signals at both room and cryogenic temperatures. The sensor research and testing revealed that the resulting signals were directly related to the resonant frequency of the sensors. The signal analysis, together with the transducer testing, indicates that a system capable of monitoring the structural capability is not only feasible but is extremely practical when the sensor resonant frequency is matched with the proper filter arrangement for the most advantageous signal-to-noise ratio.

ULTRASONICS

Ultrasonic efforts currently fall within three major areas: in-process, on-board, and integral structures. In-process ultrasonics refers to those techniques that evaluate the quality of hardware items simultaneously with the processing sequence. The applicability for ultrasonic wave propagation

to detect material inconsistencies or changes during forming, welding, bonding, or other processes is feasible and has been demonstrated for some processes.

On-board refers to a technique of bonding ultrasonic transducers to structural assemblies for the purpose of defect analysis during the operational life of that hardware. Generation of ultrasonic waves outward away from these transducers will seek out reflective interfaces created by defective material inconsistencies and return an ultrasonic warning signal of the presence of that inconsistency by magnitude and location.

Integral structural ultrasonics refers to a technique of ultrasonic application whereby a structural assembly is illuminated with ultrasonic waves of a variety of modes and after illumination, additional instrumented ultrasonic transducers operating as receivers detect and discriminate the secondary ultrasonic radiation from those inconsistencies which are generally in the form of spherical waves. This application sometimes is referred to as "burst pulse," "delta," or "acoustic spectroscopy."

Acoustic spectroscopy is a nondestructive evaluation technique that has has been designed to provide flaw detection within large areas (10 ft^2) at extremely rapid rates. Normally, ultrasonic flaw detection is accomplished by scanning a transducer over the inspection area, which can be time-consuming when looking for small flaws (2-4 ft/hr maximum). Acoustic spectroscopy employs the principle of controlled ultrasonic wave propagation from more than one stationary source and the analysis of the resultant spectrum produced for flaw detection and location. This technology has been devised by the Agrophysics Corporation (formerly the W. W. Dickenson Co.) of San Francisco, California.

Basically, the technique employs the transmission of high-powered ultrasonic shear waves produced by burst pulsing. Computers are used to control scanning and signal evaluation, which are achieved by triangulation and spectrum analysis. This technique, if properly developed, could provide an in-place ultrasonic monitoring system capable of large homogeneous area coverage with flaw detection results available almost simultaneously with initial pulsing. Transducer location for relatively homogeneous areas could be on 10-foot centers or greater. Transducer weights at the current state of the art are measured in ounces and, with more development, could be substantially less according to W. W. Dickenson.

Acoustic spectroscopy, with further development effort, could provide a rapid assessment of structural integrity of shuttle structures in many areas, from manufacturing through operations.

HOLOGRAPHIC NDE

Holographic interferometry can locate structural anomalies by detecting irregularities in surface displacement as a structure is subjected to low-level loading. Holographic interferometry is predicated on the use of a continuous-wave (CW) laser light source. When fringe control techniques became available, they were incorporated into the laser holography system. Efforts to achieve continuous-wave, off-the-table operation have been concentrated on the double-reference-beam technique since technical literature reveals an ever-growing number of engineering applications.

The alternative approach to CW-laser holography, namely pulsed-laser holography, has made significant progress this year when several pulsed-laser holography systems have become commercially available. CW-laser holography still has the advantage over pulsed-laser systems in that it makes possible real-time observation. However, for the purpose of making photographic records, double-exposure holography is normally used; as a result, the advantages of the CW system become less pronounced. Pulsed-laser holography seems to offer the quickest method of achieving a shop inspection system because of the recent advancements.

For a continuous-wave, off-the-table system, higher power and a more compact continuous wave laser, as well as improved film techniques, must be developed. Recently, argon lasers became commercially available; these lasers offer as much as ten times (one watt) the power output of the available helium neon laser system used for the holographic system evaluation. The helium neon lasers are limited in output to about 100 milliwatts.

The application of holographic nondestructive testing to candidate structures has been under study for two years. To thin-skin structures such as honeycomb, corrugated panels, Stresskin, etc., the following equation is applicable:

$$\Delta l = \frac{d^4 (1 - \nu^2)}{64 E t^3} \cdot q$$

where

E is Young's Modulus of the facing sheet (along the plane surface)

ν is the Poisson ratio of the sheet

t is the thickness of the sheet

d is the diameter of the defect (minimum defect size)

J is the deflection of the defect's epicenter. For HNDT, this value must be at least one-half the wave length of the laser beam $\left(\frac{1}{2} \times 6328 \text{ A}\right)$ and should be a minimum of about four times the wavelength, in order to make practical application possible.

q is the forcing parameter

For internally loaded structures, q corresponds to the pressure difference across the membrane and is limited by the strength of the material. The theoretical maximum can be taken as 0.8 times the yield strength of the composite structure in flatwise tension testing. The meaning for thermal or vibration loading is not completely clear, but is similarly limited.

In terms of the present state of the art, 50-mil-thick 7075 aluminum, adhesively bonded to titanium core (1/2-inch void), represents a very conservative limit for high-conductivity materials; while a 16-mil titanium facing sheet, diffusion-bonded to titanium core (1/4-inch void), represents a conservative limit for low-conductivity materials with little thermal expansion mismatch. Both limits are to be construed with respect to thermal loading. Extension to other candidate materials may be made on the basis of relative proportionality by the formula

$$\frac{E_1 t_1^3}{d_1^4 \left(1 - v_1^2\right)} = \frac{E_2 t_2^3}{d_2^4 \left(1 - v_2^2\right)} \left(\frac{q_1}{q_2}\right)^1$$

and the allowable minimum defect dimension. The symbols have the same meaning as in the previous formula. The subscript 1 refers to a material of a known holographic sensitivity. While the subscript 2 allows the unknown sensitivity of a second structure to be calculated, based on the material properties of the structure. The effective diameter of the defect, d, is taken to be a measure of sensitivity of the holographic nondestructive testing.

Off-the-Table, Continuous-Wave Holography

Methods to achieve continuous wave, off-the-table holography were centered around the basic premise of making the exposure time short enough so that the random background vibration was stopped in time-action

photography. In order to achieve a short exposure time, the light intensity level at the film plateholder must be of sufficient level to make possible a short exposure. Basically, two methods are available for raising the intensity. One method would be simply to use a laser of high enough power to achieve this intensity. However, the highest-powered CW lasers (argon) presently available are limited to approximately 1 watt, single mode, equivalent to 1.0 joule second. It is known from pulsed-laser holography, also, that exposures of about 20 nanoseconds are required for a 3-joule rod. Therefore, on a comparative basis, it can be seen that present CW lasers are not powerful enough.

Another method would necessitate the use of lenses to increase light intensity. A large Fresnel lens placed between the object and the film plateholder is a basic concept being studied. The basic method of approach is illustrated in FIGURE 45. The light intensification that can be achieved by using this technique may be calculated on the basis of the area of light collected, as shown in FIGURE 46. Here the increase in light intensity is A_1/A_2, minus the reflected light from the lens. A practical value for A_1 is several square feet while the limit for A_2 would be a few square inches. A_2 is limited by the practical size of the hologram plate that can be viewed, or about one-fourth of a 5- x 4-inch plate, which when projected back to the viewing plane becomes one-half this value, or about 2-1/2 square inches. With the use of an antireflecting coating, the light lost from the lens should be about 10 percent or less. The result is an increase in light intensity of about 100. With calculations based on the present exposure time of one second for a light cone 12 inches in diameter from an 87-milliwatt laser, exposure of about 10 milliseconds would be required.

It is not known how fast the exposure must be in order to stop the random background motion. However, with a ten-fold increase in power (about the limit of what is available now), exposures in the millisecond range could be achieved. This status is far removed from the exposures of a few hundred nanoseconds, which can be achieved with pulsed lasers. Hence, at the present time, the pulsed laser systems are far superior to the CW laser approach in the achievement of off-the-table holography.

THERMOGRAPHY

Thermographic nondestructive testing methods have been investigated since the mid-1960's. Thermal techniques function on the principle of heat energy flow for the flaw detection mechanism. Any discontinuity located in the heat flow path will result in some differences in surface temperature. This surface temperature differential can be detected by a variety of sensing methods, such as infrared detectors, liquid crystals, infrared sensitive photographic film, etc.

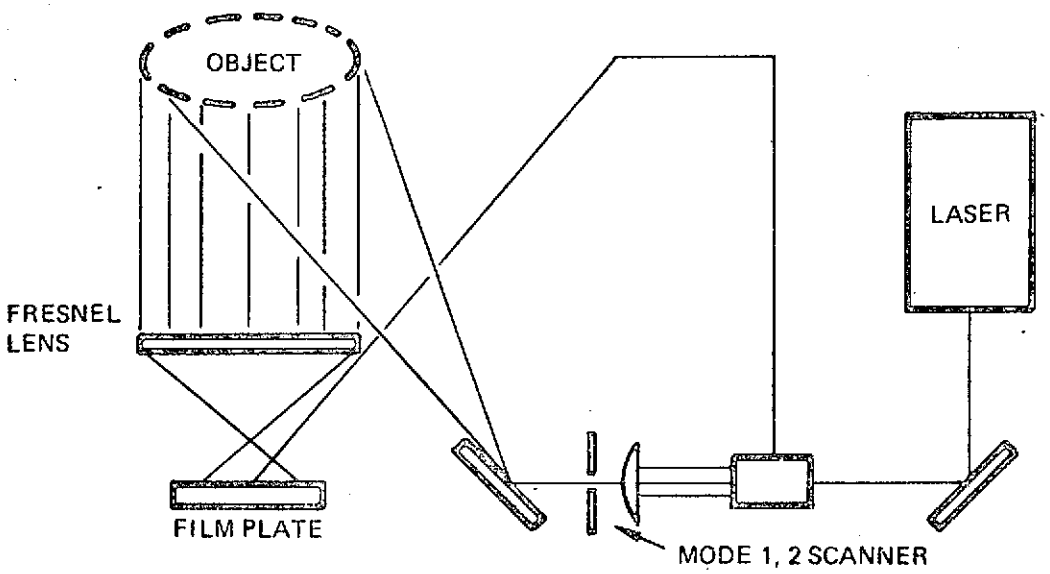

Figure 45. Holography With Intensifier Lens

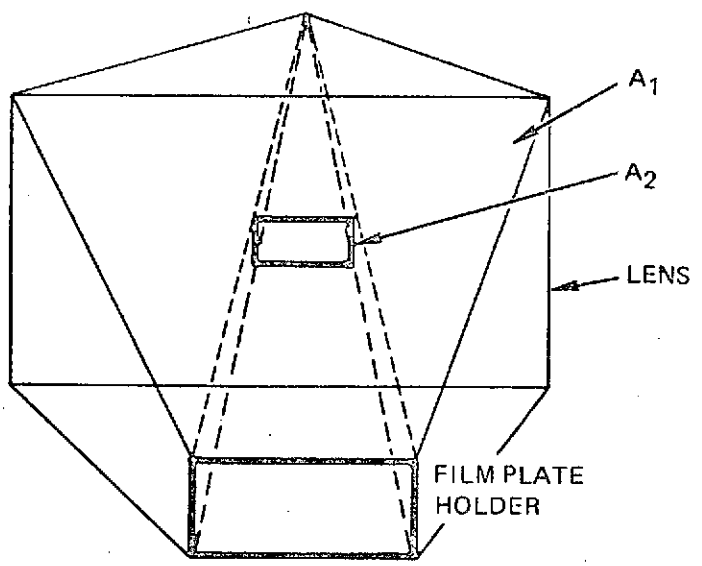

Figure 46. Increased Intensity Film Lens

Infrared Scanners

Infrared scanning detector systems are comprised basically of three elements: (1) an input optical system, (2) the infrared detector, and (3) the data processing section. The optical portion of the system collects the radiation obtained from the subject for filtering and focusing onto the surface of the detector. The detector, which is the heart of the entire system, converts this infrared energy into a form that can be monitored. Once the infrared radiation has reached the detector and the resulting signal has been generated, another system processes the signal for presentation in the desired manner. In order to obtain an increased field-of-view, a scanning mechanism is used in conjunction with the optic device. When a scanner is located in the input optical section, the signal processing electronics must be synchronized with the scanning operation. Although the initial scanner systems possessed advantages such as no contact with test part and large area coverage, limitations existed because of slow scan speed, limited detector selections and spectrum ranges, and limited data presentation modes.

In recent years, with the advent of increased military and commercial applications, significant improvements in the field of infrared technology have been achieved. Among the major improvements are detectors with increased sensitivity and spectral response, rapid scanning input optics, and multiple data presentation methods.

Several infrared detector systems are now commercially available that encompass the features that make them extremely attractive as potential nondestructive testing systems. The units included the Barnes Engineering Model T-101, AGA Corporation Model 680 Thermovision, and the Dynarad, Inc., Model 201. A comparison of the various features of these units is shown in TABLE 15.

Infrared Photography

Regular infrared photography is the technique of using a camera lens to focus an infrared image onto an emulsion sensitized to infrared radiation. The infrared image is produced as a negative record, and subsequently, is reproduced as a positive print. The sensitivity region of infrared sensitive film is approximately 700 to 900 mμ; however, results have been obtained at wavelengths out to approximately 1350 mμ. Most infrared photographic work is performed using reflected IR energy. Emitted IR energy can be recorded on IR sensitive film if the temperature of the test object is in the range of approximately 250 to 500 C (482 to 932 F). Below this temperature range, the radiation is nonactive; above it, some of the radiation is in the visible range.

Based upon this data, it can be concluded that the use of infrared film as a thermal nondestructive test device is limited. The sensitivity of the film for the detection of emitted IR energy is restricted to objects with temperatures above approximately 500 F. Some applications may exist for the combination IR film and ultraviolet lighting method for inspection of thin nonmetallic materials. In both cases, extensive evaluation tests will be required to establish the detection capability and sensitivity limits of the techniques.

Liquid Crystals

The liquid crystal thermographic technique has been shown as a feasible method of nondestructive testing in specific applications. Application development of this technique has been conducted on various materials and hardware configurations. Among the materials to which the technique has been applied were an epoxy/polyimide honeycomb structures, aluminum coldplate assemblies, nichrome wire heater elements, Haynes 188 Stresskin panels, and diffusion-bonded columbium structures.

FIBER OPTICS

Optical devices have long been used for the inspection of aircraft and aerospace structures. With the increased complexity and extended usage of advanced space vehicles, the need for optical viewing of inaccessible areas of such spacecraft is expected to become even greater. During the past decade, many advancements have been made in the manufacture of remote viewing optical devices as a result of demands in the field of medical instrumentation. These new medical systems can be adapted to aerospace applications and can provide improved viewing capability for assessing structural integrity in normally inaccessible areas. Furthermore, the coupling of these optical devices with sophisticated electronic devices has resulted in many useful and unique means of data presentation and documentation.

Although remote viewing optic devices, such as borescopes, have been in use for many years, some inherent problems have been encountered with these devices. Among the more significant problems are: (1) a limited depth of field (focusing has to be exact to obtain a clear image); (2) the image clarity and field-of-vision from small diameter scopes are limited; and (3) the light intensity is not adequate.

An evaluation of commercially available optic systems has been conducted to determine which equipment had the optimum potential for aerospace

Infrared Scanners Features	Detector	Coolant and Capacity	Focus	Field-of-V
Barnes Engineering T-101 (~$25,000)	Indium antimonide	100 cc Liquid nitrogen 4 hours continuous operation	10 inches to infinity	25 x 12.5 de full field 12.5 x 12.5 half field
AGA Thermovision Model 680 ($27,000)	Indium antimonide 2 - 5.6μ	Liquid nitrogen 4 hours between fills	0.95 in. 3.1 ft to infinity	10 x 10 deg additional lenses 25 x 25 deg 40 x 40 deg
Dynarad Thermo-Imager Model 200 series ($17,900) (Optical Detector $6800)	Indium antimonide (Opt-HqCdTe)	100 cc Liquid nitrogen 5 hours continuous operation	16 inches to Infinity	10 x 10 deg

2

Table 1

cus	Field-of-View	Frames per Second	Applicable Temp Range	Minimum Detect Temp	Size and Weight	Isc
ches ity	25 x 12.5 deg full field 12.5 x 12.5 deg half field	4 frames per sec 95 lines per frame	-20 C to 150 C extendable to 300 C, 700 C	Better than 0.2 C at 30 C	Head: 13-1/2 x 10 x 12 57 lb Display: 10 x 13-1/2 x 21 33 lb	Adju 2.5 of tot temp in im
in. t ty	10 x 10 deg additional lenses 25 x 25 deg 40 x 40 deg	16 frames per sec 1600 lines per sec	-30 C to 700 C in 10 sensitivity steps extendable up to 2000 C	Less than 0.2 C at 30 C	Head: 7.9 x 9.5 x 19.7 30 lb Display: 17.7 x 7.9 x 20.8 52 lb	Dual singl varia width Dual- 30% c selec temp range
ches ty	10 x 10 deg	60 frames per sec at 100 lines 30 frames per sec at 200 lines ($2000) (tuning fork)	-20 C to 150 C	0.3 C at 30 C	Head: 5.5 x 6.6 x 11 9.7 lb Display: 10 x 13-1/2 x 21 29 lb	Isoth width 2.5 t of se temp

3

le 15. Comparison of Infrared Scanners

Isotherms	Instantaneous Field	Added Features
Adjustable 2.5 to 20% of total temp range in image	0.1 deg 1.7 millirads	External calibrator Polaroid scope camera Light and sun filter Single-line A-trace magnetic tape recorder
Dual or single, variable width Dual-1 to 30% of selected temp range	1.3 millirads	Color monitor Filter wheel (8) Polaroid scope camera Magnetic tape recording Interchangeable optics
Isotherm width 2.5 to 20% of selected temp range	1.7 millirads	External calibration source Magnetic tape recorder Polaroid scope cameras Single-line trace multidetector systems

applications. TABLE 16 compares the commercially available devices with respect to specific attributes. The light transmission percentage, viewing angle, and scope diameter and length are shown for nine different scopes.

Table 16. Comparison of Borescopes*

Borescope	Light Transmission (percent)	Viewing Angle (deg)	Diameter (mm)
ACMI lateral	100 (std)	52	5.2
ACMI foroblique	42	30	.4.1
Sass and Wolf lateral	160	30	4.5
Sass and Wolf foroblique	75	35	3.5
Gardner lateral	110	47	5.0
Drapier foroblique	30	28	4.2
Drapier forward	30	23	4.2
Storz Hopkins lateral	200	70	4.1
Storz Hopkins foroblique	170	70	4.0

*All lengths were approximately 30 centimeters (12 inches).

Larger diameters are necessary for longer length, because the total amount of light that can be transmitted through an optical system is directly proportional to the cross-sectional area of the light transmitting bundle.

As the comparison shows, the Storz Hopkins rod optic devices system is the system possessing the optimum characteristics required for use on aerospace structures. The Storz Hopkins design differs from conventional borescopes in that rod lenses are used, an invention of Professor H.H. Hopkins of the University of Reading, England. In contrast to previous systems, the air spaces are replaced by glass, and the former glass lenses by air spaces. The spaces between the rod-like glass elements act as air lenses. With this arrangement, stray light is avoided and a much-increased contrast is obtained. The extraordinary resolving power of this system is illustrated by high contrast, which, even when the system is used extremely close to the object, results in a very realistic image. The Hopkins telescope has an angle-of-field of 90 degrees in air and produces no aberration, even over this large field. In water, the angle-of-field becomes 70 degrees, but no image errors are present. The high aperture of the rod lens system allows a considerable increase in image brightness. For this reason, the diameter of the telescope can be minimal, even with its fiber optic light

guide, so that the manufacture of extremely small-diameter instruments with good optical properties is possible. The optical system is well corrected for color, and variations of color are realistically reproduced, both in visual observation and also in photography.

Another major advantage of the Storz Hopkins optic devices is its use of a cold-light source for illumination of the area being investigated. Cold light makes it possible to locate the light source external to the part being examined. This generally means the elimination of any explosion hazard or the possibility of damage from a hot incandescent light bulb on the inserted scope. Also, with the light source located externally, less maintenance and bulb replacement are necessary.

In addition to the investigation of optic devices, methods of documenting the images obtained with the optics, using closed-circuit television systems, has been conducted. Several vidicon systems have been evaluated, including Sony, RCA, RAM, and Unitron cameras. The Unitron camera was found to be the smallest and most flexible. This camera will magnify the small 1/4-inch eyepiece image of the optice device to fill a full-sized monitor screen. This capability results from the low light characteristic of the camera and its special lens. An average borescope has an equivalent f stop of F40, which limits the types of cameras that can be employed to only those sensitive to the lowest light level of the visible spectrum. FIGURE 47 illustrates some of the television and camera systems evaluated.

RADIOGRAPHY

Radiographic nondestructive evaluation has been developed to a high degree for flaw analysis of aerospace structures. New or recent developments in X-ray equipment itself have been directed towards miniaturization of X-ray beads, better electrical and electronic support equipment, and automation of the process itself. Probably the greatest strides have been made in the fields of neutron radiography and radiographic image enhancement.

Neutron radiography has been established as an inspection method for the nondestructive testing of ordnance devices. The success of neutron radiography in contributing to improved reliability for ordnance devices in space vehicles has stimulated interest in developing this technique for advanced space vehicles.

Significant improvements in photographic image enhancement techniques have been achieved in recent years. Probably the most widely publicized effort related to the early photographs sent from space vehicles and moon probes, which were reconstructed and enhanced with great success.

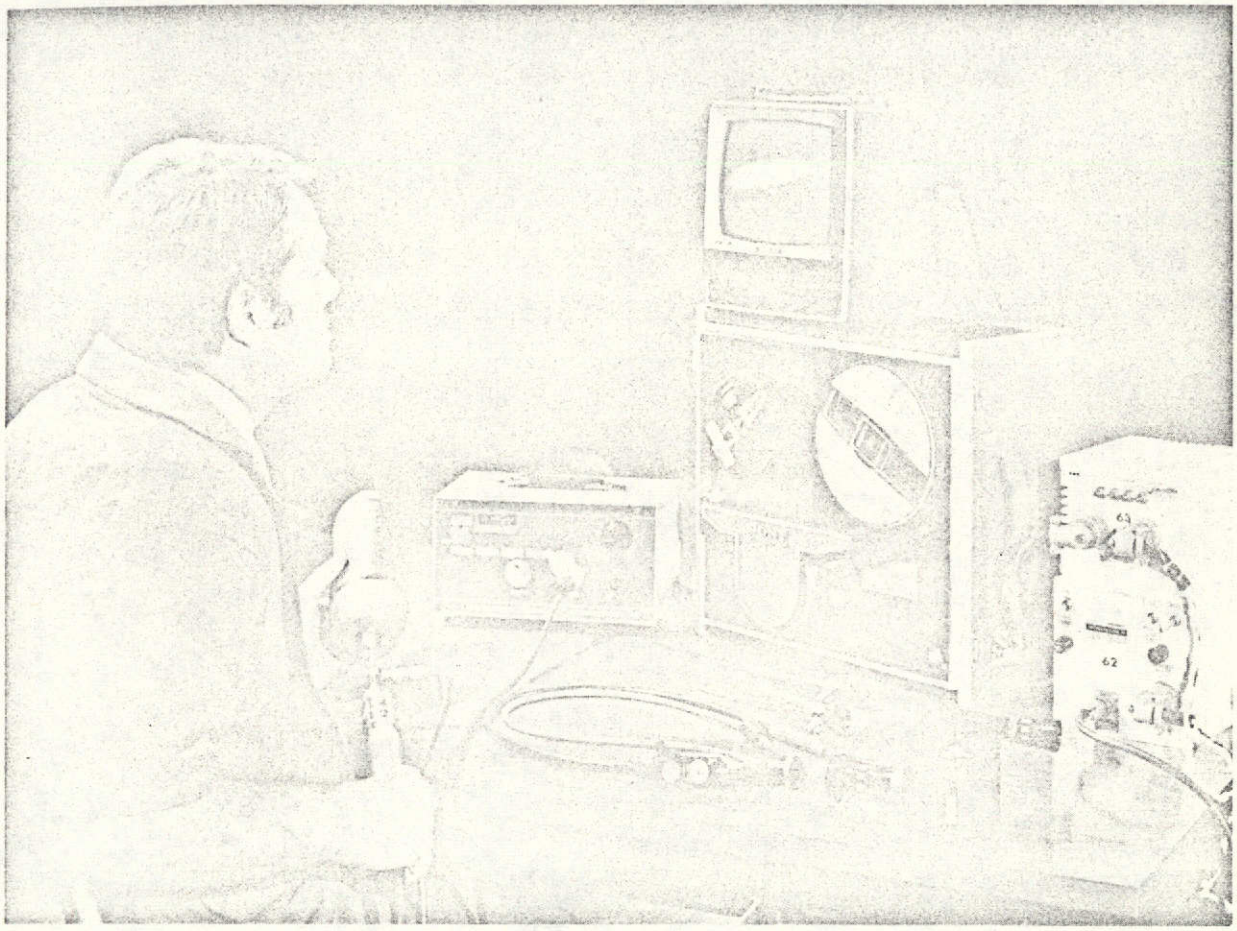

700 60-99

Figure 47. Borescope CCTV Apparatus

Basically, the principle involved is that of reducing the various densities creating the image to forms that a computer can accept (digitize). The computer can then sharpen the edges and reconstruct the enhanced image. The computer can also, conceivably, measure the area of a flaw, compare the measurement against a known standard, and make a decision—based on acceptance data—regarding acceptability.

FIGURE 48 shows an early attempt at industrial radiographic enhancement.

The four photographs of the sample radiograph were reconstructed in the following modes:

1. Quadrant 1 (upper left), normal

2. Quadrant 2 (upper right), complement

3. Quadrant 4 (lower left), normal with gamma

4. Quadrant 4 (lower right), complement with gamma

Although the quality of the results is certainly not startling, the pictures do represent a necessary and significant early step in the image enhancement of industrial radiographic film.

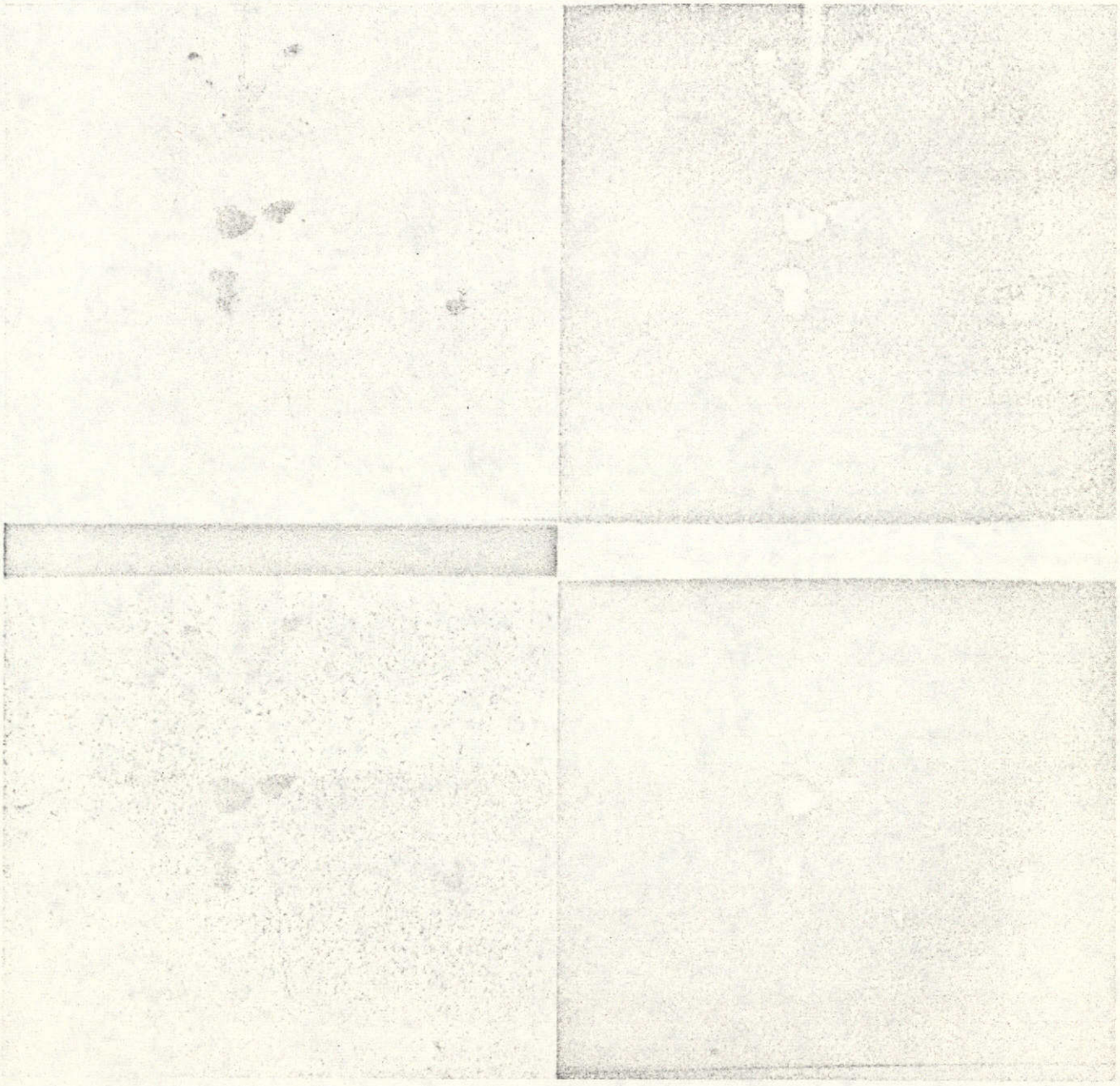

Figure 48. Radiographic Enhancement
(Courtsey Dicomed)

RECOMMENDATIONS

ADDITIONAL STUDIES

Three additional studies are recommended that will provide KSC operations and maintainability engineers and technicians with some of the necessary tools to achieve rapid vehicle turnaround. These studies are parallel efforts to the current structural integrity program described in this report but not necessary logical follow-ons. They are designed to provide the feasibility necessary to begin development of specific NDE methods, which will directly aid vehicle turnaround.

Thermal Protection System Integrity

Certain conceptual studies have shown that thermographic nondestructive evaluation methods utilizing scanning cameras can provide quality data for ablative thermal protection materials and structures. Assessment can be rapid, data can be recorded, and information can be secured immediately after severe thermal exposure. For materials protecting the basic structure of a shuttle vehicle, quality data can conceivably be obtained immediately before or after touchdown and prior to vehicle safing during the cool-down period.

Proposed implementation of thermal techniques could involve a stationary camera system by which the vehicle could pass. Alternately, a movable camera system could be developed to assure complete coverage of a stationary shuttle.

Concern for the quality of ablator materials used on the shuttle does not presently involve any material containing a surface char layer. Only those materials that are uncharred and appear similar to unexposed ablators will be of concern to further vehicle operation. This material, which will have been exposed to a thermal environment substantially less than those that produce ablation, may appear similar to unexposed material but outgassing might have occurred at the elevated temperature, and the service life of the ablator may have terminated.

A study should be conducted to achieve two basic goals. The first is to develop the capability to scan an entire vehicle moving at high relative speeds to a scanning system and to determine basic resolution and sensitivity capabilities of such a system. The second is to characterize the IR response

from uncharred but thermally exposed materials and determine, nondestructively, the remaining service life of the ablator. Ultimately, upon successful conclusion of these investigations, a total systems concept will evolve to provide an analysis of TPS serviceability.

NDE for TPS Refurbishment

During replacement of ablator, and eventually reusable, external insulation panels, rapid evaluation methods are necessary to determine attachment integrity, especially when panels are attached by adhesive bonding processes. Access to these areas will most likely be from the TPS surface, which is normally a relatively porous nonconductive material. Studies to date have shown that normal bond integrity evaluation devices such as ultrasonics have proven relatively ineffective with these structures and materials, especially from the thermally exposed side. An evaluation program should be conducted to determine those techniques that can effectively and efficiently provide bond integrity information subsequent to field repair of the thermal protection system. Such technologies as low-frequency ultrasonics, thermography, and microwave analysis are strong candidates for evaluation and study.

Ultrasonic Particle Counters

Ultrasonic energy at relatively high frequencies has been used in the laboratory and in some low sensitivity commercial systems to detect and size contaminate particles in fluid systems. This emerging technology should be developed to provide the sensitivity necessary to evaluate shuttle fluid systems for contaminate particles on installed shuttle systems and in the major subsystem configuration. Successful development of this method could provide particle determinations without fluid sampling or line entry.

FOLLOW-ON EFFORT

Transducer Development

Development of surface and shear wave transducers for on-board system considerations should be pursued. Present configurations of transducers provide very narrow-beam ultrasonic propagation, thereby limiting areal coverage. Two approaches can be considered. The first would investigate rotational possibilities for transducers to provide direction as well as distance information concerning flaws. A radar or sonar analogy can be utilized to illustrate this approach. The second approach would hopefully evolve stationary transducers with wide-beam angle capability to increase structure coverage. On-board ultrasonic systems for the shuttle must incorporate transducer designs capable of large area coverage to reduce the number of transducers required and the electronics necessary to support the total system.

Ultrasonic Triangulation and Computer Analysis

Follow-on effort must be a logical step ahead from the technology position now being held. The further development and application of the ultrasonic flaw detection method to specific structures and assemblies will provide this step. Present effort has proven that one parameter, distance, can be obtained in fairly complex structures. It is necessary to determine methods to provide the other parameter, azimuth or direction, before the actual systems development of the monitoring device can be conducted. Using the techniques of surface wave propagation, multiplexing, adhesive bonding, and other pertinent data already developed, a program to begin actual development of the system concepts to real structural assemblies for ultrasonic flaw location must be conducted. Many structures that were used during the development of the CSM and S-II programs can be test structure candidates for these further studies. Certain structural requirements that have been established for space shuttle assemblies should be brought to bear so that a representative workpiece can be selected for use. The design requirements of the shuttle must be continually considered during the duration of any resultant study by continual interface with shuttle design engineering teams.

Shuttle Structure Ultrasonic Testing Using Multiplexing Methods

The above section establishes a tentative program to develop flaw location methods utilizing triangulation and computer techniques much similar to those being developed for the acoustic emission systems. One other method that must be employed in order to aid in the reduction of the supporting electronics is that of multiplexing the ultrasonic signal to the selected number of transducers to be installed on board the shuttle vehicle. A follow-on program should be conducted to establish multiplexing techniques for ultrasonic transducers that can ultimately provide design requirements for the final on-board configuration.

PRECEDING PAGE BLANK NOT FILMED

GLOSSARY

A-SCAN. A data presentation method by which intelligence signals from a single object located are displayed. As generally applied to pulse echo ultrasonics, the horizontal and vertical sweeps are proportional to time or distance and amplitude or magnitude respectively. Thus the location and magnitude of acoustical interface are indicated as to depth below the transducer.

GAIN. The level of amplification at which the receiving circuit in an ultrasonic instrument is set. For the purposes of this study, gain values were used as a comparative measure.

INITIAL PULSE (MAIN BANG). The first indication that may appear on the screen depending upon the amount of sweep delay. This indication represents the emission of ultrasonic energy from the crystal face.

RAYLEIGH WAVE. A wave that travels on or close to the surface and readily follows the curvature of the part being examined. Reflections occur only at sharp changes of direction of the surface.

SHEAR WAVE. A wave in which the particles of the medium vibrate in a direction perpendicular to the direction of propagation.

PRECEDING PAGE BLANK NOT FILMED

BIBLIOGRAPHY

1. Anderson, R.E. Nondestructive Evaluation Development for Advanced Spacecraft. Space Division, North American Rockwell Corporation, SD 70-406 (September 1970).

2. Anderson, R.E., C.C. Kammerer, and F.H. Stuckenberg. Methods of Assessing Structural Integrity for Space Shuttle Vehicles. Space Division, North American Rockwell Corporation, SD 70-419 (October 1970).

3. Anderson, R.E., and R.G. Poe. A Study of Space Shuttle Structural Integrity Test and Assessment, Mid-Term Report. Space Division, North American Rockwell Corporation, SD 71-193 (October 1971).

4. Anderson, R.E., and F.H. Stuckenberg. Methods of Assessing Structural Integrity for Space Shuttle Vehicles, Phase II Report. Space Division, North American Rockwell Corporation, SD 71-112 (January 1971).

5. Bishop, C.R. Nondestructive Evaluation Development for Advanced Spacecraft. Space Division, North American Rockwell Corporation, SD 71-153 (September 1971).

6. Carlin, B. Ultrasonics, Second Edition. McGraw-Hill Book Company, Inc. (1960).

7. Greer, A.S., and W.M. Tooley. Feasibility Study of Ultrasonic Burst Scanning Techniques for Reentry Vehicles, Final Report. Automation Industries, TR-71-7 (31 January 1971).

8. Logistics and Maintenance Plan. Space Division, North American Rockwell Corporation, SD 71-106 (June 1971).

9. McMaster, R.C. Nondestructive Testing Handbook, Volume II. The Ronald Press Co., New York (1959).

10. Program Cost and Schedule Estimates Plan for Phase C/D, Part 1. Space Division, North American Rockwell Corporation, SD 71-107 (June 1971).

11. Program Cost and Schedule Estimates Plan for Phase C/D, Part 2. Space Division, North American Rockwell Corporation, SD 71-107 (June 1971).

12. Sugg, F. E. S-II Advanced Technology Study No. 4, MCR S06874, First Quarterly Progress Report. Space Division, North American Rockwell Corporation, IL No. NDT-21-003 (12 February 1971).

13. Sugg, F. E. S-II Advanced Technology Study No. 4, MCR S06874, Second Quarterly Report. Space Division, North American Rockwell Corporation, IL No. 145-020-71-32 (17 May 1971).

14. Sugg, F. E. S-II Advanced Technology Study No. 4, MCR S06874, Third Quarterly Report. Space Division, North American Rockwell Corporation, IL No. 047-300-71-103 (13 August 1971).